جامعة أبو بكر بلقايد
UNIVERSITÉ DE TLEMCEN

Pan African University
Institute of Water and Energy Sciences

Institute of Water and Energy Sciences (Including Climate Change)

SIMULATION OF LAND USE CHANGES AND IMPACTS ON THE WATER BALANCE OF AN UNCONFINED AQUIFER

CASE STUDY: SAISS AQUIFER, MOROCCO

Muhammudu Mukaya

Date: 04/09/2017

*Master in **Water, Policy track***

President: Prof. Joseph Kajima Mulengi

Supervisor: Prof. Abdelkader El Garouani

External Examiner: Dr. Nadia Badr

Internal Examiner: Dr. Karima Benhattab

Academic Year: 2016-2017

DECLARATION

I, Mukaya Muhammudu, do hereby declare that the thesis entitled *"Simulation of land use changes and impacts on the water balance of an unconfined aquifer (The Case of Saiss aquifer, Morocco)"*, submitted by me in partial fulfillment of the requirements for the award of Master of Science in Water Policy of Pan African University, Institute of Water and Energy Sciences (including Climate Change), PAUWES is original work and it has not been presented for the award of any other degree, diploma, fellowship or other similar titles, of any other University or Institution.

MUKAYA MUHAMMUDU

Signature

Date: 3rd September 2017

CERTIFICATION

I undersigned, Prof. El Garouani Abdelkader, Guest Lecturer at the Pan African University Institute of Water and Energy Sciences including Climate Change (PAUWES), and permanent lecturer at the Faculty of Sciences and Techniques of Fez (FST), Morocco; certify that Mr. Mukaya Muhammudu conducted his Master Thesis research under my supervision. Certified further, that this master thesis entitled *"Simulation of land use changes and impacts on the water balance of an unconfined aquifer (The Case of Saiss aquifer, Morocco)"* is an authentic work of Mr. Mukaya Muhammudu who carried out the research under my guidance.

Signature 

Date: 4th September 2017.

ACKNOWLEDGEMENTS

My first and highest gratitude is owed to the Almighty Allah whose faithfulness has seen me through the challenging situations of my academic life.

I thank my supervisor prof. EL GAROUANI Abdelkader, from the Faculty of Science and Techniques, Fez (FST-Fez), for the support criticism and all help given during the entire course of research.

My sincere gratitude to African Union and the African Union Commission (AUC), the Germany Ministry of Foreign Affairs, for awarding me the Scholarship that enabled me do this postgraduate degree.

I would also like to express my sincere gratitude to:

- The Jury members: Prof. Joseph Kajima Mulengi, Prof. Abdelkader El Garouani, Dr. Nadia Badr and Dr. Karima Benhattab;
- The Laboratory of Geo-Resources and Environment of the Faculty of Sciences and Techniques of Fez;
- Mr. Kamal Aharik, PhD student of the Geo–Resources and Environment Laboratory for his assistance and help;
- West African Science Centre on Climate Change and Adapted Land Use, Competence centre for the technical skills I gained during the internship that shaped my research.

TABLE OF CONTENTS

LIST OF TABLES

LIST OF FIGURES

ABBREVIATIONS

AEP	Actual Evapotranspiration
AHBS	Agency of the Hydraulic Basin Sebou
CCAA	Climate Change Adaptation in Africa
GIS	Geographical information system
GWD	Ground Water Depth
IDW	Inverse distance weighting
LULC	Land Use Land cover
NIAR	National Institute of Agronomic Research
PAUWES	Pan African University Institute of Water and Energy Sciences
PET	Potential Evapotranspiration
RS	Remote sensing
SCS-CN	Soil Conservation Service Curve Number
STDW	Spatiotemporal data ware house
USDA	United States Department of Agriculture
USDP	United Nations Development Programme
USGS	United State Geological Survey
WetSpass	Water Energy Transfer between Soil Plants and Atmosphere at quasi Steady State

ABSTRACT

Ground water is widely a used fresh water source upon which plants, animal and human life relies. However, over years this golden source has become under diverse threat of depletion and degradation more so in circumstances where aquifers are heavily allocated or where there are changes in recharge rates due to several factors. The inter-connectness between land use, hydrological events and processes is a contingent linkage where by any modifications and transformations made on land either due to rapid population growth and or increased rate of urbanization, in one way or the other has a direct response on the water balance components. Assessment of effects of land use and cover changes serves as a principle indicator for water resource base analysis and development of effective and efficient plans for sustainability management. This study presents a methodology of quantifying the impacts of land use change on water balance of unconfined aquifer Saiss located in the center of Sebou watershed, and between the cities of Meknes and Fes (Morocco), through the objectives of evaluating historical land use changes for the period (1987-2016) and simulating the water balance components of recharge, evapotranspiration and surface runoff. Using a spatially distributed water balance model (WetSpass), with primary and secondary input data of meteorological from eight weather stations, land use, soil texture and general morphology of the basin. The evolution of land use in the study period of 29 years indicated significant changes, urban, irrigated land, olive trees, orchards, increased by 131%, 86%, 101% and 99% whiles as, open water surface, arable lands decreased by 33% and 20% respectively. The WetSpass simulated results indicated that the annual long-term mean precipitation of 409 mm was spatially distributed within the basin as, evapotranspiration (205 mm), run-off (76 mm) and recharge (126 mm) under land use condition 1987 and as 274 mm, 26 mm and 107 mm respectively under land use 2016, hence an increase of 33% evapotranspiration and decrease of 65% run off, decrease of 15% recharge due to land use change. For sustainability of Saiss aquifer, water abstraction for any intended use should not exceed the safe yield from the current annual ground water recharge of 107 mm (230 Mm^3) of 2016. This study recommends practical remedies of artificial recharge, use of recycled waste water in agricultural fields and adoption of modern efficient irrigation technologies.

Key words: Land use change, water balance, WetSpass, Saiss aquifer

RESUME

L'eau souterraine est une ressource dont dépend la vie végétale, animale et humaine. Cependant, au fil des années, cette ressource précieuse est menacée d'épuisement et de dégradation. Les niveaux piézométriques des aquifères diminuent à cause de la forte exploitation et à cause de la diminution de la recharge annuelle, cette diminution de recharge est liée au changement de l'utilisation du sol et les processus hydrologiques. Actuellement, l'évolution de la population et d'urbanisation ont un effet direct sur les composants du bilan hydrique. L'évaluation des effets de l'occupation du sol est un indicateur principal pour analyser et élaborer des plans de gestion adéquats des ressources en eau. La méthodologie adoptée permet de quantifier les impacts du changement d'utilisation des sols sur le bilan hydrique de la nappe phréatique de Saiss située dans le centre du bassin versant de Sebou, entre les villes de Meknès et Fès (Maroc). Le but est d'évaluer les changements de l'utilisation des sols pour la période (1987-2016) en simulant les composants du bilan hydrique de la nappe (Recharge, évapotranspiration et ruissellement de surface). On a utilisé le modèle spatialisé (WetSpass), ce modelé utilise comme entrés les données météorologiques à partir de huit stations météorologiques, la variation de l'occupation des sols, la texture du sol et la morphologie générale du bassin. L'évolution de l'utilisation des sols pendant la période d'étude de 29 ans a révélé des changements importants dans les zones urbaines, les surfaces irriguées, les plantations d'oliviers et les vergers, qui ont augmenté de 131%, de 86%, de 101% et de 99% alors que les sols qui sont occupés par les surface d'eau libre et les terres arables ont diminué de 33% et 20% respectivement. Les résultats simulés de WetSpass ont indiqué que la précipitation moyenne annuelle à long terme de 409 mm est repartie entre l'évapotranspiration (205 mm), ruissèlement (76 mm) et la recharge (126 mm) sous les conditions d'utilisation du sol en 1987. La répartition a évolué en 2016 avec 274mm pour évapotranspiration, 26 mm pour le ruissèlement et 107 mm pour la recharge. Donc, il s'agit d'une augmentation de 33% de l'évapotranspiration, une diminution de 65% de ruissellement et une diminution de 15% de la recharge due au changement d'occupation du sol. Pour la durabilité de l'aquifère de Saiss, l'extraction de l'eau pour toute utilisation prévue ne doit pas dépasser le rendement sûr de la recharge annuelle actuelle d'eau souterraine qui est de 107 mm (230 Mm^3) en 2016. Cette étude recommande des remèdes pratiques de recharge artificielle, l'utilisation d'eaux usées recyclées dans l'agriculture et l'adoption de technologies d'irrigation modernes et efficaces.

Mots clés : Occupation du sol, Bilan hydrique, WetSpass, Aquifère de Saiss

Chapter 1: GENERAL INTRODUCTION

1.1. Background

The principal "reservoir" of available fresh water is underground. It contributes a significant 0.61% of the less than 1% of earth's total fresh water available to humans (Kimberly, 2012). Upon this water, plant, animal and human life relies. For effective management, a scientific understanding of the interactions in the hydrological cycle is essential (Sayena, 2012).

Imitating the data environment of the unknown underground processes through models which characterize the hydrological cycle's attributes both temporal and spatial (Dams *et al.,* 2008), is thus a key practice in modern hydrological studies. Estimating the hydrological water balance components is essential to water resources management, especially in areas where the major water supply source is groundwater. This however requires a good grasp of the area hydrological processes, many besides, climate change, are increasingly becoming influenced by changes in the land use resulting from activities of humans. The effects of land use change are especially pronounced in regions undergoing rapid urbanization (Wagner *et al.*, 2013), increasingly depending on agriculture and areas limited in surface water.

Land use changes influence the input, storage and output of water within catchments, attributes whose relationship is described by the catchment's water balance (Ellen, 2008). Driven by human activities, such as urbanization, mining, industrialization, agriculture (Meiyappan & Jain, 2012), these changes significantly impact on the water balance (Awotwi , 2009).

Any alteration or transformation of the land cover causes a response to the hydrological system which brings about a rise or a fall in water levels; increase the discharge from the system. This lowering or rising of groundwater levels depends on whether or not demanding groundwater discharge exceeds its recharge. Amounts of this depend, among others, on weather factors including precipitation, temperature (Keisuke, 2017).

The shallow aquifer Saiss Basin, located in the center of Sebou watershed, represents 11% of Morocco's annual water endowment, providing water for 1.8 million habitats in the Saiss plain (UNDP, 2013). However, its level of ground water has been decreasing over the last 30 years due mostly to a fall in the level of precipitation and limited seasonal recharge. The result is a net annual loss of 100 Mm^3 in its water balance (Legrouri *et al.*, 2012). Over exploitation among other factors,

accounts for a decline in groundwater levels of about 70 meters over 1981–2006 in this Saiss basin (UNDP, 2013)**.**

However, while this is true, the Saiss basin also constitutes about a quarter of Morocco's arable land and sustains some 8,000 commercial and subsistence farms (Legrouri *et al.*, 2012). In the past decades, Morocco has experienced significant changes in land use due to population increase, urbanization due to the spread of settlement and the increased development of the land mainly for agriculture and industries.

The impact specifically of these land use changes, besides the climatic factors and over exploitation, remain largely unaccounted for so far as the water balance of the Saiss aquifer is concerned, even though providing a scientific understanding of the process of land use and land cover change, the impacts of different land use decisions, and the ways that decisions are affected, the hydrological cycle and increasing variability, are priority areas of research (Abraha, 2007).

The influence of land use changes is thus significant and increasingly a growing concern; more so under circumstances where aquifers are heavily allocated or where they are subjected to recharge changes. Indeed, their impacts are likely even more intense for unconfined aquifer systems which respond rapidly to changes in the recharge regime (Salem, 2013). Despite this, the relationship specifically between changes resulting from land use and the water balance of unconfined aquifers remains a wide research gap in the annals of hydrologic studies.

Few studies of it are available on a global scale, and even much fewer in Africa, despite the continent undergoing accelerated land use changes owing to exploding populations, urbanization, industry and agriculture.

In Morocco, the studies (Chadli et al., 2016; Briak et al., 2016; Chadli, 2016; Benaabidate et al., 2010) on the subject of land use changes have been associated to sediment yield, run-off, soil loss ,water quality, among other factors but not water balance of unconfined aquifers. The Saiss shallow aquifer of Morocco is thus hydrologically a priority research subject as no records exist as regards impacts of land use changes on its water balance.

The challenge of course is the scarcity of a well-documented and consistent observed record of land use change for the previous 30 years and their corresponding impacts on the general water balance. However, several hydrologic models, including SWAT, Hec-HMS, WaSim, WetSpass,

complemented with remote sensing and GIS techniques, can be chosen from and calibrated to address this challenge. Indeed, it is the intention of this study to further simulate land use changes and their impacts on the water balance of Saiss aquifer.

Considering data limitations, and for purposes of flexibility, the WetSpass model has been adopted for this study, with emphasis on its suitability of spatially simulating water balance components of ground water recharge, evapotranspiration and run-off, using long-term climatic inputs on monthly, seasonal and annual scales, and how each responds to land use change. For impact assessment, GIS spatial analysis has been concurrently used for simulation.

The WetSpass model calculates the water balance of a grid cell while considering the fractions of vegetation, bare soil, open water and impervious area (Pan *et al.*, 2011). Its successful application for the estimation of groundwater is diverse, and can be found in (Dams *et al.*, 2008; Armanuos *et al.*, 2016; Mustafa, 2017; Tilahun and Merkel, 2009 and (Tilahun and Merkel , 2009), among others.

1.2. Statement of the Problem

Globally, aquifers have come under grave threat of depletion and degradation (Legrouri et al., 2012). Morocco is not exceptional, her shallow Saiss aquifer threatens to deplete. It is affected by declining levels of precipitation, accompanying a 1 ^{o}C increase in average temperature (Legrouri *et al.*, 2012). These causes can further be argued to be associated to changes in the use of land owing among others, to Saiss basin's accelerated population growth of 21.3% of the total Moroccan population, a rate faster than the country's average national growth (OPID, 2016).

Operating at a 100 M cubic meters per year recharging deficit (Legrouri *et al.*, 2012), and since 30 years ago, decreasing in levels of ground water, the Saiss basin aquifer runs the danger of depletion unless levels of abstraction as well as recharge are restored to sustainable levels and land use properly managed. Already, spring waters fed by the aquifer have since 1970, declined by 45%, from 24 m^3/s to 15 m^3/s (Legrouri et al., 2012). With regard to its water balance, the contribution of land use changes to Saiss aquifer's current condition is still unknown. However, the occurrence of landscape changes due to land use is apparent. Urbanization is at a massive 49%, just slightly below the national average of 55%. It has been typified by establishment of 74 urban centers (CCAA, 2010). The agriculture industry on the other hand is expanding uniquely; farmers are

intensifying as well as diversifying their production, opting for the commercially lucrative but water intensive crops (CCAA, 2010).

Until now, hydrological models have predicted that unless changes in the use of water, and recharge and precipitation occur, in the time duration of averagely 25 years, Saiss aquifer will dry up completely (Legrouri et al., 2012), To this, imbalance between water exploitation and water recharge, climatic variances and others are contributing factors, however, understanding the impact of land use changes on Saiss aquifer's water balance as undertakes this study, could be the missing link to its sustainable exploitation.

1.3. Research questions and Objectives

1.3.1 General research question.

What is the impact of land use change on the water balance of unconfined aquifer of Saiss?

1.3.2 Specific research questions

1) What is the variation of land use pattern of the Saiss basin in the last 29 years?
2) What is the appropriate hydrological model to simulate the water balance components?
3) What are the impacts of land use changes on water balance components in the Saiss Aquifer?

1.3.3 General objective

The general objective of this research is to simulate the land use change impacts on the water balance components (evapotranspiration, ground water recharge, surface run-off) of Saiss basin using GIS techniques and WetSpass model.

1.3.4 Specific Objectives.

1) To assess the historical land use pattern of the Saiss basin over the last 29 years
2) To set up an appropriate hydrological model for estimation of water balance component.
3) To evaluate impacts of land use changes on water balance components in the Saiss aquifer under different land uses.

1.4. Significance of the Study

Land use change has significant impacts on natural resources, socio-economic and environmental systems. Assessment and knowledge of the types and influences of land use changes on a hydrological system is a principle indicator for resource base analysis and development of effective and appropriate response strategies for sustainability of natural resources. This study will contribute to the body of literature on impacts of land use changes on the water balance of water resources in Morocco and within the Saiss basin to be particular and to trigger further research.

Legislators and policy makers will find the study results a useful reference and resource for making informed decisions regarding water resources and land use management policy and strategies. Moreover, the study presents a method to quantify land use and its impact on water balance regimen, achieved through a method that combines the hydrological model; WetSpass to simulate the main water balance components and GIS techniques for analysis of the land use changes.

1.5. Scope and Limitation of the Study

Limited to the simulation and assessment of the impacts of land use changes on the main water balance components, the study was conducted on the shallow aquifer Saiss Basin, located in the centre of Sebou watershed, and geographically corresponding to the plain of Fez - Meknes.

The water balance was estimated basing on the conservation of mass, taking precipitation as the inflow component and actual evapotranspiration, surface runoff, groundwater recharge as the out flow elements. WetSpass model was used to simulate the water balance components using long - term average weather data from eight weather station within and around the study area for 29 years.

1.6. Study Structure

The structure of the study has been undertaken in three phases, namely:

1.6.1 Pre-field work

The activities conducted before the field work itself; problem definition, literature review on which model to use, the exact data required by the model, and which calibration method to use. Related works, journal works, and previous studies including discussions with supervisors were done in this phase.

1.6.2 Field work

This involved collecting field observation data and from meteorological stations, and all the input data, not acquired during the pre-field work but which was required for the study.

1.6.3 Post-field work

This phase of the research comprises thesis preparation through data processing and analysis, water balance model development, results analysis and presentation

1.7. Thesis Outline

This research thesis was laid out in five chapters (Figure 1.1) and table (1.1) summaries what is entailed in each chapter.

Table 1.1: Thesis report outline

Chapter one	Represents the research background information, problem statement, research questions and objectives, significance and scope of study, outline and general structure of the research.
Chapter two	Detailed comprehensive review of the literature related to this study and research gaps identified that justified the research study at hand.
Chapter three	Presents a detailed description of the study area, information of the location, hydrology, geology, population, administration, social and economic context and climate.
Chapter four	Presents a detailed methodology applied in this research and the data processing and modeling tools. The trend of land use change detection analysis is explained, including the acquiring of required data, processing and analysis.
Chapter five	Covers a chorological discussion of the results and findings from the data analysis, assessment of land use change impacts on the water balance of the Saiss basin, conclusion and policy insights.

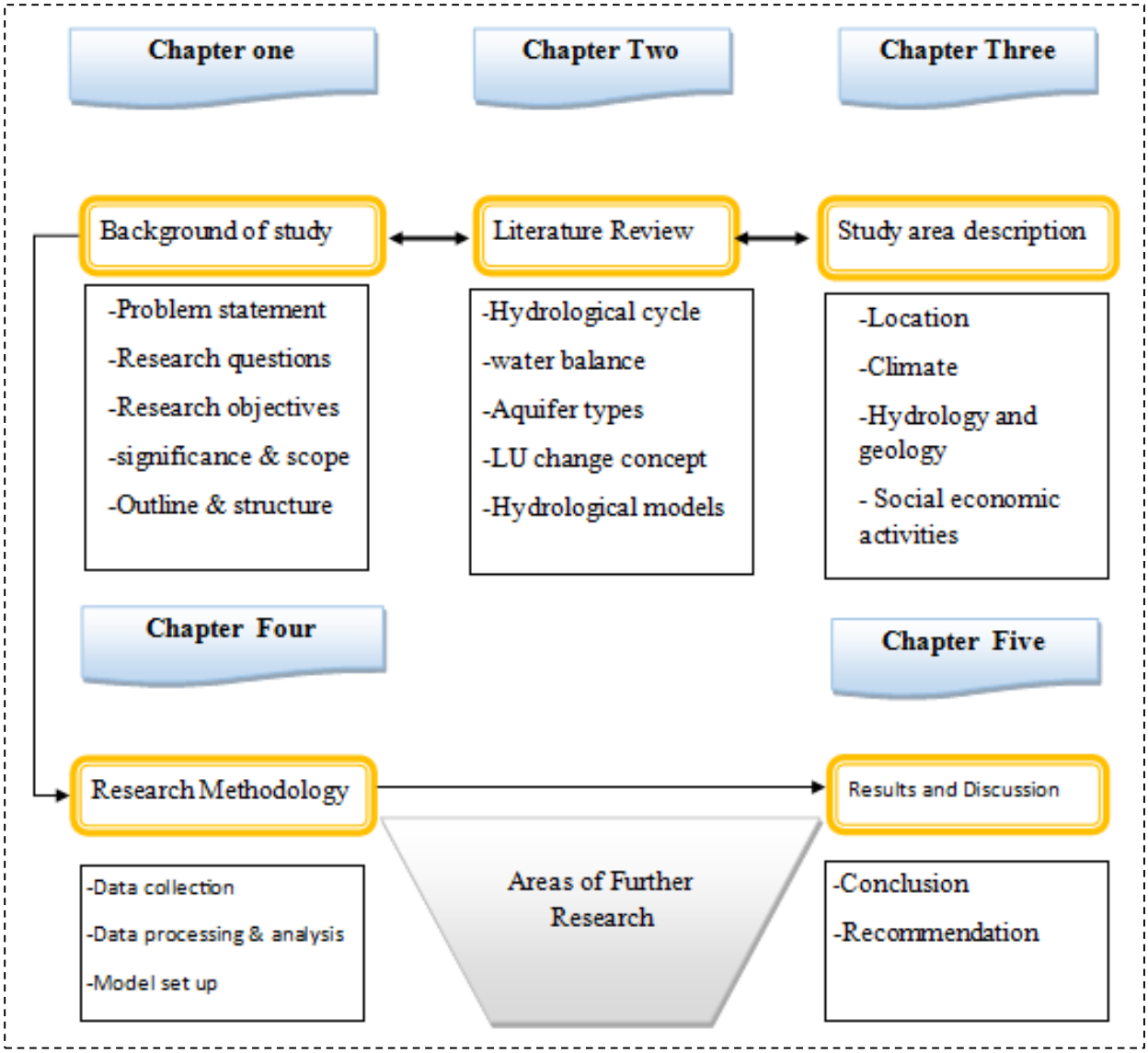

Figure 1.1: General layout of the research thesis

Chapter 2: LITERATURE REVIEW

2.1. Introduction

The interaction between land use, and hydrological events and processes is a contingent linkage. Much of what happens to surface water or ground water, has roots on land development (Stephen and Jan, 2014). In order to compensate present as well as offset future negative effects, impacts of land use changes on the hydrological system, significant yet determinable, deserve pre-emptive planning. In this section, several models for quantifying land use change impacts, and approaches toward land use change modeling are discussed. Also discussed are the concepts, including the salient features of literature about land use and water balance, and groundwater interactions on related studies, the drivers of land use transformation and their impact on the sustainability of the shallow Saiss aquifer.

2.2. Hydrology, Hydrological Cycle and Water Balance

2.2.1. Hydrology

Hydrology is the geoscience which describes and also predicts occurrence and circulation of water, including distribution of earth's water, and its atmosphere. Beneath almost the whole earth there is water present; this water is called groundwater (Sanna, 2015). The groundwater surface marks the line between the unsaturated zone and the saturated zone. The use of groundwater as freshwater supply is universal. About 30% of all of freshwater is regarded as groundwater (Rodhe, 2014).

2.2.2. Hydrological cycle

The hydrological cycle is the natural continuous movement of water from the atmosphere, on soil surface and below and then back to the atmosphere. It follows a continuous circulation of water between the atmosphere, oceans as well as vegetation and land, as schematized in (Figure 2.1).

The hydrological cycle has components, including precipitation (rainfall, dew, snowfall, sleet, hale among others), runoff (interflow, surface runoff and base flow), Interception, evaporation, depression storage, transpiration, percolation, infiltration, and for unsaturated zones, moisture storage.

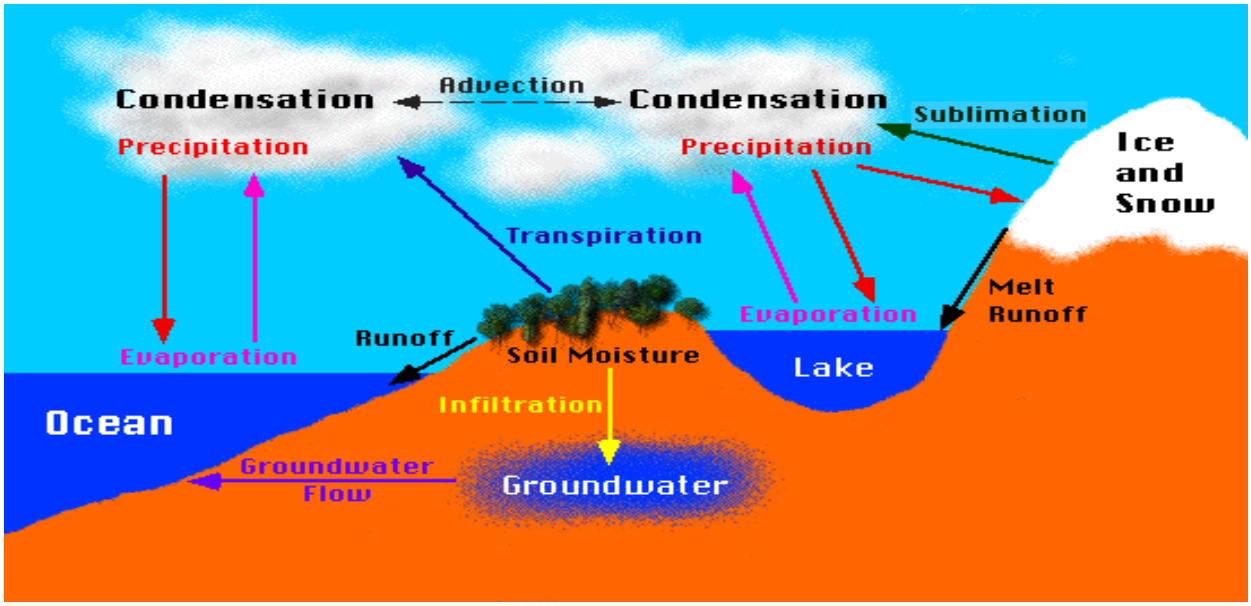

Figure 2.1: Illustration of water cycle or Hydrologic Cycle.

(https://www.slideshare.net/ariannefalsario/hydrological-cycle-water-cycle)

Overall, the water cycle constitutes a typical example of a closed system. In it, total amount of water remains the same, with practically no amount of water added to the cycle or lost. Indeed, water only moves from one storage type to another storage type. Nevertheless, whereas the hydrologic cycle constitutes a system that is closed, there exists naturally, a balance that is maintained between water exchange within the system. The potential of human activities to destabilize and cause changes in this water balance resulting in impacts that are knock on is high

2.2.3. Water balance

A water balance is described as an assessment of the key components of a hydrologic system, and involves interactions between groundwater and surface water systems. Its purpose is to describe various ways through which the supply of water is expended. Using the water balance approach, the hydrologic cycle of a definite area can be described, as well as examined for any time period. Overall, for any area of the earth's surface, the water balance is established by calculating total precipitation input against totals of various outputs (Kumar, 2012)

2.2.4. The Water balance and principle of Conservation

Water balance is described by a general hydrologic equation principally stated as the law of conservation of mass with regard to the water cycle. In simple terms, this water balance equation is expressed as:

$$Conservation: inputs(I) - Outputs\ (O) = Change\ in\ Storage\ (S)$$

$$I - O = \Delta S \quad \ldots\ldots (2.1)$$

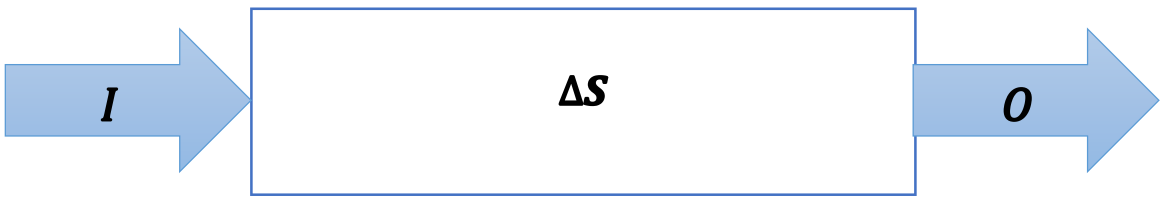

Figure 2.2: Water balance equation

Accordingly, water balance equations are easily examined for any given area and for any given time span. Thus, constructing a general water balance for a given area necessitates evaluating all inflow, outflow, and water storage components of the domain flow in accordance with how they are each bound by land surface, groundwater reservoir impermeable base that is underlying, and the imaginary vertical planes of boundaries of the area *(Kumar, 2012)*.

In studies of water balance especially, groundwater balance, the data that that may be needed over a specified period of time includes;

Rainfall data: rainfall data for every month of a sufficient range of station rain gauges found within and/or around the area of study, including their locations should be available.

Data for land use and for patterns of cropping: data for land use is required for the purpose of estimating losses of evapotranspiration from the water table through an area that is for instance if it is heavily forested.

Data for the cropping pattern is required in the estimation of spatial as well as temporal distributions of ground water with regard to withdrawals, if necessary. Rates of pan evaporation

per month should equally be available at least in some locations for the purpose of estimating consumptive requirements use for different crops.

River data: river stage data per month and data for discharge including cross-sections of the river are needed at some locations for the estimation of inter-flows of the river aquifer.

Canal data: water releases per month into the canal, including its distributaries, as well as monthly running days, are required. To also account for seepage losses that occur through canal system, test data for seepage loss is required in different reaches as well as distributaries of canals

Tank data: tank gauges per month and releases of water should also be available. Furthermore, depth against area; as well as depth against capacity, curves are required for computing evaporation as well as seepage losses in tanks. Data for field tests is necessary for computing capacity of infiltration for use in evaluating recharge resulting from depression storage.

Water table data: Monthly water table data from adequate number of observation wells that are well distributed, including their particular locations, are needed. Available data has to comprise the water table's reduced level as well as depth to the water table.

Groundwater draft: this is required in the estimation of withdrawals from underground. Thus, the number of every type of well working within the area, its corresponding hours of running per month and the discharge, are necessary and should give a comprehensive inventory of the wells lack, this may be obtained through carrying out some sample surveys.

Aquifer parameters: data about the coefficient of storage and the transmissivity are all necessary at adequate number of locations within the study area.

2.2 Aquifers

The geological formation storing groundwater enclosed in a layer of porous rocks, sand or gravel, is termed as an aquifer. The aquifer water is available for supplies as agricultural use of drinking and industry. Depending on whether the aquifer stands in direct contact with the unsaturated zone or not; it is confined or unconfined (Sanna, 2015). Specifically, an aquifer is a geologic unit that can store and transmit water at sufficient rates to supply wells (Pengfei, 2004). Aquifers are major sources of underground water for humans and their substantial exploitation threatens those wetlands that constitute groundwater-dependent ecosystems (Stigter et al., 2014).

Generally replenished by effective rainfall, rivers, and lakes (Kumar, 2012), aquifers can be of two major types: **unconfined or confined**. Water table aquifers, those with no confining layer above, are called unconfined aquifers (Figure 2.3). They are in direct contact with the atmosphere through the unsaturated zone. Whereas those with a confining layer are called confined aquifers

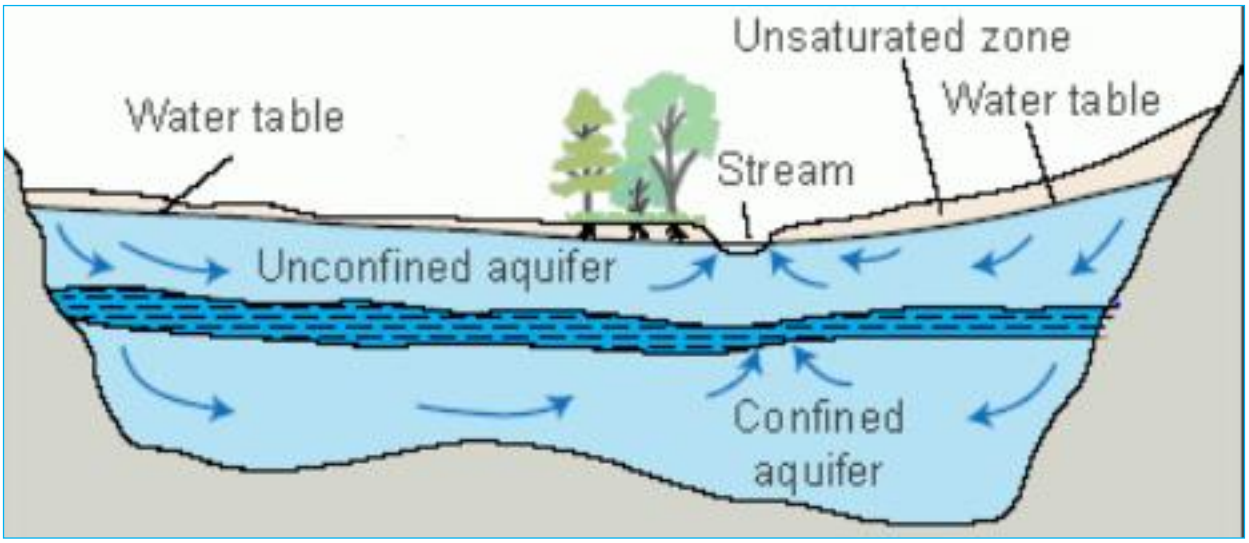

Figure 2.3: A cross-section view of an unconfined aquifer (Kumar, 2012)

The main supply of water to confined aquifers is leaking from surrounding aquifers except for more shallow ones where precipitation and draining can reach the aquifer (Drobot, 2014). The confining layer is built up by soils less permeable than the layer above - and by that a basin is formed. Water infiltrates through the porous confining layer until it reaches the next aquifer. The unconfined aquifers mainly get the water inflow from the rainfall and they are characterized by low water table depths and very common in arid and semi-arid areas. These aquifers are recharged by seasonal stream flows and can be depleted directly by evaporation.

Morocco is hydrogeologically diverse with about 126 aquifers, of which about half are shallow aquifers (less than 200 m) (Closas and Villholth, 2016). Due to a widening surface water deficit, these have increasingly become used as 'strategic sources' of water (Benaabidate and Cholli, 2011) to supplement the available surface water (Priyantha *et al.*, 2006)

In a study that completed a chronological evolution of the piezometric surface of the Saiss basin shallow aquifer by observing its fluctuation at several piezometers, the evolution evinced the continued decline of groundwater level, a decrease due to the combined effects of reduced water supplies (precipitation) which has reduced the natural recharge of groundwater, and increased abstraction of shallow aquifer waters for agricultural purposes (Benaabidate and Cholli, 2011).

2.3 The Concept of Land Use Change

Land is overall used to satisfy a multiplicity as well as a variety of human needs, including serving numerous and diverse purposes. When land users choose to use it for different purposes, land use change is what occurs, resulting into desirable as well as undesirable impacts. Analyzing land use change therefore involves analyzing relationships between land and people. Where, when, how, and why, does land use change occur? Many models exist that attempt to answer these inter-linked questions.

The first stage in studying land use change is to measure and asses the land use change that is actually involved. This is considerably affected by the level of scale at which the observation record is undertaken – spatial and temporal scale primarily but also social, economic and political (Briassoulis, 2000). However, in a related way, impacts of land use change, including degrees of severity to which they are attached, are especially influenced by scale of analysis.

Land use changes involves transformation of one land use class to another , for instance logging of forested areas for settlement or conversion arable land into forests and vice vasa (Wagner *et al*, 2013). As a result of various driving factors, economic or social just as examples, the alterations or changes from one land use type to the other, poses several impacts both on the natural resources and to people directly or indirectly. Land use change and the associated land cover change have a significant influence on soil distribution and topography, often leading to water balance components changes (Awotwi, 2009).

Land use change is a result of direct as well as indirect decisions aimed at altering current land uses at an individual level of land ownership, regional, national or even international bodies that are interested in land. Assessment and evaluation of the effects land use change on the watershed

water balance components is a resourceful tool for sustainable water resources management (Zhi *et al.*, 2015).

2.4 Impacts of Land Use Change on Water Balance Components

Changes in the use of land affect how precipitation is partitioned through the vegetation and soil into the major components of the water balance, including interception, infiltration, evapotranspiration, runoff from the surface and also groundwater recharge (Warburton *et al*, 2012).

2.5.1 Evapotranspiration (ET) and Moisture

Because evapotranspiration is actually a major input in the equation of the water balance, effects, particularly of the use of land, with regard to evapotranspiration have to be evaluated for purposes of estimating groundwater recharge with various patterns of land use (Priyantha *et al* , 2006). A basic illustration of the physiological and physical factors that govern the evapotranspiration process, taking into consideration vegetation parameters, is crop evapotranspiration. Overall, it is possible to estimate crop evapotranspiration (ET_{crop}) as the product of the crop coefficient K_c and the reference crop evapotranspiration ET_0

$$ET_{crop} = ET_0 \times K_c \quad \text{..... (2.2)}$$

There are many methods employed in empirical estimation of reference evapotranspiration (ET_O). However, depending on data requirements, the methods are categorized as Pan Evaporation, temperature based methods, combination methods and radiation.

In areas where meteorological data sources are limited, the estimation of the recharge of ground water is almost impossible. And so, upon considering the requirements for data of each method of estimation, the temperature based method is more feasible as an alternative for consumptive use operation, and for calculating reference crop evapotranspiration. The SCS Blaney Criddle method and Thornthwaite are a widely employed temperature based theoretical method. Using data that is measured on temperature only and presenting it as the main physical factor that governs processes of evapotranspiration, coupled with the annual percentages of sunshine hours per month, this method is simple enough.

Overall, SCS Blaney Criddle method gives:

$$ET_0 = K_t\left(T \times \frac{P}{100}\right) \quad \text{(2.3)}$$

$$K_t = 0.0173T - 0.314 \quad \text{(2.4)}$$

T - Mean monthly temperature(°F); ρ represents the percentage of daylight of a specified year that occurs during a given month.

Thornthwaite formula is given as follows

$$PET = 16 * \left\{\frac{10T}{I}\right\}^{a} \quad \text{(2.5)}$$

Where;

T: average monthly temperature (^{0} C)

I: annual thermal index, it is equal to the sum of the monthly thermal indices, $I = \left(\frac{T}{5}\right)^{1.514}$

a: Correction factor of each month , $a = 0.49239 + 1792 * 10^{-5} * 1 - 771 * 10^{-9} * I^2 + 675 * 10^{-9} * I^3$

It is important to note that ET is especially a complex process combining evaporation and transpiration, two sub-processes that are mostly non-linear in nature (Ghaffari *et al.,* 2010). An example is in conversion of land cover from the plant cover and to the impervious areas where transpiration can be decreased while evaporation can be increased (Pai and Saraswat, 2011).

Specifically, ET is also affected by crop density which controls rainfall interception, leaf area index, canopy resistance and plant-available water capacity, e.g., dense vegetation cover (e.g., perennial grassland) has higher crop density, leaf area index, and permeable soils compared to land for agricultural (e.g., row crops) (Kim *et al.*, 2013).

Land-use change also affects aerodynamic roughness; taller vegetation for example trees has a higher aerodynamic roughness as well as a lower aerodynamic transport resistance to, for example, grass which is a shorter vegetation. Land use and land cover (LULC) changes also influence hydrological processes (Wu *et al.*, 2013) by altering interception rates, soil water,

evapotranspiration (ET), infiltration, and groundwater, leading to changes in surface runoff, stream flow and flood frequency (Baker and Miller, 2013).

Historical land use change and climate change brought about a significant changes in the water balance components in the Bad River, Skunk Creek and Upper Big Sioux River watersheds (Manashi, 2016). In related studies, the Taleghan Catchment, Iran, the trend of water balance components in the mean annual water yield including surface runoff, lateral flow, and groundwater flow during the years were not similar (Hosseini *et al.*, 2012). Figures revealed that a trend of increase in the surface runoff occurred after degradation in land uses during the time. However, the lateral and groundwater flows declined in the same period.

Regarding the water cycle, land use plays an influential role. It does this through changes in ET, soil water holding capacity, and the vegetation's ability to intercept precipitation (Mao and Cherkauer, 2009). ET is one of the most significant components of the hydrologic budget, which is a combination of two sub-processes - evaporation and transpiration. Evaporation is water loss from open water bodies, wetlands, bare soil, snow cover, etc., while transpiration is water loss from living plant surfaces (Manashi, 2016).

Therefore, land-surface characteristics influence the process of ET. Changes in land use, land cover, crop rotation and crop types mainly influence ET in a watershed. In the Upper Mississippi River, land conversion from perennial vegetation to seasonal row crops led to a reduction in ET between 1940s-2003 (Zhang and Schilling, 2006).

Forest areas promote elevated ET because of low albedo, deep roots and water interception. However, a decrease in forest area also caused a reduction in ET (Baker and Miller, 2013). Similar results were reported in China (Liu, et al., 2008) and mid-Western US (Roy *et al.*, 2009). For aquifers, upland forested catchments are important recharge zones, because forests are often situated in areas with high annual precipitation and are associated with soils that have high infiltration capacities (Tu_Min, 2006).

As such, land use conversion from native vegetation (grassland) to agricultural or developed land would result in a decrease in ET and soil water content (Wu *et al,* 2013). Even so, in contrast to this, other studies reported that woodland and grassland conversion to agricultural land led to

increases in ET (Deng *et al.*, 2015). It is important to note that ET is a complex process combining evaporation and transpiration, two sub-processes that are mostly non-linear in nature (Ghaffari *et al.*, 2010). An example is in land cover conversion from plant cover to impervious areas where transpiration can be decreased while evaporation can be increased (Pai and Saraswat, 2011).

2.5.2 Surface runoff

The hydrologic effects of change in land-use are manifest in many ways and at different spatial and time scales (Awotwi *et al.*, 2014). The most obvious are: instant and direct effects on catchment runoff quantity as well as quality. Surface runoff can be estimated using the Soil Conservation Service Curve Number (SCS-CN) method. It is a model that was developed by the United States Department of Agriculture (USDA), and computes direct runoff using an empirical equation that takes the watershed coefficient and rainfall as inputs.

The curve number (CN) represents the watershed coefficient, and particularly represents the potential of runoff of the soil complex and land cover. This method is highly established for estimating direct runoff arising from storm rainfall, and is popular because of its simplicity and convenience. Moreover, when employed in the calculation of direct runoff, this method doesn't consider such factors as distribution of rainfall, and rainfall duration or rainfall intensity except rainfall volume. The relationship between runoff (RO) and rainfall depth (P) characterizes the SCSCN method.

$$RO = \frac{(P-0.2S)^2}{(P+0.8S)} \quad \text{(2.6)}$$

S designates potential maximum retention afterwards when runoff begins whereas P represents precipitation. Note that the retention factor is related to land use as well as soil conditions of a particular watershed through the specific curve number. This is actually determined by: -

$$S = \left(\frac{100}{CN} - 10\right) \times 25.4 \quad \text{(2.7)}$$

Where CN is the curve number while S is given in millimeters

Note that S is, for convenience, expressed in CN terms, a dimensionless water parameter which ranges between 0 and 100.

Studies have evinced that runoff coefficient changes with surface types (Mengistu, 2009). The impervious surface of urbanized catchments results in local decreases such as in infiltration, in canopy interception as well as in the water-holding ability (Zhou *et al*, 2013).

Land use changes, such as urbanization and agricultural activities cause, greater surface runoff (Pai and Saraswat, 2011). Urban areas have large paved areas in the landscape that increase impervious surfaces. Accordingly, little rainfall can soak in and enter the soil profile, which produces greater surface runoff (Jacobson, 2011). In Cedar River basin, it was predicted that surface runoff would increase as a result of urban expansion that was projected (Wu *et al.*, 2013).

Intensive agricultural activities can also reduce surface roughness (Baker and Miller, 2013) that contribute to lower interception (Ghaffari *et al.*, 2010) and less pore space availability in soil to store water leading to greater runoff generation.

Furthermore, deforestation can also cause greater runoff. In East Africa, the conversion of land from forests into agricultural land increased surface runoff (Baker and Miller, 2013). In a similar manner, decreasing grassland and increasing agricultural land decreased recharge of groundwater and base flow in the semi-arid Zanjanrood basin in Iran (Ghaffari *et al*, 2010). In Minnesota, Wisconsin, and Michigan, strong correlations between the spatial and the seasonal variations concerning the water balance, including changes in the land use type were found (Mao and Cherkauer, 2009).

2.5.3 Stream flow and flood

Groundwater flow and surface runoff are especially key components of stream flow. Groundwater flow is a result of infiltrated water while the surface runoff is contributed to from rainfall. The source of stream flow is surface runoff during excess precipitation, and ground water during dry times. Increasing land use conversion (especially for urbanization, deforestation, grassland depletion) can potentially lead to an increase in stream flow and flood frequency (Schilling, et al., 2014). Land use changes alter vegetation cover and surface roughness that affect the timing and magnitude of surface runoff and groundwater discharge, leading to changes in stream flow, and magnitude and frequency of floods (Pai and Saraswat, 2011).

During storm events, greater surface runoff can exceed the flow carrying capacity of the stream within the watershed which may increase the risk of potential flooding. In the study of hydrologic response to land use changes in the Great Lakes states, namely, Minnesota, Wisconsin, and Michigan, it was found that greater risk of flooding was caused by deforestation (Mao and Cherkauer, 2009).

In a chine, a similar study concluded that increasing forest land can reduce flood potential while depletion of forests may increase flood potential in the wet season and drought severity in the dry season (Guo *et al.*, 2008). Moreover, grassland expansion can reduce flood potential due to a decrease in stream flow. This is because Grassland has higher ET compared to agricultural land, and may encourage higher infiltration, leading to a reduction of flood potential in a watershed. In the Raccoon River watershed in Iowa, cropland conversion to grassland reduced the occurrence and frequency of flooding (Schilling, et al., 2014).

2.6 Patterns of Land Use Change in Morocco

Land-use change can have local, regional and global hydrologic consequences. Over the last 250 years, not less than half the land that is ice-free globally has directly been modified as a result of human activity, mostly by native forest conversion to agricultural land for arable farming (70%), pasture land (30%) (Meiyappan and Jain, 2012). These changes in land use can eventually be credited to the growth of population and to increasing demand for food.

In North and West Africa, considerable changes in the cover of land have taken place over the previous four to five decades largely owing to population increase, and the inherent increase in the use of land resources for agriculture and economic development, and the spreading of settlement and the (Abbas *et al.*, 2010).

Over the previous three decades, the Arab region where Morocco is found has experienced a development boom, with rapid population growth. To meet accompanying increases of food demand, the majority of countries have come to prioritize food security as well as socio-economic development by pursuing policies to expand land for agriculture and for irrigated agriculture practice. Still, many have fallen short in in considering the limited availability of water, or even the need for conserving as well as demand management (UNDP, 2013).

In Morocco, groundwater has largely become used as a 'strategic resource' to expand the growing irrigation industry, to lessen water stress and improve the resilience of farmers, instigated through improvements in the drilling techniques as well as in the convenience of newer pumps (Closas and Villholth, 2016).

The strong drivers of agricultural development, including the limitations of the previous groundwater management policy in Morocco have caused the continuous overuse of Saiss's groundwater resources. Aquifer levels are dropping and some farmers have to abandon agriculture as they cannot keep up with the increasing depth to water in their wells (Houdret, 2012). However, irrigated agriculture is still expanding and enabling the growth of lucrative citrus export businesses, while benefitting mostly economic elite (Houdret, 2012).

Sebou basin is among the main regions in the country with an agricultural vocation. It has 20% of irrigated utilized agricultural area (i.e. 357,000 ha), and 20% of the utilized agricultural area of Morocco (i.e. 1,800,000 ha) (CCAA, 2010). Land use is relatively diversified with a predominant share of grain crops (60%), the remaining being occupied by fruit plants (14.4%), legume plants (6.6%), industrial crops – sugar beet and cane (4.2%), oilseed crops (3.6%), vegetable crops (3.1%) and forage (1.7%) (OPID, 2016).

Owing to the fastest growing populations, urbanization is high, the industrial sector is booming, and because the state of Morocco does not dictate which crops farmers should, grow, farmers are increasingly opting for water intensive crops that have high capital returns. The implication of this requires an understanding of Saiss aquifer's water balance in regard to the changes in its land use that are taking place.

2.7 Hydrological Models

A Hydrological model is literally a mathematical depiction of the components of a given hydrologic cycle. Although developed for several reasons, a hydrological model is designed to particularly meet at least one of two primary objectives: to get a good understanding of hydrologic processes in a watershed and of how the watershed's changes may affect these phenomena (Asmamaw, 2013), and for hydrologic prediction (Tadele, 2007). The utilization of a flow model for groundwater specific to a complex hydrological site leads to the knowledge of a site's

hydrogeology which comes not from the data, but from the model. In modeling a catchment's hydrological response, an important issue is the detail level at which land cover properties are represented, both where land cover patterns are stable and where they are changing over time. (Emiru, 2009).

Several approaches have been tested and tried all over the world for assessing the impacts of change in land cover. Each of these can however be classified between those which bare distributed physically based and those which are semi-distributed conceptual hydrological models. Here physically-based is taken to stand for a catchment's physiographic information, and in a simplified manner, climatic factors, while conceptual stands for a catchment's hydrologic state, including processes of flow at any instant.

Spatially distributed physically based hydrological models constitute largely rational ways of modeling impacts of changes in land cover on the runoff dynamics of a river catchment. In this kind of approach, characteristics of the land surface are represented by land cover parameters and spatially organized in grid layers. Accordingly, parameters are measured to have physical meaning, or simply estimated and optimized model calibration. This class of models is very much demanding in regard to their data requirement as well as their computational effort, that may increase further with increases in the catchment's size (Emiru, 2009).

Conversely, semi-distributed conceptual models are capable of capturing the dominating hydrological processes at appropriate scales, and with accompanying formulations. Widely compared with others, conceptual models are indeed often taken as a compromise that is in-between the requirement for simplicity and that for firm physical basis, despite the limitation in regard to the derivation of their model parameters directly from field measurement, and which make calibration a must.

Overall, the application of models to studies of hydrology is now indispensable as a tool employed to examine and understand the natural processes that occur at any given watershed scale. Numerous computer-based models for hydrologic studies exist and are available for hydrologic modeling. They are largely utilized for analyzing stream flow, for flood forecasting and groundwater development, including protection, surface and groundwater conjunctive use management, the distribution system of water, climate as well as study of the impacts of land use

change, ecology and a wide range of activities related to the management of water (Ber and Ashish , 2013). Owing to high levels of availability, the vast ranging features as well as potential applications of models, it is today difficult for users to make a choice of a specific model that is both most convenient and also most suited to a given problem. For the purpose of spatial simulation of recharge, various models exist, including among others, SWAT, MODFLOW, WaSim, DREAM, AnnAGNPS, GSSHA, HYPE, Hec-HMS, MIKE-SHE, PRMS, WetSpa, WinSRM and WetSpass.

2.7.1 HYPE

HYPE stands for: Hydrological Predictions for the Environment (Lindstrom *et al.*, 2010). It is a hydrological model used for assessing water resources in small-scale and also in large-scale. Overall, it is a process-based and semi-distributed, as well as conceptual model used to simulate several multi-basin regions, including wide variations in soil types, geomorphology, topography and land uses. HYPE notably integrates elements of landscape as well as hydrological compartments that are along flow paths filled with turnover of nutrients and transport. Calculations for this model are accomplished on a time step that is daily, and in sub-basins that are coupled. Parameters of the model are associated with soil type, land use, else for the whole catchment, be common. Thus, owing to parameter values coupling to physiography, the HYPE model is most suited for simulating in catchments that are ungauged (Strömqvis *et al.*, 2012). Summarily, the HYPE model uses just a maximum of ten data files of input, independent of resolution and size of the domain (Lindstrom *et al.*, 2010).

2.7.2 PRMS

PRMS stands for Precipitation Runoff Modeling System, a modular designed, and physically-based, and distributed- parameter model for watersheds developed for the purpose of evaluating effects of several precipitations, and climate combinations, including land use on the stream flow, yields from sediment, and basin hydrology in general (Markstrom *et al.* , 2008). The PRMS model simulates snowpack formation of snowpack and melt. It is also suited for the simulation of stream flow, including hydrologic components of it, from basins dominated by snowmelt. PRMS is able to function as a lumped but also as a model that is of a distributed parameter type.

2.7.3 Hec-HMS

Hec-HMS refers to Hydrologic Modeling System. It is a model designed for continuous modeling as well as hydrologic modeling that is event-based. The Hec-HMS model enables many different options for users to model several components of the hydrologic cycle. Initially developed for the purpose of simulating processes of precipitation-runoff of systems of dendritic watersheds, it was later modified for solving wide possible ranges of different problems across water supply of large river basins, flood hydrographs, as well as small urban or natural watershed runoff (USACE-HEC, 2010). Four major components constitute the Hec-HMS model in regard to modeling watershed, namely, Meteorological model, Basin model, Control specification, and lastly Input data.

2.7.4 SWAT

SWAT refers to Soil and Water Assessment Tool. It is a physically-based continuous-time, conceptual, long-term, distributed watershed scale hydrologic model that is constructed for the purpose of predicting impacts of land management on sediment, hydrology, and the contaminant transport found in large and complex catchments. It can simulate surface runoff, and percolation, erosion and return flow, pesticide fate irrigation, transport and groundwater flow among others and can be applied to large ungauged watersheds in rural areas with above 100 watershed numbers (Kusre *et al.,* 2010).

2.7.5 MIKE-SHE

MIKE SHE (DHI, 2007) Model is a comprehensive deterministic, distributed, and physically based modeling system capable of simulating all major processes in the land phase of the hydrologic cycle. This model covers a full set of pre- and post-processing tools, including a flexible mix of simple and advanced solution techniques used for each hydrologic process. MIKE SHE model includes the interception, precipitation, infiltration, evapotranspiration, saturated and unsaturated zones' sub flows, surface flow, as well as flow in ditches or channels

2.7.6 Water balance model (WetSpass Model)

WetSpass stands for: ***W***ater and ***E***nergy ***T***ransfer between ***S***oil, ***P***lants and the ***A***tmosphere under a quasi-***S***teady ***S***tate. It is a model based on physical parameters used for estimating long-term mean groundwater recharge spatial patterns of evapotranspiration and surface runoff,

accomplished by employing physical and empirical relationships (Batelaan and De Smedt, 2007). WetSpass is mostly suitable for studying effects that are long term, and of changes in land use on water regimes of watersheds. It enables and eases an exact definition of different land use types.

WetSpass, integrated in GIS ArcView as a raster model, is often coded in avenue. Its inputs include grids of land use, precipitation, groundwater depth, temperature, potential evapotranspiration, slope wind-speed and soil. Parameters such as soil types and land-use are related to the model as attribute tables, each referred to respective specific grids (Woldeamlak and Batelaan, 2007). Computing the Water balance is accomplished at the level of a raster cell, given the model is a type that is distributed.

As indicated in the (figure 2.4), individual raster water balance is accordingly obtained by adding up independent water balance for bare soil area, vegetated area, impervious area and open-water bodies, captured in equations below. Overall, total water balance of any given areas is calculated as the summation of the water balance of respective raster cells.

$$ET_{raster} = a_v ET_v + a_s E_s + a_o E_o + a_i E_i \quad \text{(2.8)}$$

$$S_{raster} = a_v S_v + a_s S_s + a_o S_o + a_i S_i \quad \text{(2.9)}$$

$$R_{raster} = a_v R_v + a_s R_s + a_o R_o + a_i R_i \quad \text{(2.10)}$$

ET_{raster}, S_{raster}, and R_{raster} denote the total evapotranspiration, surface runoff, groundwater recharge of a respective raster cell, each characterized by vegetated area, bare soil, and open water, and impervious area components respectively designated as a_v, a_s, a_o and a_i.

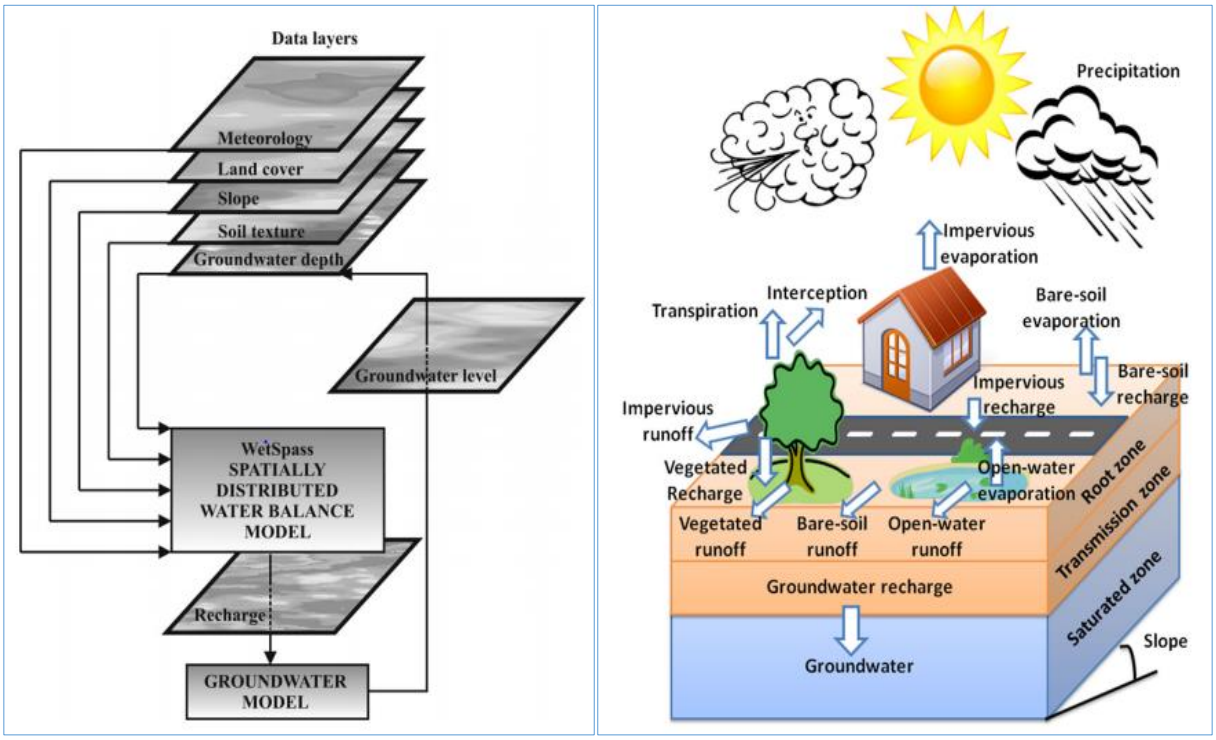

Figure 2.4: Representation of water balance of a hypothetical cell (K.Abdollahi, 2012).

2.8 Geographic Information Systems (GIS) and Remote Sensing

A Geographical Information System is that system which is used for capturing and storing, analyzing as well as managing data, including associated attributes which are spatially referenced to earth (Renny, 2012). GIS as too that is computer-based and that displays, and stores, analyzes, and retrieves, as well as generates spatial attributes and non-spatial attributes, and provides suitable alternatives for efficiently managing large and complex databases.

It is applicable in hydrologic modeling for the purpose of facilitating processing, management and the interpretation of the hydrological data. Remote Sensing refers to the science of obtaining the information regarding an object, an area, or a phenomenon by analyzing data that is acquired through the use of a device which is not in any way, in contact with the object, the area, and/or the phenomenon that is under investigation (Bawahidi, 2005).

Remote sensing data and Geographic Information System are proving to be key tools for analyzing land use and hydrology. This is especially so since several data needed for hydrological and land-use analysis is easily got from remotely sensed images (Renny, 2012). Indeed, remote sensing has

a capability of acquiring signatures instantaneously over large areas. Spectral signatures allow for the extraction of information pertaining to the use of land, and to land cover, emissivity, surface temperature and energy flux (Gumindoga, 2010).

Where urban expansion processes are taking place, using vegetation indices in studies of changes of land-use has previously been conducted. By use of image techniques, land use and changes in land cover can be analyzed using Landsat Multi Scanner (MSS) data and Landsat Thematic Mapper (TM) (Gumindoga, 2010). These are however limited to using spectral indices, i.e., the Leaf area index (LAI) and the Soil Adjusted Vegetation Index (SAVI) to detect areas where vegetation covers decrease. The combination of land-use and with land cover from Landsat images and statistical census on land-use data have however proved more successful than only using vegetation indices in studies (Renny, 2012).

In this study, statistical, non-parametric and trend analysis methods will be employed to detect trends relationships between land-use and discharge and therefore water balances. Many studies have piloted direct measurements of ET, and scaled their values to catchment level transpiration (Ford *et al.*, 2007), however, remote sensing likely provides more appropriate spatial data as well as parameters at given appropriate scale to be used in distributed hydrological models (Stisen, Jensen *et al.*, 2008) and groundwater models (Li *et al*., 2009).

Remote sensing and GIS have, among others, been employed for investigating springs (Sener *et al.*, 2005), determining the groundwater dependent ecosystems (Münch and Conrad, 2007), determining the recharge potential zones (Shaban *et al.*, 2006), as well as for mapping the recharge of groundwater and the discharge areas (Tweed *et al.*, 2007). Its tools enable organizing a considerable groundwater quantity, including surface water information, plus advancing analysis through their capability in mapping and managing data (Sayena, 2012).

2.9 ArcGIS

ArcGIS refers to a system for manipulating maps and also geographic information. It is suitable and used for the following; Creating as well as using maps, managing any geographic information and in a database, analyzing mapped information, Sharing, discovering, and using given geographic information everywhere behind firewalls within an organization, with selected groups,

public using ArcGIS Online, compiling geographic data and Using maps as well as geographic information through a range of web and mobile applications, custom desktops, and embedded hardware. The system enables and gives an infrastructure useful in making maps. It also makes geographic information to available throughout the organization, and across community, including openly on the web (ESRI, 2012)

Chapter 3: STUDY AREA DESCRIPTION

3.1 Location and limits

The shallow aquifer Saiss Basin (Figure 3.1), is located in the center of Sebou watershed, and between the cities of Meknes and Fez respectively at 33°53 N-34°04 N latitude and 5°30 W-4°57 W longitude at an altitude about 400 m and with a surface area of 2200 km^2. The Sais aquifer plain, also knowns as Fez-Meknes plain, is 95 km in length and 30 km in width, it is delimited by, the prerif and pre-rifal wrinkles of Zalagh and Tghat in the North, River Sebou in the East, River Beht towards the West and the middle Atlasic causes in the South.

Fez-Meknes forms a complex depression, under which the topographic elevation of Aïn Taoujdate divides the two parts (eastern and western) of the plain with a general orientation in WNW-ESE facing NE, where the plain of Fez extends as the lower part of Saiss(Benaabidate and Cholli, 2011).

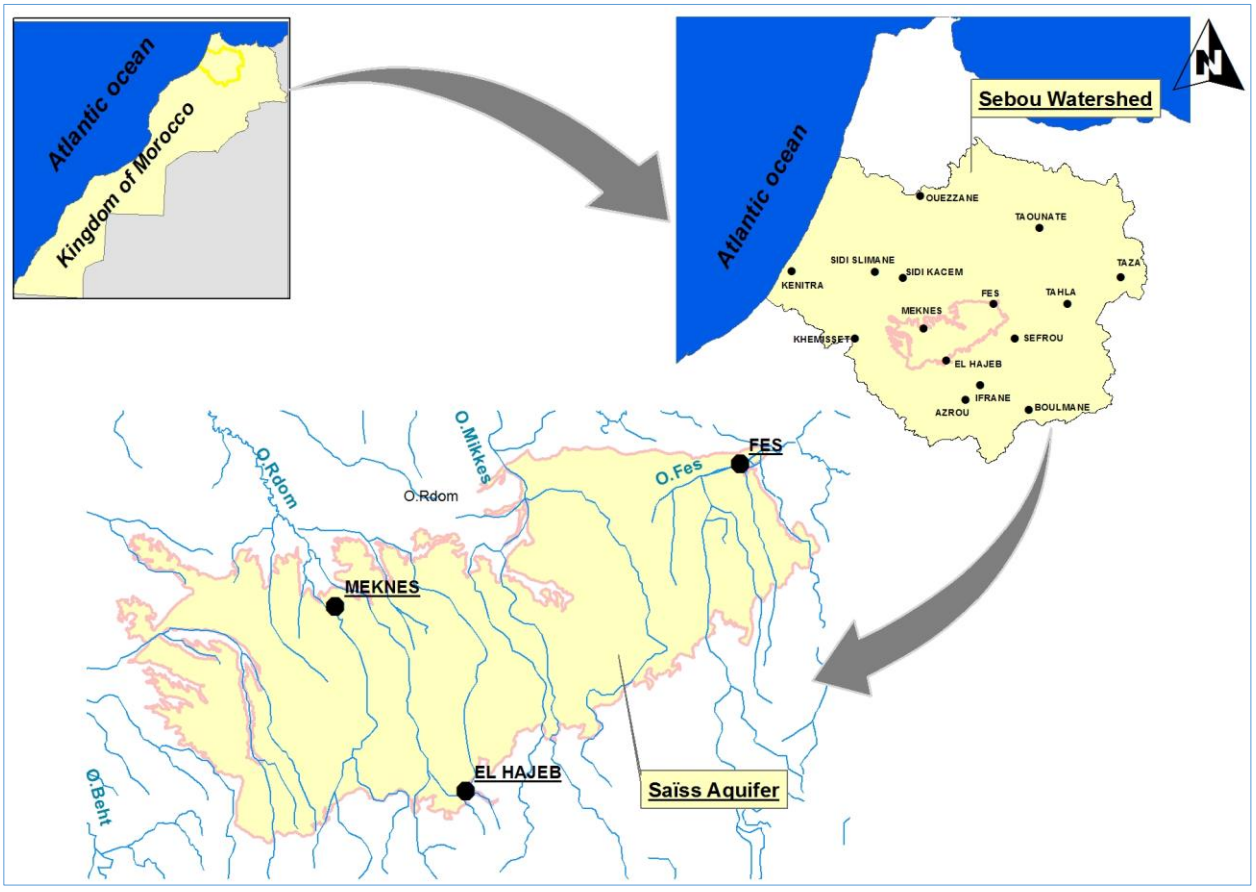

Figure 3.1: Location of Saiss shallow aquifer basin

3.2 Human geography and socio-economic context

The human geography of the basin is marked by the two major cities Fez and Meknes. These two cities alone are home to the total population of the basin, which amounts to about 1.9 million people as indicated by the population census of 2014. Agriculture and handicrafts play an important part in the economic activity of the region. The main crops are viticulture, arboriculture, cereals and legumes. Artisanal activity revolves around the textile industry, tanneries, agri-food and building materials. The rural population is poorly distributed in the basin because of land use patterns. The density of the population is higher in the viticultural areas than in the cereal-growing areas. The agricultural activities are supported by the irrigation technologies given the erratic nature of the precipitation in the Saiss plain. Irrigation represents the engine of economic development in the Saiss plain. Despite the succession of years of drought, Morocco succeeded modernization and Conversion of irrigation systems (drip into arboriculture) of agriculture irrigated. This has led to a notable evolution in the production and policy adopted by the State for water economics with almost 93% of irrigated areas are pumped from the groundwater. The distribution of the main irrigated perimeters in the plain are shown in the following map.

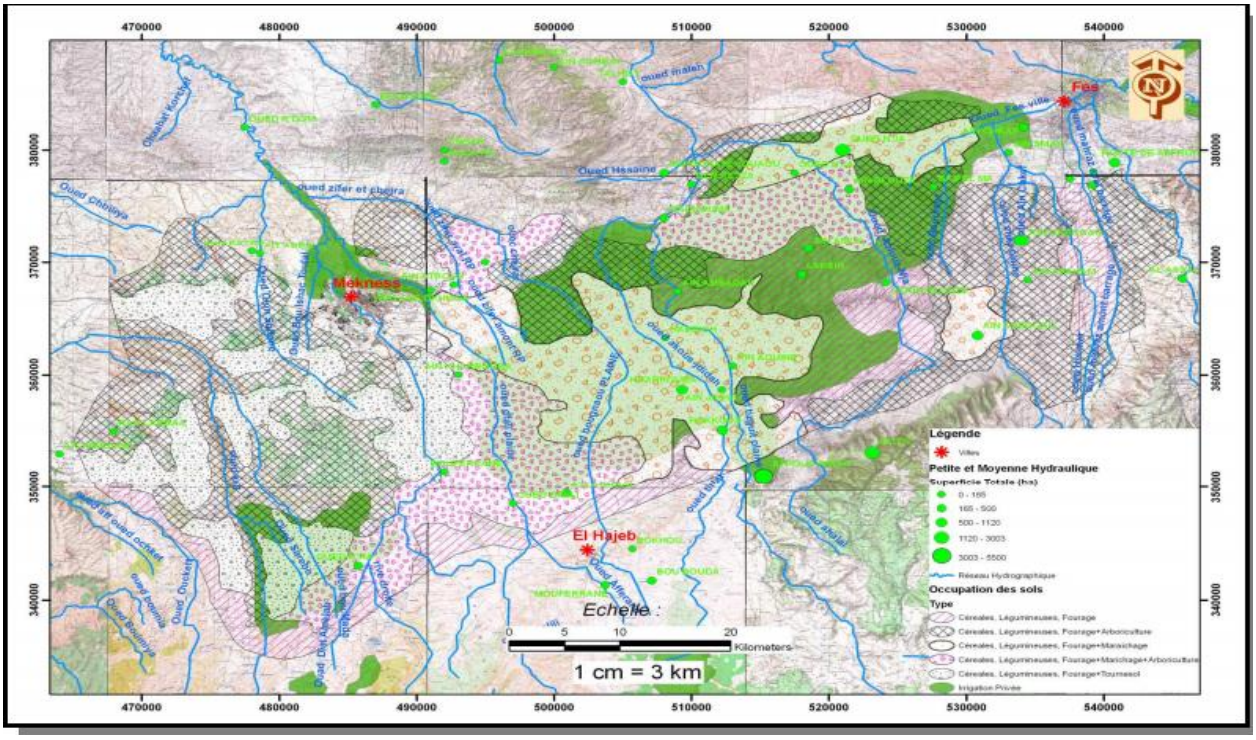

Figure 3.2: Irrigated perimeters within Saiss plain(Chamayou, 2014)

3.3 Administrative framework

Administratively, the plane of the Saiss belongs to the territory shared between 2 Province (Fez and Meknes) and includes some of the provinces listed below according to the following table

Table 3.1: Administrative division of the Saiss plain (ABHS)

Regions	Provinces	Communities
Fez- Boulemane	Fez	13
	Sefrou	3
	Moulay Yacoub	1
Meknes-Tafilelt	Meknes	16
	El Hajeb	14
	Ifrane	1
Rabat-Sale-Zemmour-Zaer	Khemisset	1

Communities belonging to the territory of the Saiss, totally or partially, are listed in the (table 3.2)

Table 3.2: Percentage of the integrated surface in the Saiss plain.

Province	Community (Rural /Urban)	% surface
FEZ	Agdal	100
	Ain Bida	80
	Ain Bou Ali	9
	Ain Chkef	100
	Zouagha	100
	Ain Kansra	2
	Oulad Tayeb	100
	Sidi Harazem	80
EL HAJEB	Agourai	100
	Ait Bourzouine	100
	Ait Harz Allah	55
	Ait Naamane	13
	Ait Ouikhalfen	6
	Ait Yaazem	100
	Bittit	100
	El Hajeb	60
	Iqaddar	40
	Jahjouh	50

	Laqsir	100
	Ras Ijerri	20
	Tamchachate	1
KHEMISSET	Sfassif	4
	Ain Orma	60
	Ain Taoujdate	100
	Ait Ouallal	100
	Al Machouar- Stina	100
MEKNES	Boufakrane	100
	Dar Oum Soltane	50
	Dkhissa	34
	Majjate	100
	Meknes	100
	M'haya	30
	Mrhassiyine	1
	Oued Jdida	70
	Ouislane	96
	Sabaa Aiyoun	100
	Sidi Slimane Moul Al Kifane	100
	Toulal	100
MOULAY YACOUB	Sebaa Rouadi	40
SEFROU	Aghbalou Aqorar	7
	Ain Cheggag	52
	Kandar Sidi Khiar	8
IFRANE	Tizgite	6

The great proportion of the communities is situated on the edge of the plain, municipalities that are located entirely on the plain account for 50% of the area. The distribution of municipalities according to their positions and the provinces of the plain is shown in the (Figure 3.3) Administratively, the Saiss plain straddles the zones of action of the 6 provinces and these include, Meknes, Fez, Ifrane, El Hajeb, Sefrou and Khemisset.

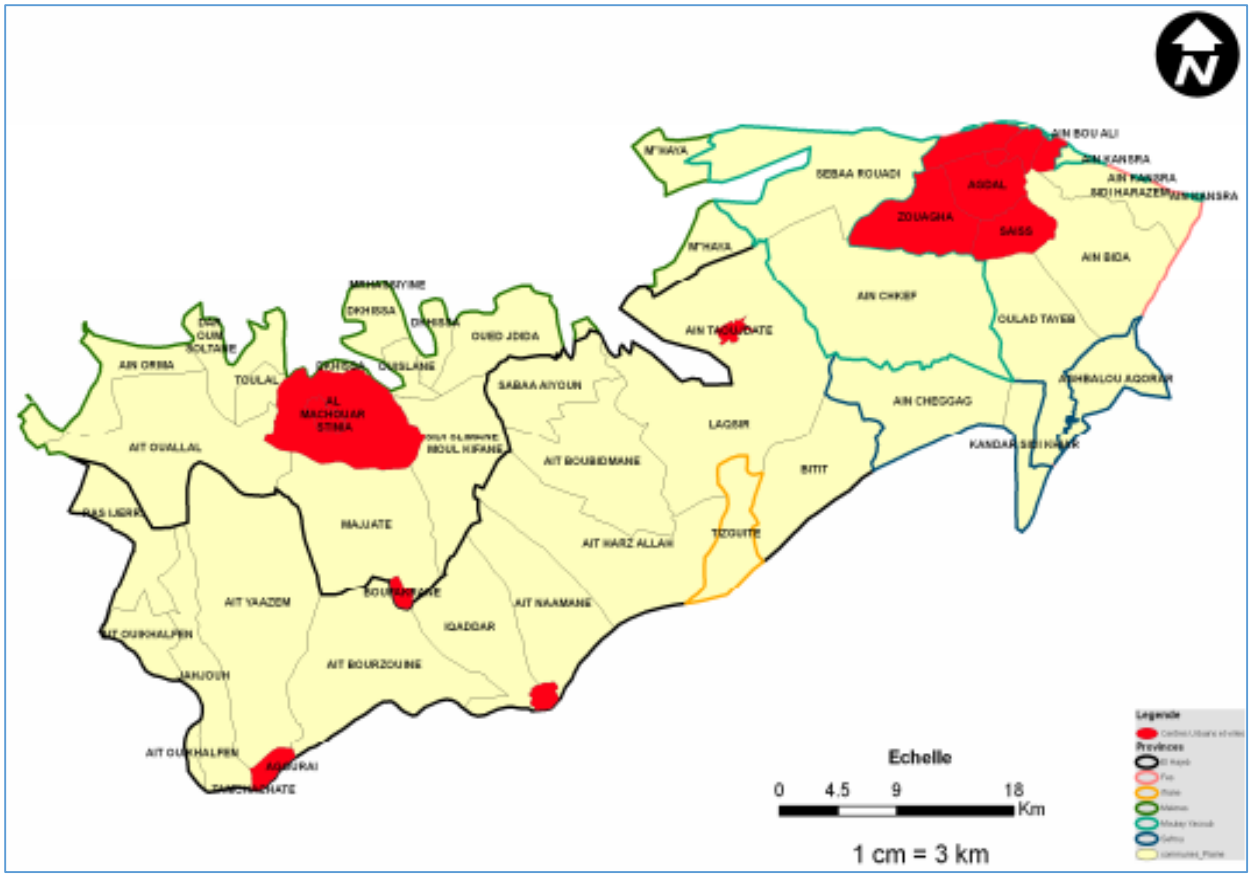

Figure 3.3: Location of municipalities basing on positions and the provinces of the plain

3.4 Hydro-climatological context

Fez-Meknes basin lies in the semi- arid Mediterranean zone with oceanic effect, characterized with temperate winters and with mean annual precipitations varying from 400 to 550 mm and annual air temperature varying between 10˚C for minimum temperatures and 20˚C for maximum temperatures.

The basin of Fez-Meknes has a poorly developed hydrological network that is essentially limited to four major rivers. From West to East, is the El Kell river which is a tributary of the river Beht, the river R'dom which is a confluence of the river Boufekrane and the river Ouislane, the river Mikkes and river Fez

All these rivers, with the exception of river Fez, are from the middle Atlantic atoms where they lose a good part of their flows in karstified limestones. Their rates are replenished within the basin through water emissions more or less diffuse that constitute emergencies and deep groundwater

aquifers. This type of feeding by localized emergences is the origin of several minor rivers that originate inside the basin. The direction of their flow is generally SSE-NNW, with the exception of River N'ja and river Fez which flow respectively from east to west and from west to east.

The total area of the five main watersheds is approximately 3800 km^2, of which 2200 km^2 is the area drained over the Meknes-Fes basin, the rest corresponding to the watersheds dominating the plateau of the Middle Atlas.

3.5 Geology and Lithology

The Saiss plain is a Neogene basin that forms part of the South Rifain. This groove represents the front country of the Rif Cordillera, and is considered as an intra-chain basin since it is framed by the Rifain chain in the North and the Meseto-Atlasic chain at South. The plain comprises mainly of the sands, sandstones, conglomerates and Sahelian Pliocene lacustrine, lime stones and locally in the travertine(Cirac, 2008). Cuts derived from lithological columns stratigraphic drilling Plateau Meknes indicates that the Plio-Quaternary deposits show a wide variation faces of a well to another (figure 3.4).

The plain of Fes - Meknes forms two topographically distinct sets, separated by a geological accident of orientation EW called Ain Taoujdate flexure. The plateau of Meknes in the west and the plain of the Saiss in the east can be seen. The plateau of Meknes raised in relation to the plain of Saiss, presents altitudes of the order of 1000 m in its southern part. These altitudes decrease with an average gradient of 12% to 500 m in the northern part where the shelf suddenly straightened in contact prerifaines wrinkles (Cirac, 2008).

Like the plateau of Meknes, the Saiss plain (collapsed compartment), has higher altitudes in the south (700 m) from the middle atlas with steeper descending slopes which gradually fades to bring the plain to an altitude of the order of 400 m before it straightens up fairly steeply in contact with the pre-Faerian wrinkles.

Apart from Aïn Taoujdate flexure, which clearly separates the Fes-Meknes basin in two different levels, other accidents have also affected the basin. Accidents in the basin fall into two different origins. Those resulting from the Atlasic tectonics that extend into the plain and which constitutes the ante-neogenous substratum, show an NE-SW direction and those coming from the Rifaines tectonics show a cross-direction to the first NW-SE.

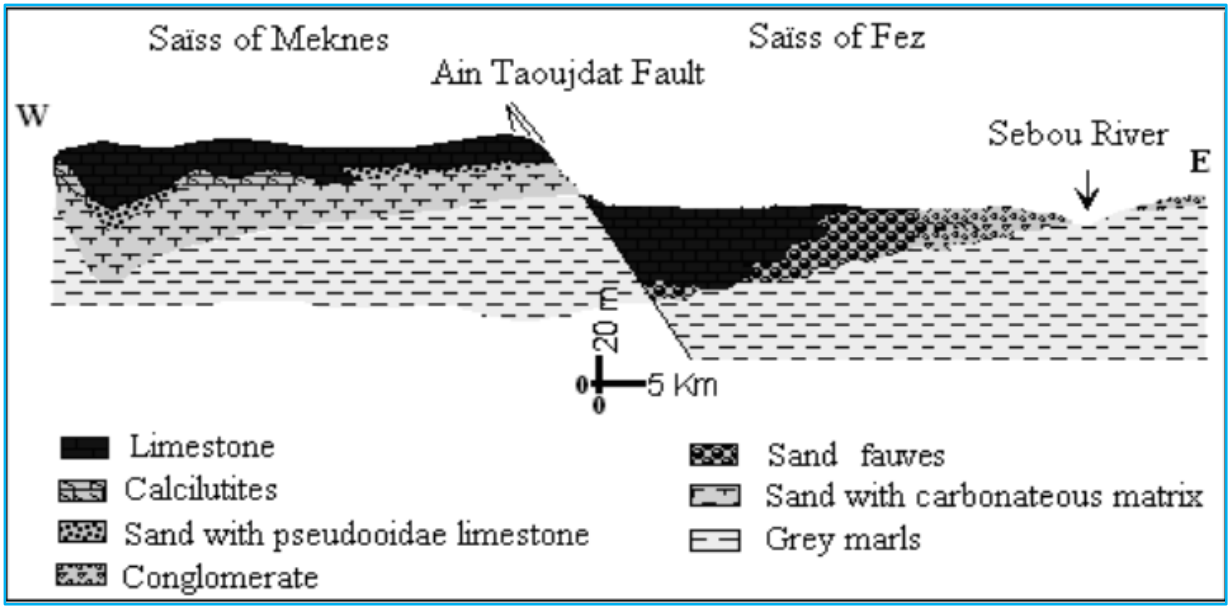

Figure 3.4: Lithology of Saiss basin (Cirac, 2008)

3.6 Hydro-Geological Context

In the Fez - Meknes basin, there are two major aquifers two main aquifers; 1) deep aquifer sheltering the Lias formations. This aquifer is free along the way Atlas Causse and north captive under the powerful marl Miocene that trap water and 2) phreatic aquifer (Saiss shallow) which sits in the pliovillafranchian formations and which extend over an area of 2200 km².

Due to its size and good productivity, this reservoir plays a decisive role in regional economic development, particularly in the development of the hydro-agricultural sector. These two layers communicate in places through the geological accidents that affect the ante-neogenous substratum.

3.7 Water Points and Sources

The Saiss plain comprises majorly of four categories of water points across its geological formations. They include wells, bore-holes, well-bores and piezometers (figure 3.5).

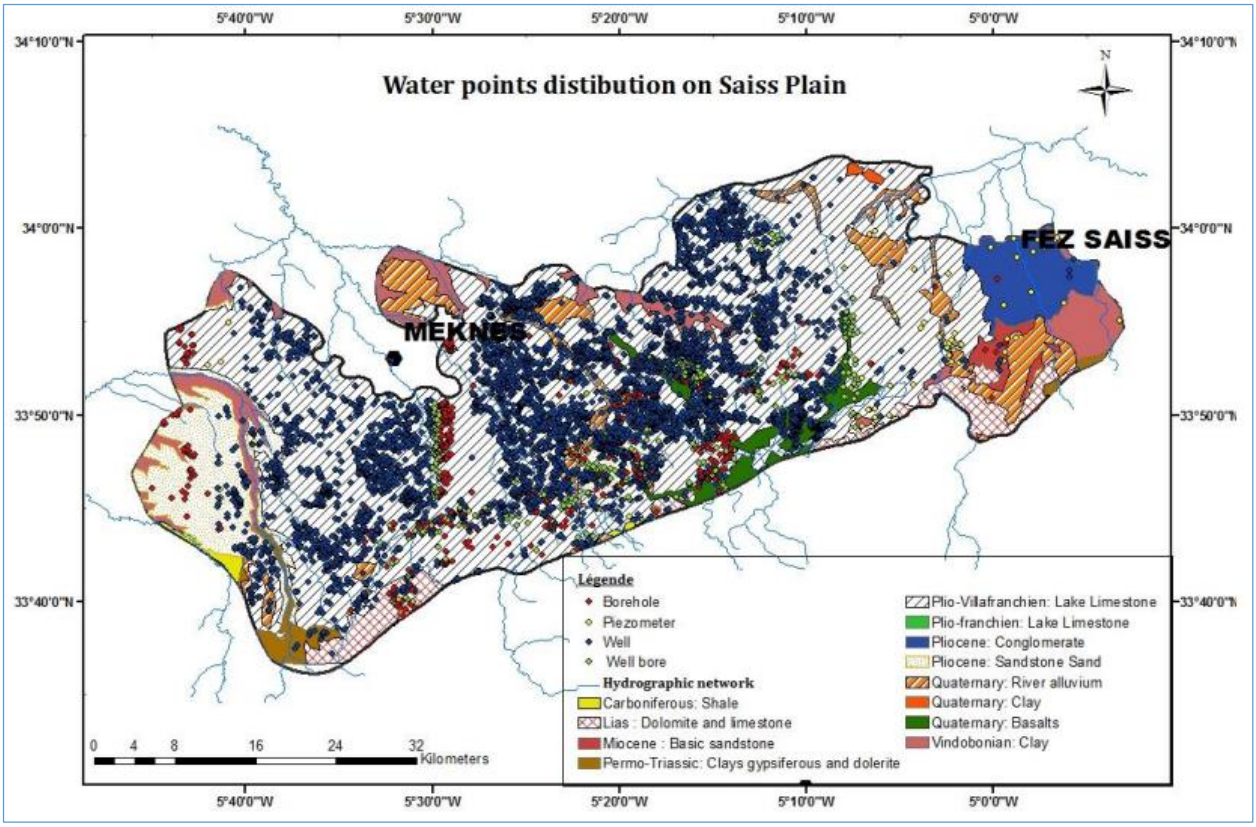

Figure 3.5: Water points across Saiss, adopted from (Laraichi et al, 2016):STDW

3.8 Water Table Formation

The water table in the Fes-Meknes basin is subdivided into two important units by Aïn Taoujdate's flexure. In the west there is a more elevated unit called Plateau of Meknes, and to the east, below, the unit called the Saiss plain. The pliovillafranchian formations which shelter the water table do not present the same faces everywhere. In general, three types of faces constituting the aquifer;

1) **Wild Sands**, they were deposited on the Miocene gray marls in a structural depression between Meknes and Ain Taoujdate. They seem never to have covered the Sais of Fez east of Ain Taoujdate (in the process of emersion) and their extension would not have passed the slope of Ain Taoujdate. The greater thickness in the sector of Meknes and in the west (more than 45 m) decreases gradually towards the East

2) **Conglomerates,** they present themselves as a synchronous alluvial and deltaic spreading of the fawn sands and appear above the Miocene gray marls and the calcareous lake slab. They consist of Jurassic limestone pebbles, sandstones and quartzites in a travertine cement. The

conglomerates follow the tawny sands east of the slope of Ain Taoujdate. They extend only in the Saiss of Fez and to the East of it.

3) **Lacustrine limestones**, they overcome the wild sands and conglomerates and present themselves in two levels, lower beige limestones (lower Saiss) and upper gray limestones (upper Saiss), separated by a horizon of black clays of small thickness.

However, the water table circulates locally in cracked basalts of the Quaternary and in massifs of travertines. The substratum consists mainly of the blue marls of the Tortonian. In the Plateau of Meknes, the sheet rests in places on primary schists. The water supply to the groundwater aquifer is mainly through the infiltration of rainwater and the supply of water from the deep aquifer. A third component, however, is the return of irrigation water.

3.8.1 Plateau of Meknes

In the Plateau of Meknes, the water table circulates mainly in the sand, sandstone and conglomerates of Sahelian. To the west of the Plateau, the aquifer consists of a sandy clay complex up to 70 m thick, resting on the blue marls of the Tortonian. Further south, the substratum of this complex consists of primary schists.

3.8.2 Plain of Saiss

The Saiss plain also has variable faces of aquifer levels. To the west of the plain of Saiss, there are powerful Pliocene lacustrine limestones that shelter the aquifer. To the east these lacustrine limestones pass laterally to conglomerates which become the only aquifer level. In the bowl of Douyet, north of the plain of Saiss, the groundwater aquifer flows in a fairly powerful series of lacustrine limestone resting on calcareous-dolomitic micro-conglomerates. In this region, in times of high recharge the water table is flush in the form of poorly drained ponds. Piezometrically the dominant flow is generally from south to north with the individualization of both flow directions.

Chapter 4: METHODOLOGY, DATA COLLECTION AND PROCESSING

3.1 Introduction

This chapter describes the methodology adopted to evaluate the impact of changes in land use, on the water balance components of the Saiss aquifer in Sebou basin, the nature of model input data, their sources and processing approaches. The overall methodology involves simulation under two land use conditions of 1987 and 2016, using the Geographical Information System (GIS) and a spatially distributed water balance model (WetSpass).

3.2 Methods and Materials

In order the answer the research questions specified in the objective of this research, careful and step by step approach was employed to collect necessary data input and best choice of method of processing the data sets. The figure (4.1) shows the research

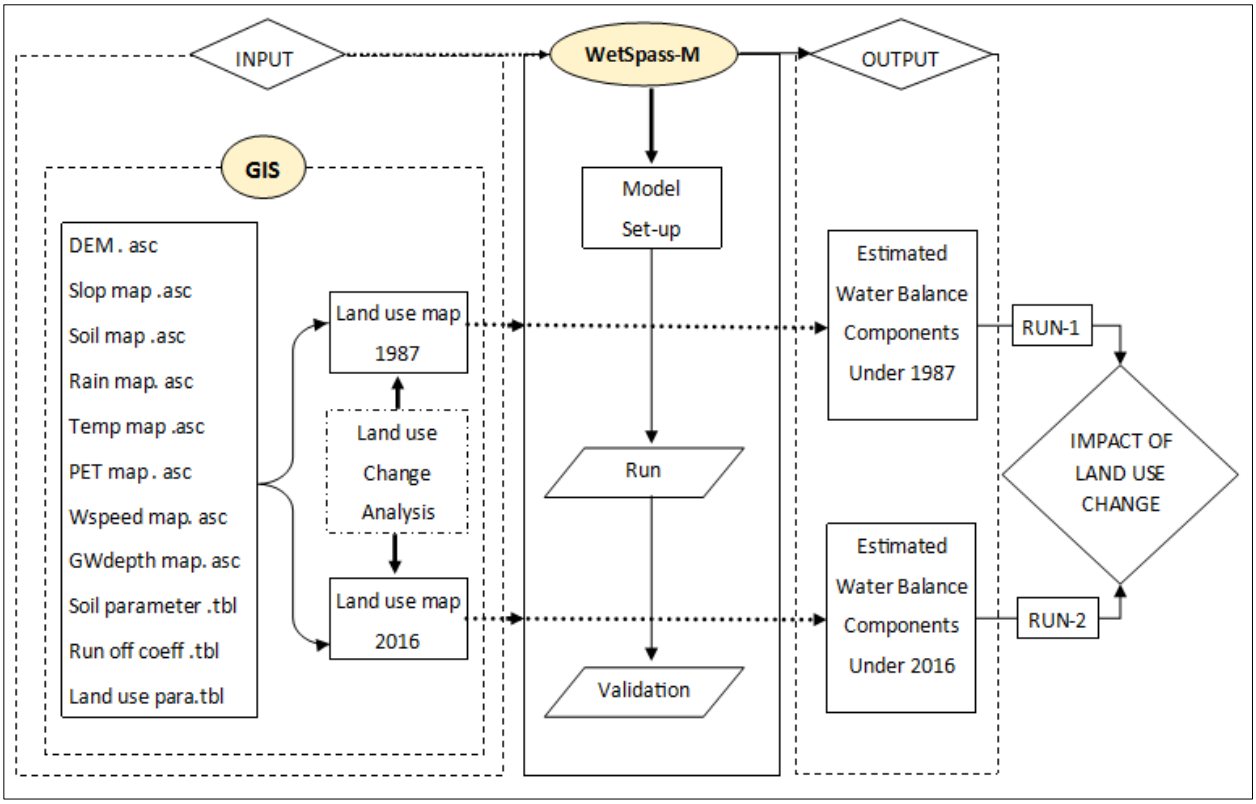

Figure 4.1: General research methodology

3.3 The Water Balance Model (WetSpass)

A Water and Energy Transfer between Soil, Plants and Atmosphere (WetSpass), under quasi-Steady State is a physically based model for the assessment of long-term average spatial patterns of surface runoff, evapotranspiration and groundwater recharge, using empirical and physical relationships(Batelaan and De Smedt, 2007).

The python- WetSpass model was selected for this research since it is highly suited for studying long term impacts of land-use changes on the water regime in a catchment and is a raster-based water balance model in which for each grid cell rain-fall is split into evapotranspiration, interception, surface runoff and groundwater recharge.

The model operates on input data of precipitation, temperature, wind speed, number of rain days, potential evapotranspiration referred to as climatic data, distributed land use, soil texture, slope and groundwater depth all as the basic model required input data.

For the heterogeneity within each member cell according to the different land use categories, four cell fractions namely impervious surface, vegetated cover, open water and bare soil are defined per grid cell(Armanuos et al., 2016 ; Batelaan and De Smedt, 2007).

The water components of each sub-cell fraction are used to estimate total water balance of a raster cell and in all time sets groundwater recharge is deduced as the residual component of the water balance of each sub- cell.

The (figure 4.2) gives a generalized summary of the four major hydrological processes of, interception, surface runoff, evapotranspiration and groundwater recharge that occur within the model.

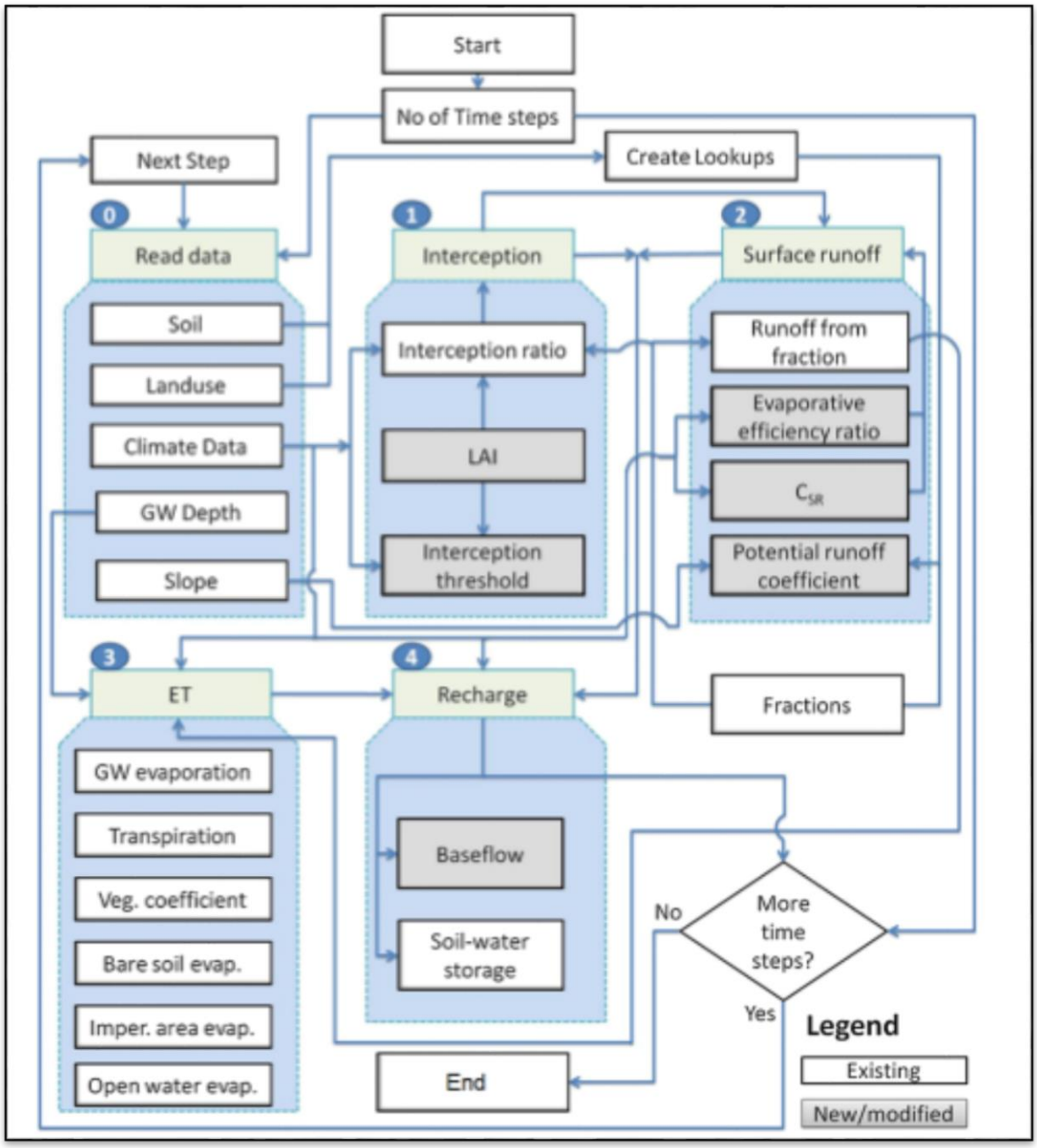

Figure 4.2: The general flow chart of WetSpass model.(adopted from Armanuos et al., 2016).

3.3.1 The WetSpass water Balance Components

Water balance computation is accomplished at a raster cell level, since the model is of a distributed type. Individual raster water balance is accordingly obtained by adding up independent water balance for bare soil area, vegetated area, impervious area and open-water bodies (Woldeamlak and Batelaan, 2007), as captured in equations 4.1- 4.3. Overall, total water balance of any given areas is calculated as the summation of the water balance of respective raster cells.

3.3.2 Calculation of Water Balance per Raster Cell

Bare soil area, vegetated area, impervious area and open-water bodies are water balance components used to calculate the water balance of a raster cell.

$$ET_r = a_v ET_v + a_s E_s + a_o E_o + a_i E_i \quad \text{(4.1)}$$

$$S_r = a_v S_v + a_s S_s + a_o S_o + a_i S_i \quad \text{(4.2)}$$

$$R_r = a_v R_v + a_s R_s + a_o R_o + a_i R_i \quad \text{(4.3)}$$

ET_r, S_r, and R_r denote the total evapotranspiration, surface runoff and groundwater recharge of respective raster cell, each characterized by vegetated area, bare soil, open water, and impervious area components respectively designated as a_v, a_s, a_o and a_i. Discussions of the computation of each of these components of the water balance are as follow.

The starting point for computation of the water balance of each of the components of a raster cell is a precipitation event, followed by runoff, interception, Evapotranspiration and recharge in a systematic manner. This order becomes a prerequisite for the seasonal time scale with which the processes will be quantified (Salem, 2013). The water balance for the respective components is set forth below.

Vegetated Area

For a vegetated area, the water balance depends on the mean seasonal precipitation P, interception fraction (I), surface runoff (S_v) , actual transpiration (T_v), and groundwater recharge (R_e), each with the unit $[LT^{-1}]$ and related as in the equation:

$$P = I + S_v + T_v + R_v \quad \text{(4.4)}$$

Interception (I)

The interception fraction (I) represents a constant percentage of the annual precipitation value, depending especially on the vegetation type. Indeed, the fraction reduces with an increase in the annual total amount of rainfall given that throughout the simulation period, the vegetation cover is assumed constant.

Surface runoff

Surface runoff is calculated relative to the amount of precipitation, intensity of precipitation, interception and capacities of soil infiltration. First however, the potential surface runoff (S_{v-pot}) is calculated as:

$S_{v-pot} = C_{sv}(P - I)$……..…….. (4.5)

C_{sv} is the surface runoff coefficient for vegetated infiltration areas, and it is a function of the type of vegetation, type of soil and the slope, in groundwater discharge areas, saturated surface runoff takes place, resulting to a high surface runoff coefficient. This is a consequence of reduced dependence on the soil, type of vegetation and the siting of the area to a river. It is indeed, often assumed constant. In the second phase, actual surface runoff is then calculated from the S_{v-pot} by considering the differences in intensities of precipitation related to capacities of soil infiltration.

$S_v = C_{Hor}S_{v-pot}$…… (4.6)

C_{Hor} is a coefficient for describing that component of seasonal precipitation contributing to the Hortonian overland flow, for groundwater recharge areas, it is equal to one (1) because all precipitation intensities contribute to surface runoff, and only storms of high intensity are able to generate surface runoff in areas of infiltration(Woldeamlak and Batelaan, 2007).

Evapotranspiration

In calculating the evapotranspiration value, a reference value of transpiration is taken from the open-water evaporation value and vegetation coefficient as indicated in the Penman equation:

$T_{rv} = cE_o$…… (4.7)

In this, T_{rv} refers to the reference transpiration of a vegetated surface, E_o = potential evaporation of open water and c = vegetation coefficient. In addition, it is also possible to calculate the vegetation coefficient as the ratio of reference vegetation transpiration (Penman-Month) to potential open-water evaporation (Penman)(Woldeamlak and Batelaan, 2007). This is given by:

$$c = \frac{1+{}^{\gamma}/_{\Delta}}{1+{}^{\gamma}/_{\Delta}\left(1+{}^{r_c}/_{r_a}\right)} \quad \text{(4.8)}$$

γ = the psychometric constant

Δ = slope of first derivative of the saturated vapor pressure curve (slope of saturation vapor pressure at prevailing air temperature), r_c = Canopy resistance

r_a = Aerodynamic resistance given by the following formula

$$r_a = \frac{1}{k^2 u_a z_a}\left(ln\left(\frac{z_a - d}{z_o}\right)\right)^2 \quad \text{(4.9)}$$

Where: K= Von Karman constant (0.4) , u_a, = Wind speed at measurement level, z_a = 2 m

d= Zero-plane displacement length , z_o = Roughness for the vegetation or the soil

${}^{\gamma}/_{\Delta}$ = Penman coefficient (varies with temperature, can be obtained from the table 4.1 below.

Table 4.1: γ/Δ variation with temperature (Woldeamlak and Batelaan, 2007).

T (^{0}C)	**-20**	**-10**	**0**	**5**	**10**	**15**	**20**	**25**	**30**	**35**	**40**
${}^{\gamma}/_{\Delta}$	5.864	2.829	1.456	1.067	0.763	0.597	0.445	0.351	0.273	0.251	0.171

The actual transpiration T_v for vegetated groundwater discharge areas is equal to the reference transpiration because there is no water or soil availability limitation. It is indicated as:

$T_v = T_{rv}$, provided $(G_d - h_t) \leq R_d$ (4.10)

G_d = Ground water depth (L) , h_t =Tension saturated height (L) , R_d = Rooting Depth (L)

Where the groundwater level is below the root zone, for vegetated areas, the actual transpiration is indicated as:

$T_v = f(\theta)$ Provided $(G_d - h_t) > R_d$……..…… (4.11)

$f(\theta)$ = function of the water content.

For a time-variant situation, $f(\theta)$ is indicated as:

$f(\theta) = 1 - a_1^{w/T_{rv}}$……..…. (4.12)

$w = P + (\theta_{fc} - \theta_{pwp})R_d$……...…. (4.13)

a_1=Calibrated parameter related to sand content of a soil type

$w =$ Available water for transpiration

$\theta_{fc} - \theta_{pwp}$ = Plant available water content

Recharge

Ground water recharge, which is the last component, is then calculated as a residual term of the water balance, namely:

$R_v = P - S_v - ET_v - I$……..…… (4.14)

ET_v = Actual evapotranspiration, and equal to the sum of transpiration T_v and E_s(Evaporation from soil base found in-between vegetation). The spatially distributed recharge is thus estimated from the soil type, vegetation type, groundwater depth, slope, and climatic variables of potential evapotranspiration, precipitation, wind-speed and temperature (Abdollahi, 2012). Furthermore, recharge is associated with discharge areas given the concept that even in discharge areas, there is a thin unsaturated zone present, even though this may be different in the summer season. Specifically, during summer, potential transpiration is high due to vegetation.

3.3.3 Bare-soil, Open water and Impervious surfaces

In calculating the water balance for bare-soil, open-water, and impervious surfaces, a similar procedure as that of the vegetated surfaces is followed. As such, interception and transpiration terms are not there. In this case therefore, ET_v becomes E_s

3.3.4 Model validation

The water balance model, WetSpass was parameterized under conditions of humid climatic conditions, to adopt it to semi- arid conditions as a case for this and noted in (Abdollahi *et al.*, 2017), the model necessitates calibration to partake in the actual simulation of the water balance in local catchment. The model calibration is done by varying the local model parameters A1, LP, alpha (*α)* and *a* which are related to recharge, surface runoff, actual evapotranspiration and interception by Gafsa *et al.* (2017), further changing the soil and run off coefficients relating the location in question , which was accomplished by use of literature related to semi – arid conditions. By manually changing the above four parameters, the calibration is accomplished when an acceptable agreement is attained between the simulated and measured discharge or ground water heads. Appendix (8.1 and 8.2) show model simulations and calibration parameters.

3.3.5 WetSpass model input and output data

The water balance model requires five generalized typology of data, climatological data (precipitation, temperature, wind speed, potential evapotranspiration), basin configuration (land use /land cover types, groundwater depth and slope), soil texture and topography of the study area. All these input data are a combination of ESRI ascii grid file format and tbl table files.

Table 4.2: WetSpass input maps and tables.

Maps (ESRI ascii/ Arc info Grid files)	Tables (tbl) format
Topography Precipitation Temperature Potential evapotranspiration Wind speed Groundwater depth Slope	Soil parameter Run-off coefficient Land use parameter

On the other hand, the water balance model simulates seven grids maps of same format of the input data and these include; monthly and yearly run-off, evapotranspiration, interception, transpiration, soil evaporation, groundwater recharge and error in water balance distribution over the entire basin.

3.4 Data Collection and Processing

The required data for simulation of impacts of land use changes on water balance of the Saiss basin were collected from local and secondary sources, which included the elements of meteorological, morphological, hydrogeological and vegetation as shown in table (4.3). The interdependent connections among all the mentioned elements in any given watershed, highly influence the water balance components. The model input data were preprocessed and prepared into grid raster maps with same number of rows and columns of selected geographical, hydrogeological and meteorological elements in the Saiss plain. The weather data series (1987-2016) of precipitation, temperature, wind speed and for potential evapotranspiration were obtained from service of the Agency of the Hydraulic Basin Sebou (AHBS).

Table 4.3: Water balance model input data

Input	**Source**	**Initial spatial Resolution**	**Applied spatial Resolution**	**Initial temporal resolution**	**Applied temporal resolution**	**Processing tools**
DEM	SRTM	30 m x 30 m	100m x 100m	Static raster map	Static raster map	ArcGIS 10.3
Slope map	From DEM	30 m x 30 m	100m x 100m	Static raster map	Static raster map	ArcGIS 10.3
Land use map	Landsat	30 m x 30 m	100m x 100m	Composite map of 1987 and 2016	Composite map of 1987 and 2016	ArcGIS 10.3 ENVI 5.1
Soil map	NIAR	100m x 100m	100m x 100m	Static raster map	-	WetSpass lookup tab
Rain fall map	Observed rainfall	100m x 100m	100m x 100m	Daily	Monthly sum	IDW/ArcGIS
PET map	Calculated	100m x 100m	100m x 100m	Daily	Monthly sum	Spline
Temperature map	Observed temperature	100m x 100m	100m x 100m	Daily	Monthly mean	Spline
W/speed map	Observed wind speed	100m x 100m	100m x 100m	Daily	Monthly mean	IDW
GW depth map	Observed GW depth	100m x 100m	100m x 100m	Monthly	Monthly mean	Kriging

3.4.1 Digital Elevation Model and Slope map of Saiss.

The Digital Elevation Model (DEM) and two imageries of Landsat 5 TM of 1987 and Landsat 7 ETM+ of 2016 were downloaded from the United State Geological Survey (USGS) earth explorer in Geo TIFF format and they were processed into different land use classes which were the basis for detection of land use-cover change during this period of 29 years. The DEM was further processed to prepare elevation map and slope map of the Saiss basin shown in figure (4.3).

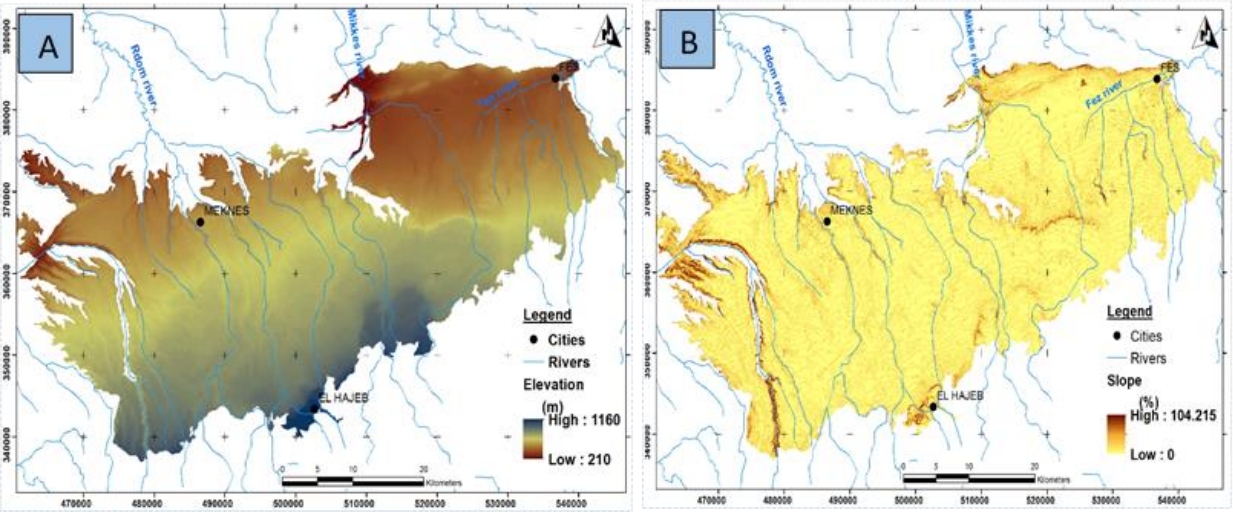

Figure 4.3: Elevation map (A) and slope map (B) of the Saiss basin.

3.4.2 Soil map of Saiss basin

The soil map was digitized from the map (1/50000) of National Institute of Agronomic Research (Institut de La Nationale Recherrche Agronomique), Pedology Regional Labaratory, Meknes (Labaratoire Region de Pedologie), (NIAR) using ArcGIS 10.3.

The soil texture obtained was re-coded according to the USDA texture codes which are related to the WetSpass soil codes (Appendix 8.3). The extracted soil map was further resampled using resample (data management) tool in ArcGIS, to give a resolution of 100 m x 100 m, with 870 rows and 493 columns, chosen in conformity with same pixel size of the DEM and slope map. The Saiss basin soil map figure (4.4) linked to the look up table of WetSpass was converted to ESRI ascii file format executable by WetSpass model.

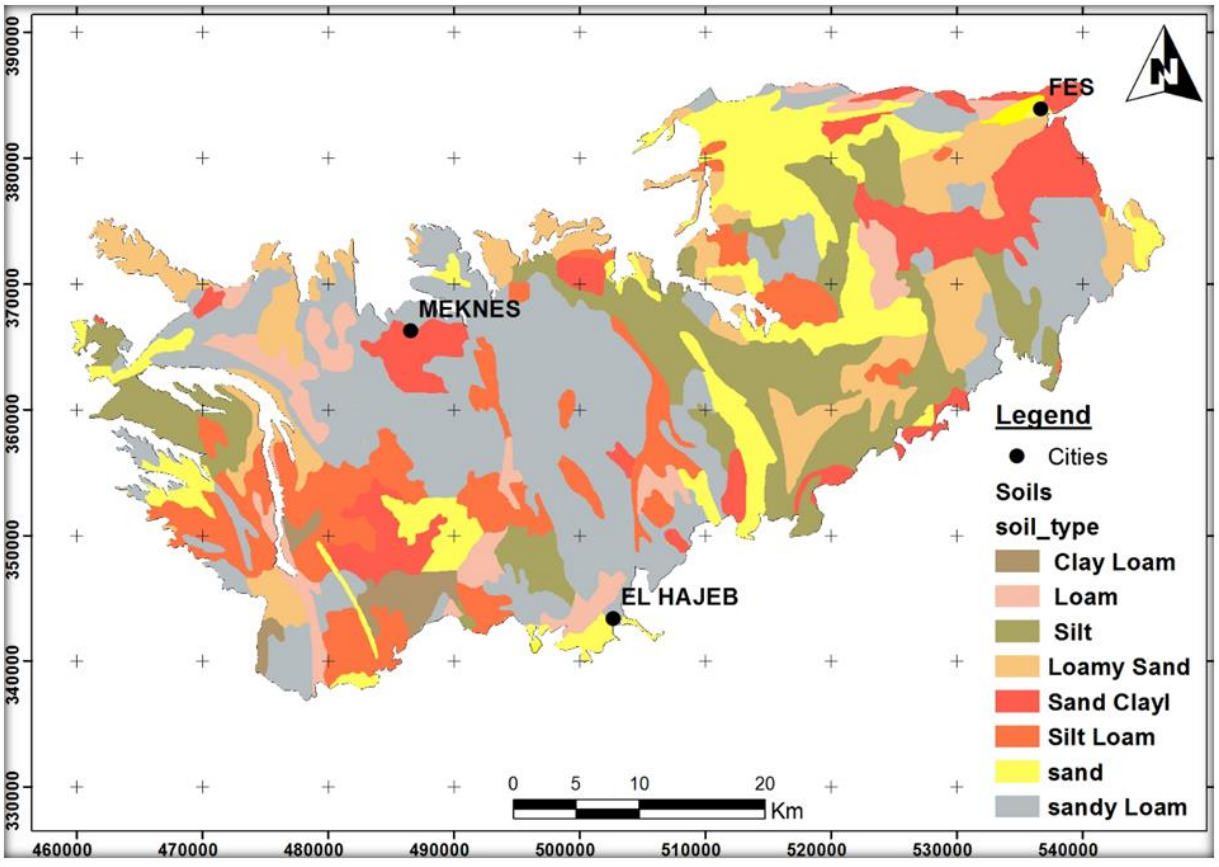

Figure 4.4: The soil texture map of the Saiss basin

3.4.3 Precipitation

Representing the fundamental element of the hydrological water balance, the Saiss basin recognizes rainy periods in winter, spring and occasionally in summer. The typology of these precipitations vary depending on the mode and the cooling conditions.

Geographic positioning influences the distribution and variation of precipitation. Table 4.4 and figure 4.5 show the position and the spatial distribution of the eight (8) weather stations (for rainfall, temperature and evapotranspiration) taken into account for the purpose of this research.

Table 4.4: Geographical positioning of the rainfall stations and observation periods.

Station	X (m)	Y(m)	Z (m)	Observation period	
				Original	Extracted
Meknes Airport	487500	365000	550	1973-2016	1987-2016
Fes Meteo	536916	385074	410	1916-2016	1987-2016
Fes DRH	535400	384800	410	1973-2016	1987-2016
O_Soltane	524000	323200	1640	1934-2016	1987-2016
Sefrou	552000	359000	820	1922-2016	1987-2016
El Hajra	507044	373136	750	1971-2016	1987-2016
Source Bittit	519660	355000	760	1977-2016	1987-2016
Dar El Arsa	543300	399700	130	1973-2016	1987-2016

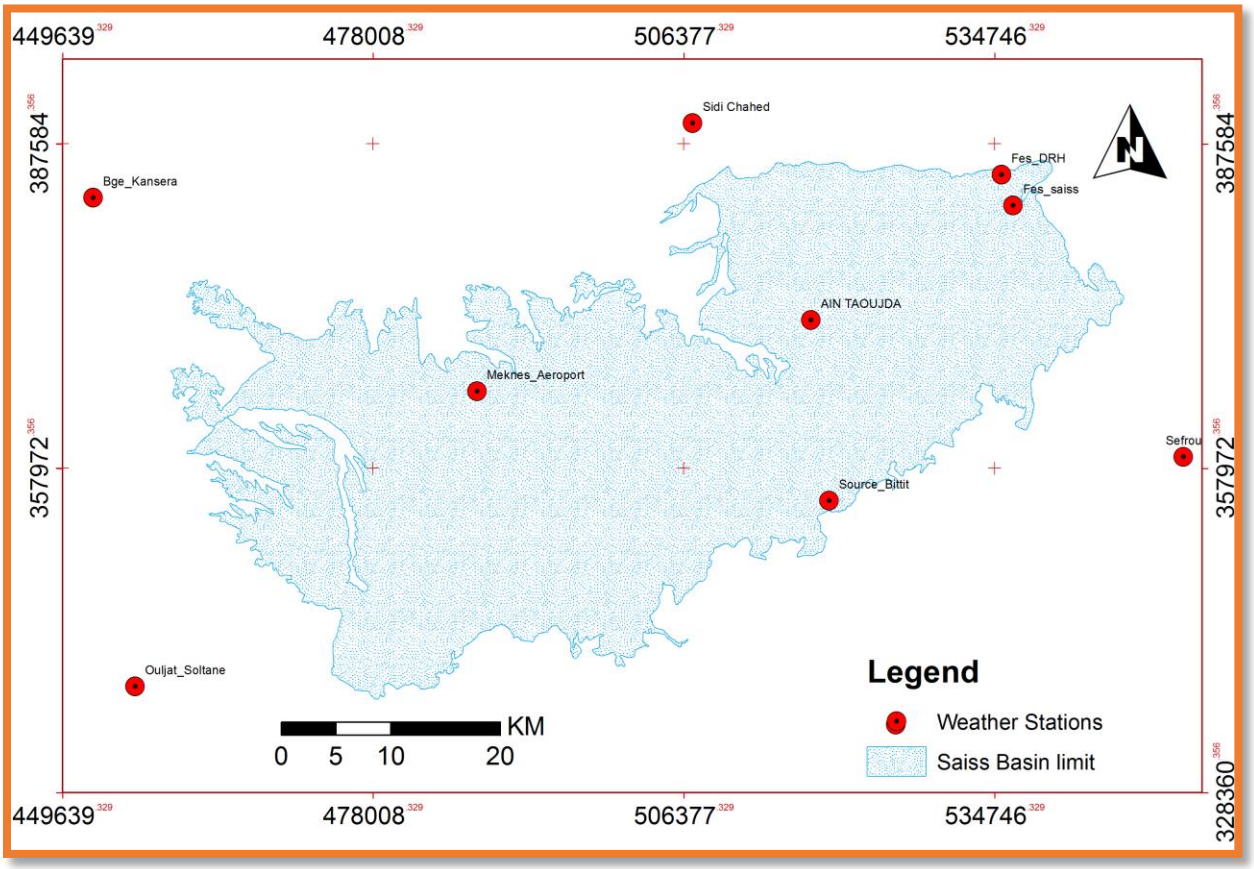

Figure 4.5: Spatial distribution of the eight weather stations within the basin

The rainfall stations are distributed irregularly in the plain, which influences the results recorded at the rainfall stations and the overall representation of the rainfall amount and nature of its coverage in the Saiss basin.

3.4.3.1 Rainfall reliability analysis from all stations

a) Data control using the Double Cumulative Method. This method is used for the criticism of the rainfall data normally from outside organizations whose reliability is unquestionable. This method consists of taking the cumulative precipitation of the reference station (Reliable data) in the abscissa axis and the station to be controlled in the ordered axis. The application of this method to stations belonging to the Saiss basin contains heterogeneities and existing anomalies in the recorded precipitation series. This operation must precede any use of rainfall data. (Appendix 8.4) Shows the variation in the pattern of precipitation curves and presence of anomalies in the precipitation recorded of the stations under consideration.

b) Frequency analysis of precipitation recorded. This is a mathematical procedure that consists of submitting the recorded data to tests and statistical laws to identify the appropriate method of adjustment to data treaties. There are a multitude of laws that allow for adjustments of data, among which include;

- Gumbel

$$F(x) = e^{-e^{-u}} \quad \text{with, } u = \frac{x - x_0}{s} \qquad \text{.....(4.15)}$$

- Gauss law

$$F(x) = \frac{1}{\sqrt{2\pi}} \int_{-\infty}^{u} e^{\frac{u^2}{2}} du \quad \text{with } u = \frac{x - \bar{x}}{\delta_x} \qquad \text{.....(4.16)}$$

- Galton law (normal log)

$$F(x) = \frac{1}{\sqrt{2\pi}} \int_{-\infty}^{u} e^{\frac{u^2}{2}} du \quad \text{with } u = a\log(x - x_o) + b \qquad \text{.....(4.17)}$$

The following table (4.5), shows the results obtained for the required data adjustments of the undistributed and irregular raw rainfall collected from the different weather stations.

Table 4.5: Results of statistical adjustment of rainfall data

Station	Observation	Law	Mode	Test Value	Mean	Cv	Frequency
Meknes Air	29	Gumbel	387	7.244	467	0.376	0.071
Fes Meteo	29	Goodrich	310	4.033	386	0.393	0.330
Fes DRH	29	Goodrich	333	1.233	364	0.350	0.946
O_Soltane	29	Gauss	352	5.833	352	0.264	0.142
Sefrou	29	Goodrich	488	3.381	487	0.283	0.003
El Hajra	29	Goodrich	273	7.253	430	0.377	0.083
Source Bittit	29	Goodrich	412	2.046	475	0.343	0.781
Dar El Arsa	29	Galton	338	5.261	433	0.363	0.201

Each station adapts to a specific statistical law based on the recorded data, the Value of the test allowed to define which of the adjustment laws was suitable for the samples. The (Appendix 8.5) details the results of statistical adjustments to precipitation.

3.4.3.2 **Variations in precipitation over time**

a) Monthly variations. For the stations controlling the Saiss plain, the precipitation regime is of Mediterranean type, the wet period ranges from November-April and the dry period Covers from May to September.

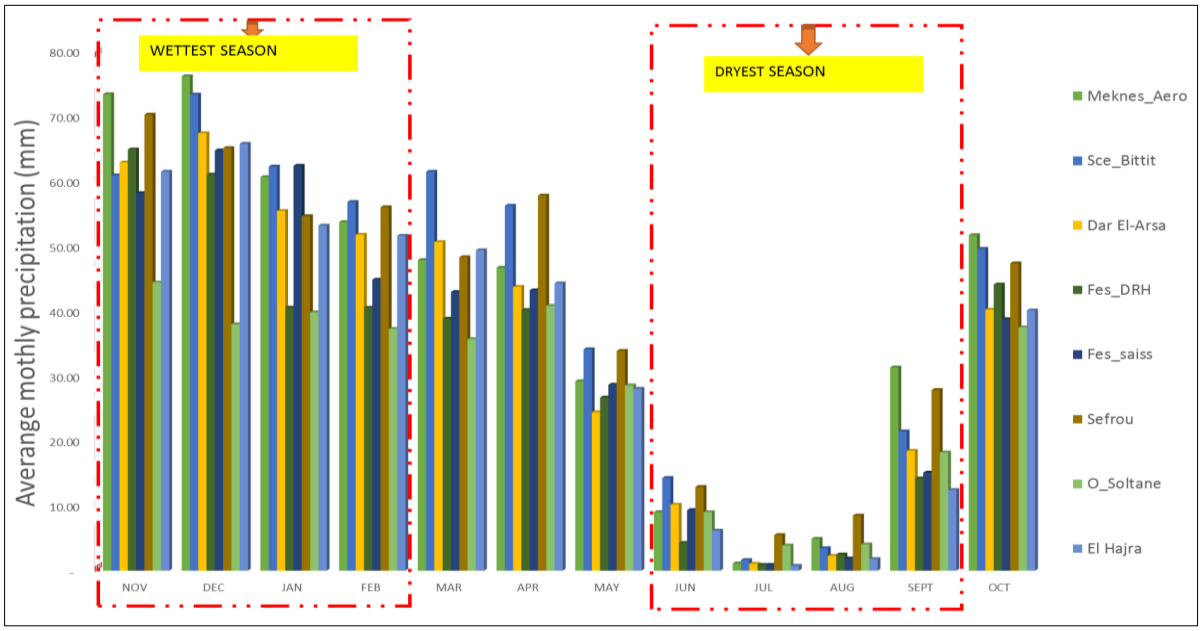

Figure 4.6: Average monthly precipitation in the Saiss basin (1987 to 2016).

The greatest amount of precipitation is recorded at the Meknes-Aero station, followed by the Sci_Bittit station. The month of December is generally the most wet while the months of July and August are the driest.

Table 4.6: Monthly precipitation of climate stations (AHBS)

STATION	SEPT	OCT	NOV	DEC	JAN	FEB	MAR	APR	MAY	JUN	JUL	AUG
Meknes_Aero	31.25	51.60	73.29	76.04	60.53	53.62	47.77	46.60	29.13	9.00	1.11	4.89
Sce_Bittit	21.42	49.51	60.80	73.23	62.16	56.72	61.36	56.14	34.04	14.26	1.63	3.44
Dar El-Arsa	18.43	40.14	62.79	67.28	55.33	51.68	50.55	43.65	24.36	10.15	1.07	2.27
Fes_DRH	14.19	44.01	64.79	60.92	40.46	40.44	38.76	40.09	26.64	4.26	0.89	2.49
Fes_saiss	15.09	38.68	58.07	64.64	62.28	44.75	42.87	43.12	28.60	9.32	0.89	1.88
Sefrou	27.78	47.28	70.15	65.01	54.53	55.90	48.20	57.69	33.80	12.87	5.47	8.47
O_Soltane	18.18	37.43	44.33	37.90	39.73	37.19	35.62	40.74	28.50	8.99	3.87	4.03
El Hajra	12.41	40.02	61.37	65.67	53.07	51.51	49.28	44.20	27.97	6.15	0.75	1.77
MEAN	**19.84**	**43.58**	**61.95**	**63.83**	**53.51**	**48.97**	**46.80**	**46.53**	**29.13**	**9.38**	**1.96**	**3.66**

The annual mean precipitation of Saiss basin ranges from 349 mm to 477 mm with the mean values of 413 mm, while as the monthly mean precipitation recorded in the Saiss basin varies between 1.96 mm in July and 63.83 mm in the month of December.

That is a variation of about 62 mm per year. Precipitation is such an important irregularity marked by strong Recordings in the Meknes –Aero station. On the other hand, the seasonal distribution of precipitation shows considerable variability in The inputs of precipitation between seasons

Table 4.7: Seasonal variations of precipitation in the Saiss plain

STATION	Winter	Summer
Meknes Airport	238.0	46.2
Sce_Bittit	253.5	40.7
Dar El-Arsa	224.8	31.9
Fes_DRH	180.6	21.8
Fes_saiss	214.5	27.2
Sefrou	223.6	54.6
Ouljat Soltane	150.4	35.1
El Hajra	219.5	21.1

The following (figure 4.7) shows the seasonal distribution of rainfall at stations belonging to the plain of Saiss

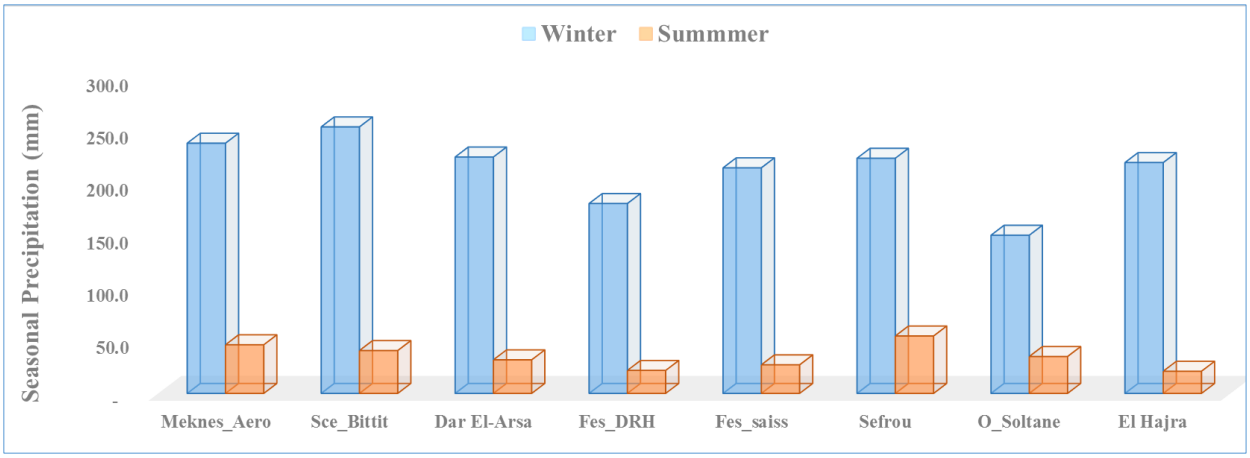

Figure 4.7: Seasonal distribution of precipitation in some stations on the Saiss plain

The wettest period (November, December, January and February) is the rainiest season for the stations belonging to the Plains of Saiss with a percentage of rainfall that reaches 62% of the annual precipitation.

b) Inter-annual variations - Monitoring of precipitation by stations over the period 1987-2016 shows that annual regime is made on the basis of an average calculated on Period of observations

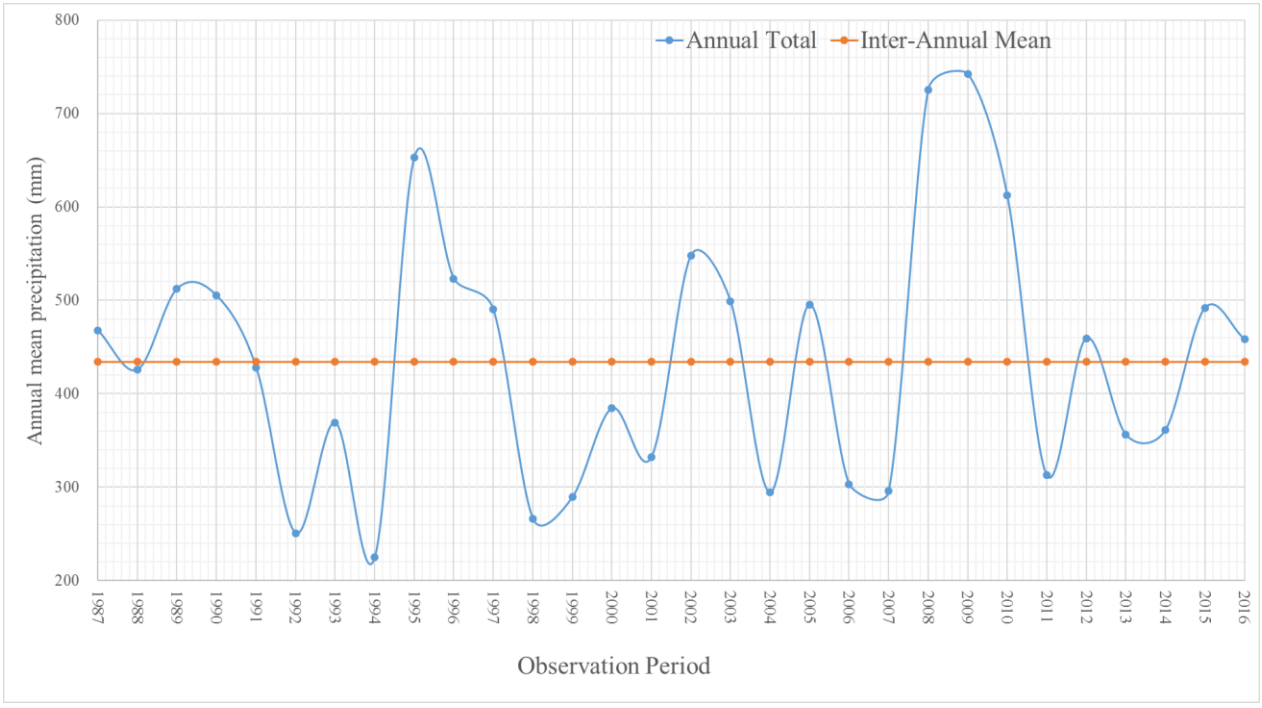

Figure 4.8: Inter-annual variations in precipitation

The previous figure shows that the precipitation regime shows an irregularity of Contributions to the area controlled by the weather stations with the basin. Annual precipitation values were calculated from average monthly precipitation, which were also obtained from daily time series for data sets across all stations, it was further subdivided into both seasonal (wettest and driest) and annual. These three data clusters were purposely obtained for the spatial representation of precipitation in the entire basin using interpolation technique by the kriging method. This Method is based on mathematical approaches based on the altitude-distance relationship Between the pairs of points which are separated by the distance h. The spatial variation is quantified by the semi-variogram equation defined as follow.

$$y(h) = \frac{1}{2n}\sum_{i=1}^{n}\left\{Z(x) - Z(x_i + h)\right\}^{z} \quad \text{..... (4.18)}$$

The application of this methodology to the available data contributed to the creation of the Maps of spatial variations of precipitation in the Saiss plain for wet , dry season and annual (figure 4.9) , which were then convert into ESRI ascii format as is a requirement for the WetSpass water balance model

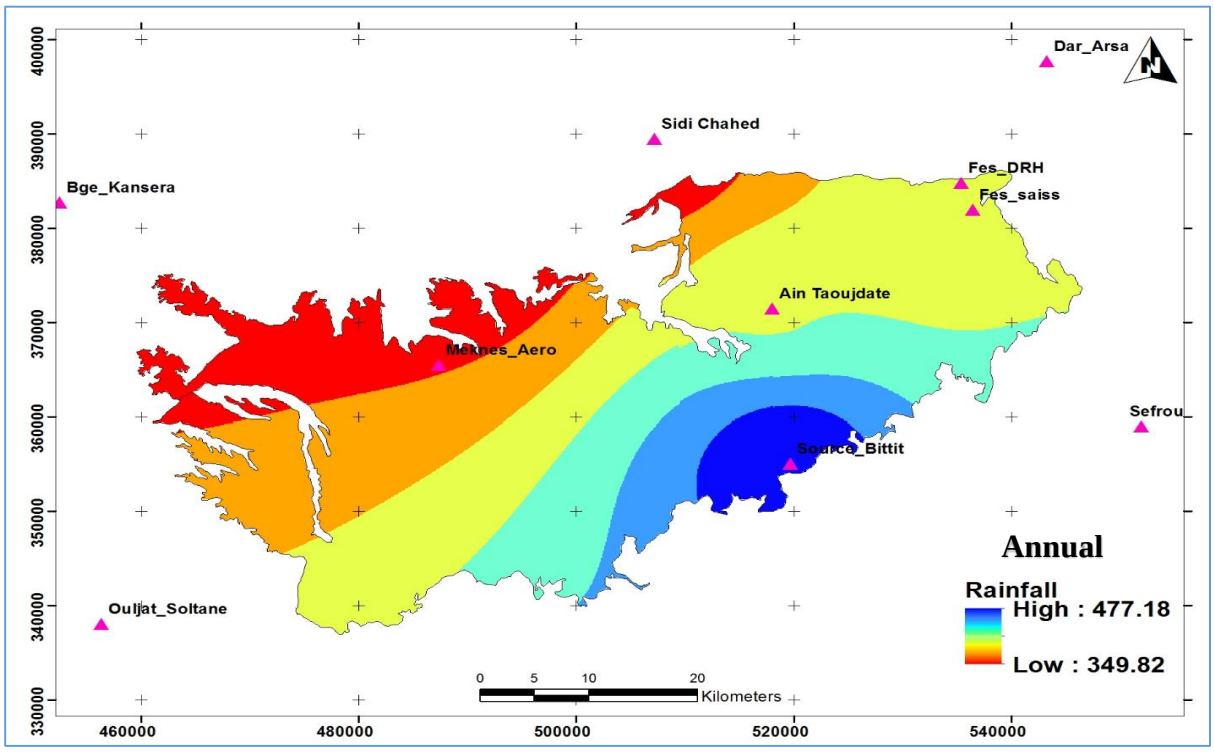

Figure 4.9: Long-term annual spatial distribution of precipitation of the Saiss basin.

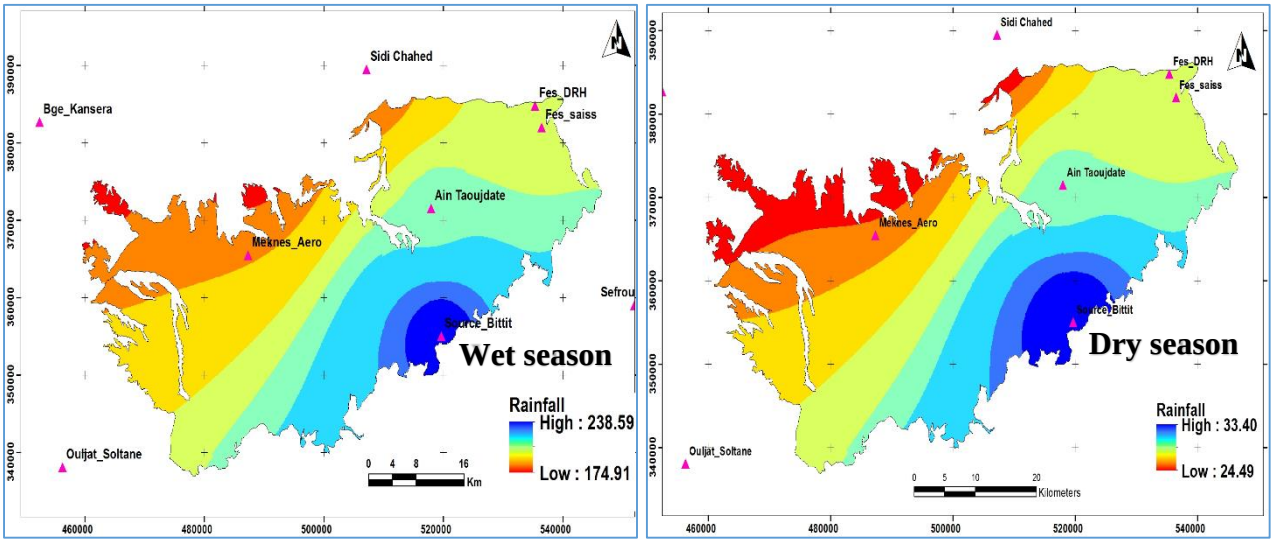

Figure 4.10: Seasonal spatial distribution of Precipitation in Saiss basin (1987-2017)

3.4.4 Temperature

The average annual and average monthly temperatures for the period 1987 -2016 were calculated from the maximum and minimum values. These temperature records were obtained from eight stations just as precipitation. The average monthly temperatures recorded from all the stations nearly presented the similar values as indicated in the (figure 4.11)

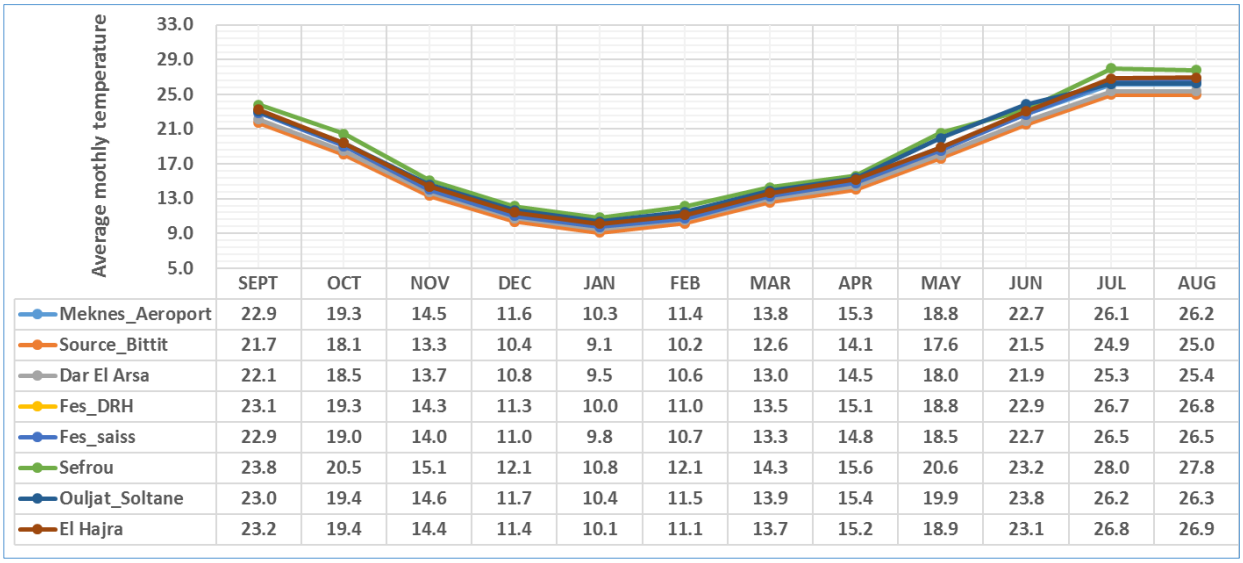

	SEPT	OCT	NOV	DEC	JAN	FEB	MAR	APR	MAY	JUN	JUL	AUG
Meknes_Aeroport	22.9	19.3	14.5	11.6	10.3	11.4	13.8	15.3	18.8	22.7	26.1	26.2
Source_Bittit	21.7	18.1	13.3	10.4	9.1	10.2	12.6	14.1	17.6	21.5	24.9	25.0
Dar El Arsa	22.1	18.5	13.7	10.8	9.5	10.6	13.0	14.5	18.0	21.9	25.3	25.4
Fes_DRH	23.1	19.3	14.3	11.3	10.0	11.0	13.5	15.1	18.8	22.9	26.7	26.8
Fes_saiss	22.9	19.0	14.0	11.0	9.8	10.7	13.3	14.8	18.5	22.7	26.5	26.5
Sefrou	23.8	20.5	15.1	12.1	10.8	12.1	14.3	15.6	20.6	23.2	28.0	27.8
Ouljat_Soltane	23.0	19.4	14.6	11.7	10.4	11.5	13.9	15.4	19.9	23.8	26.2	26.3
El Hajra	23.2	19.4	14.4	11.4	10.1	11.1	13.7	15.2	18.9	23.1	26.8	26.9

Figure 4.11: Average monthly temperature for Saiss basin (1987 -2016).

The Saiss basin temperature varies gradually, with average monthly maximum of 26 ^{0}C (in august, summer) and minimum of 10 ^{0} C (in January, winter).

These data were segmented into seasonal averages and the temperature inputs were interpolated to prepare ESRI ascii grid raster map of the entire basin temperature using 3D analyst tool>Raster>interpolation: Spline. (Figure 4.12 and 4.13)

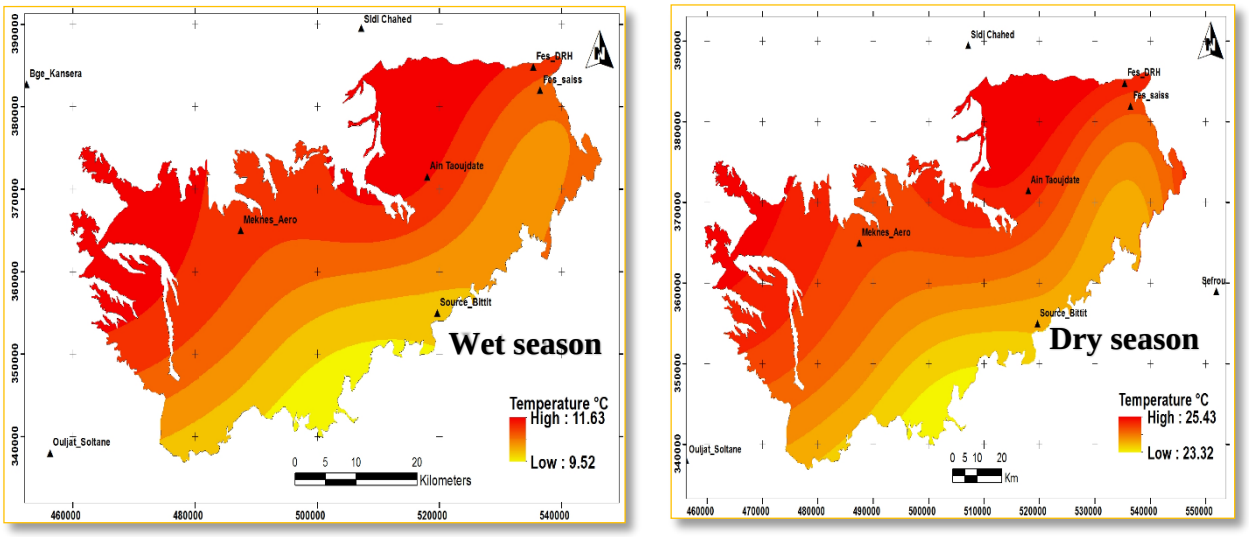

Figure 4.12: Long-term seasonal spatial distribution of Temperature in Saiss (1987-2017)

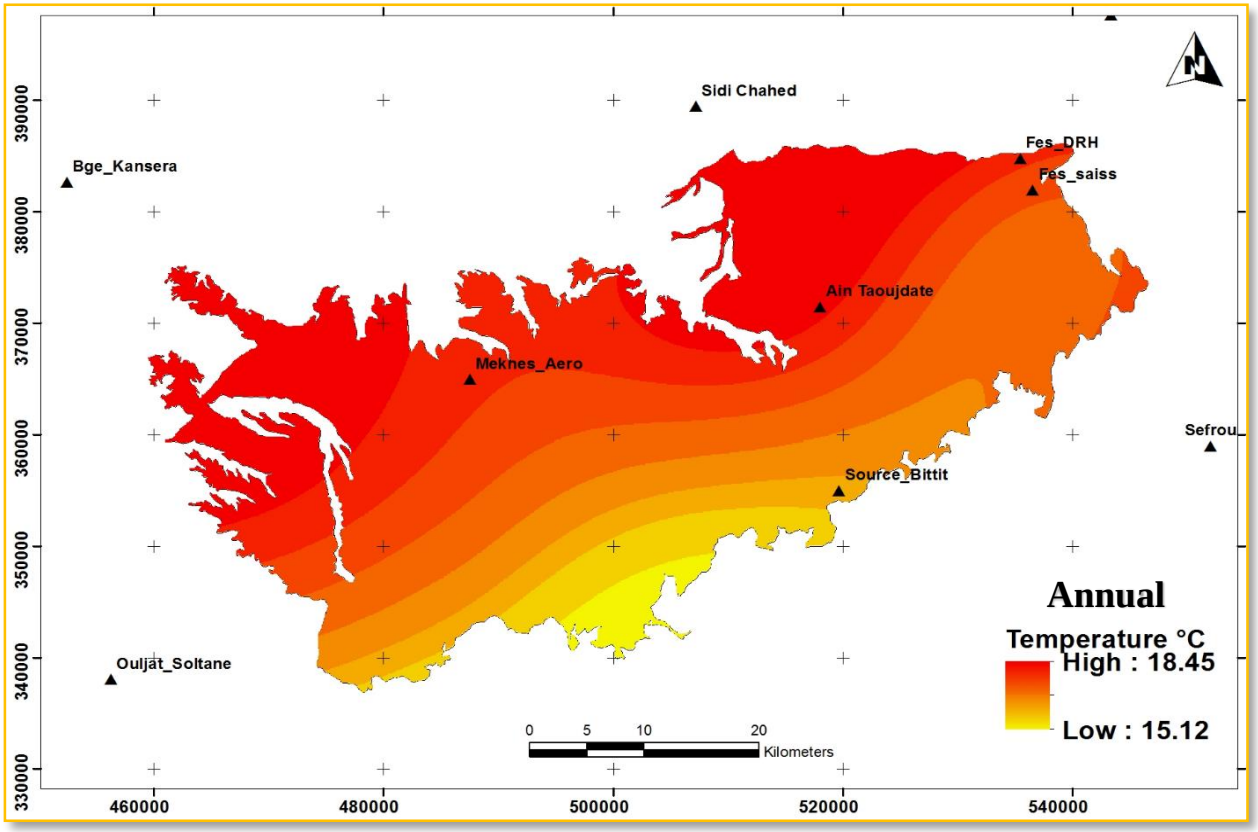

Figure 4.13: Long-term annual spatial distribution of Temperature in Saiss (1987-2016)

3.4.5 Evapotranspiration and Potential evapotranspiration

It corresponds to the amount of water transferred from the soil to the atmosphere by evaporation and transpiration of plants. Potential evapotranspiration can be estimated by several empirical formulas among which include, Turkish, Thorn Thwaite. For this study, Thornthwaite formula established in 1984, was used to estimate monthly potential evapotranspiration as a function of the monthly average temperatures and the latitude of this Saiss using the average monthly temperatures from all eight stations as follows;

$$PET = 16 * \left\{ \frac{10T}{I} \right\}^{a} \quad \text{......} \quad (4.19)$$

Where;
T: average monthly temperature (^{0} C)

I: annual thermal index, it is equal to the sum of the monthly thermal indices, $I = \left(\frac{T}{5} \right)^{1.514}$

a: Correction factor of each month , $a = 0.49239 + 1792*10^{-5}*1 - 771*10^{-9}*I^{2} + 675*10^{-9}*I^{3}$
The monthly evapotranspiration of the mentioned stations for the period 1987-2016 is presented in the (figure 4.14) below.

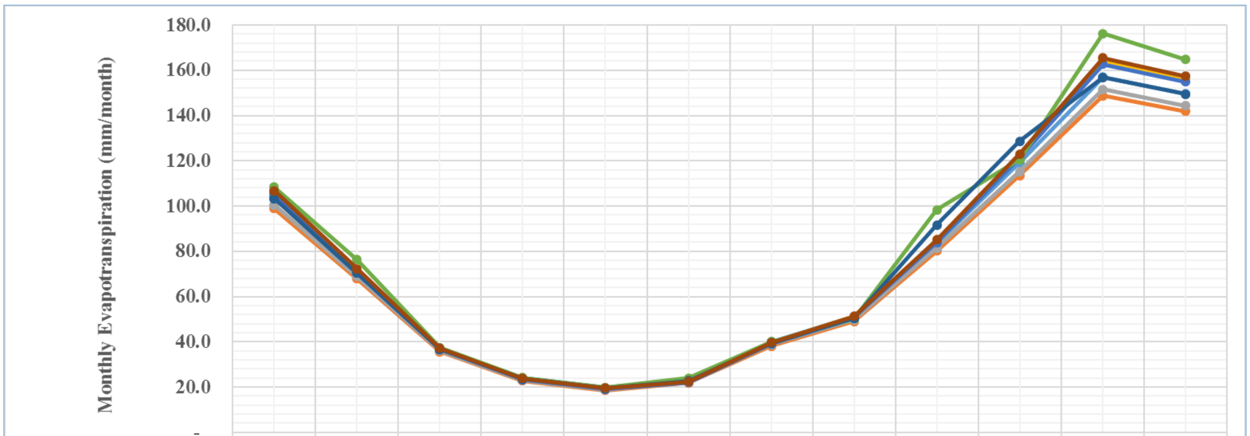

	SEPT	OCT	NOV	DEC	JAN	FEB	MAR	APR	MAY	JUN	JUL	AUG
Meknes_Aeroport	103.7	70.9	37.2	24.1	19.7	23.2	39.9	51.1	83.7	119.1	157.0	149.5
Source_Bittit	98.9	67.9	35.6	22.7	18.5	21.9	38.1	48.9	80.1	113.5	148.8	141.8
Dar El-Arsa	100.5	68.9	36.1	23.2	18.9	22.4	38.7	49.7	81.3	115.3	151.5	144.3
Fes_DRH	106.3	71.9	37.0	23.6	19.4	22.3	39.5	51.2	84.7	122.4	164.5	156.6
Fes_saiss	105.3	71.3	36.6	23.3	19.1	22.0	39.1	50.7	84.0	121.2	162.6	154.9
Sefrou	108.3	76.3	37.5	24.1	19.7	24.0	40.1	50.3	98.4	120.6	176.3	164.8
Ouljat_Soltane	103.3	70.4	36.7	23.6	19.4	22.8	39.4	50.5	91.6	128.7	156.8	149.4
El Hajra	106.9	72.2	37.1	23.7	19.5	22.4	39.7	51.4	85.1	123.0	165.4	157.4

Figure 4.14: Variation of monthly evapotranspiration with Saiss basin (1984-2016)

All the eight station exhibit nearly the same trend in the distribution of the evapotranspiration with lowest values in the month of January(winter) and highest in July (summer). The mean value across all the stations in the basin vary considerably with the mean precipitation and temperature, and ranges from 19 mm/month(January) to 160 mm/month(July) as shown in the (figure 4.15) below.

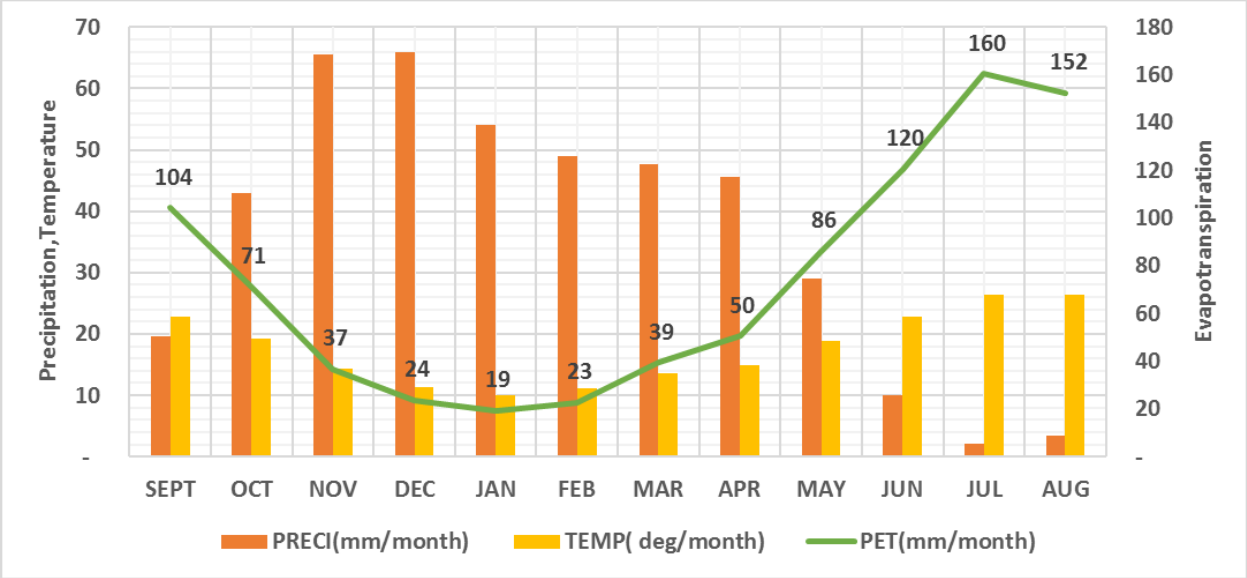

Figure 4.15: Variation of evapotranspiration with precipitation and temperature across Saiss

The calculated values of the potential evapotranspiration as indicated in (figure 4.15) above from all the weather stations within the Saiss were used to generate interpolated raster grid maps of winter season, summer and annual using the spline method as for the temperature.

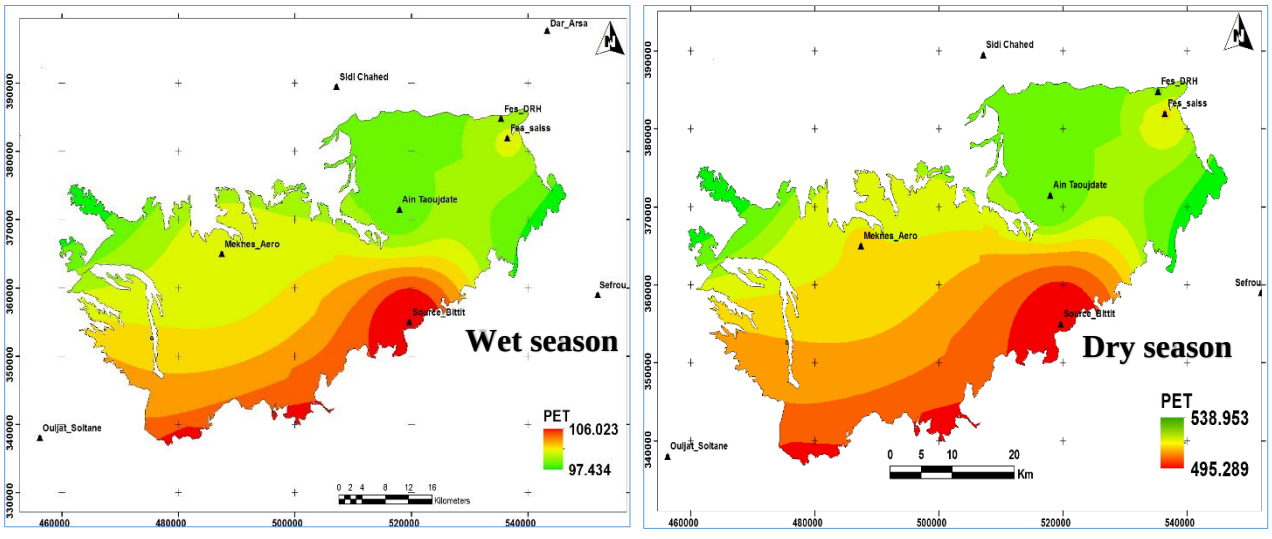

Figure 4.16: Seasonal spatial distribution of Evapotranspiration in Saiss (1987-2017)

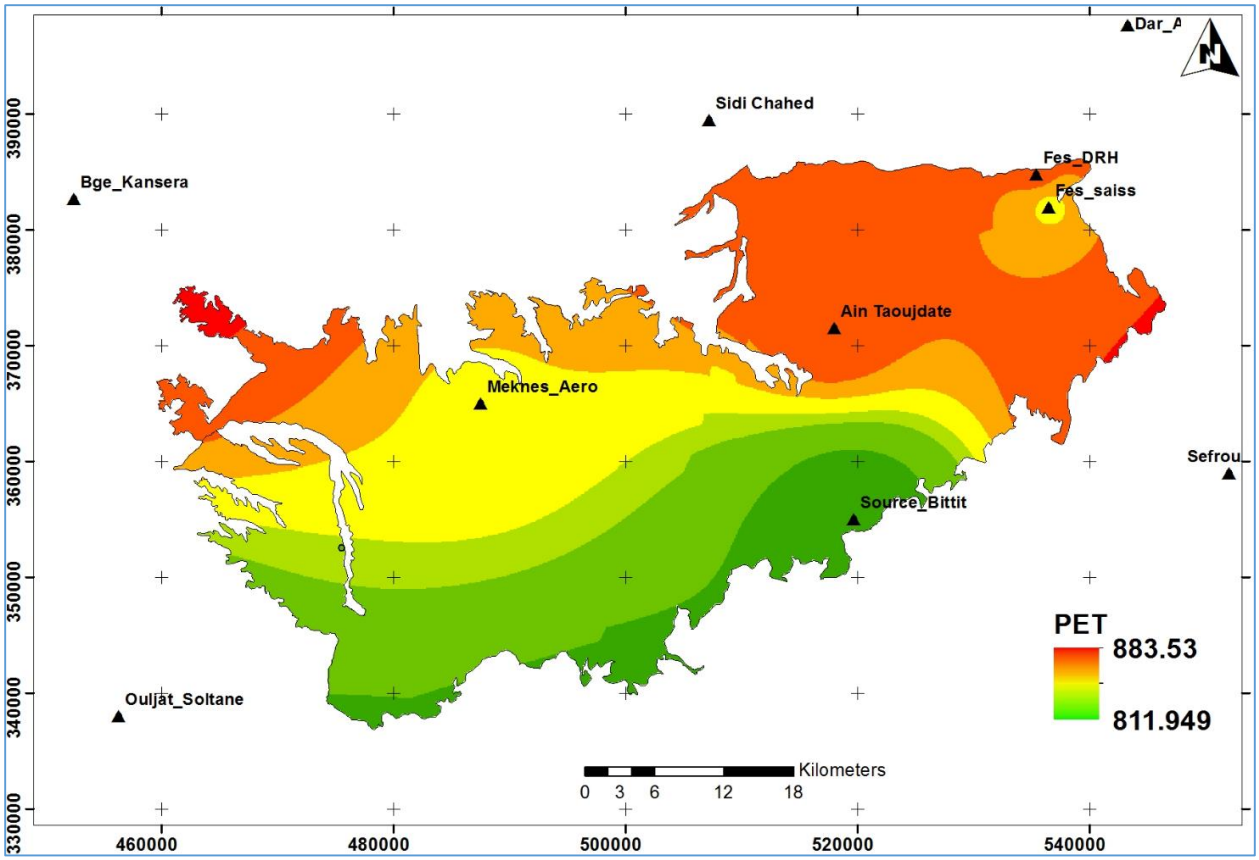

Figure 4.17: Long-term annual spatial distribution of Evapotranspiration in Saiss (1987-2016)

3.4.6 Wind Speed

Due to limitation in finding adequate wind speed data from the representative weather stations within the Saiss basin, the average seasonal and annual wind speed for the study period were obtained from Global Weather Data for SWAT, The National Centers for Environmental Prediction (NCEP) at https://globalweather.tamu.edu/. Twenty-one (21) space stations were obtained within and around the study area and 15 stations (Figure 4.18 A) were selected for the representation of wind speed data. The extracted data were processed in Microsoft Excel to obtain seasonal and annual average wind speed(m/s). The (Appendix 8.6) shows the data table of wind speed that was used to interpolate wind speed maps which was convert ESRI ascii format, (figure 4.18), using 3D analyst tool>Raster>Interpolation: IDW method.

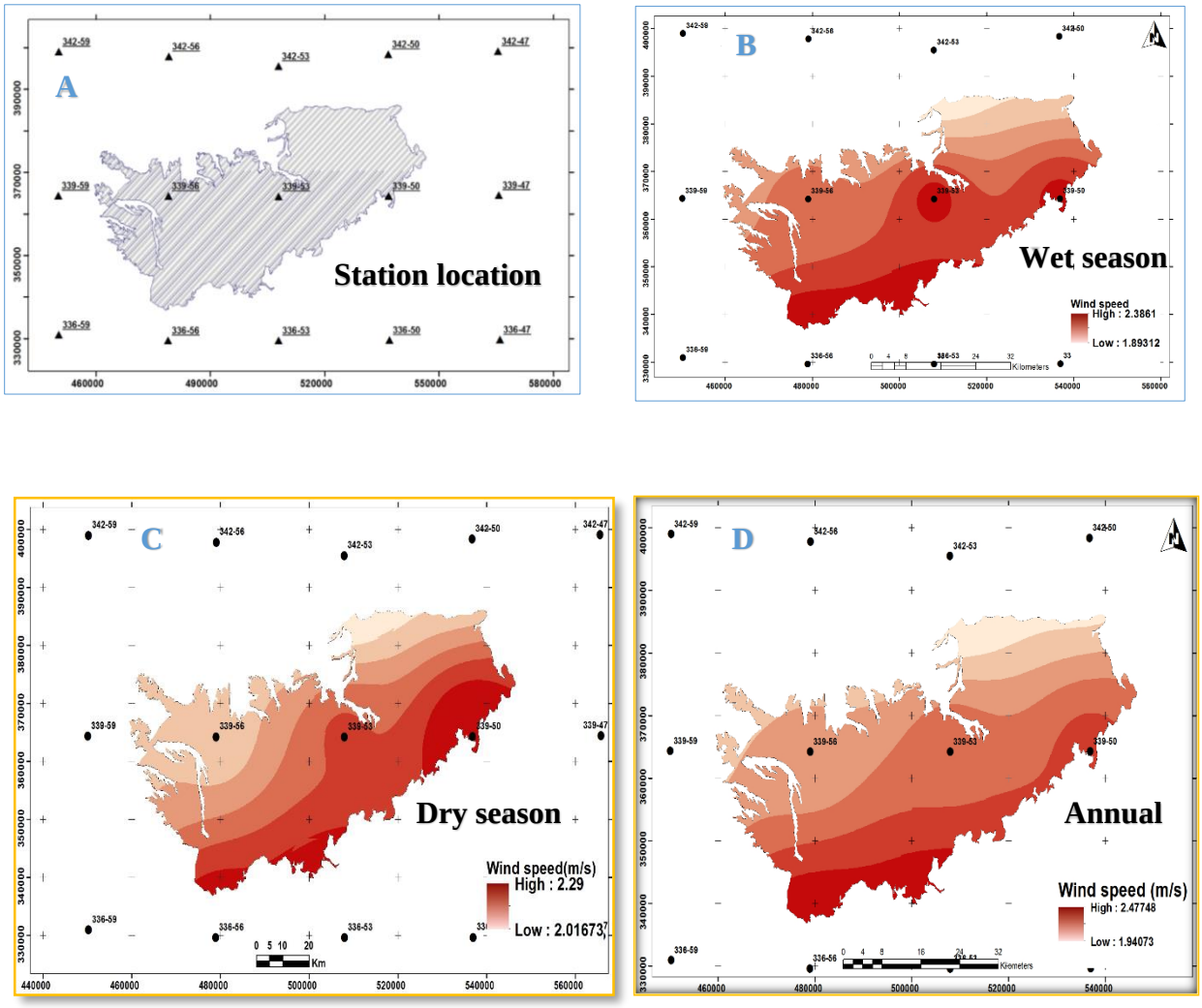

Figure 4.18: Location of stations(A), Seasonal mean wind speed (B & C), Annual mean (D)

3.4.7 Ground water depth

Ground water table of more than 20 m depth has insignificant influence on groundwater evaporation as consider by the WetSpass model(Tilahun and Merkel, 2009).

Several piezometric data were obtained from AHBS, with water table depth ranging from as low as 1 m to a maximum of 75 m, the Appendices (8.7 and 8.8) show locations and ground water table records of all the piezometers that were considered for generation of groundwater maps for this study as inputs for the model, using Kriging method (figure 4.19).

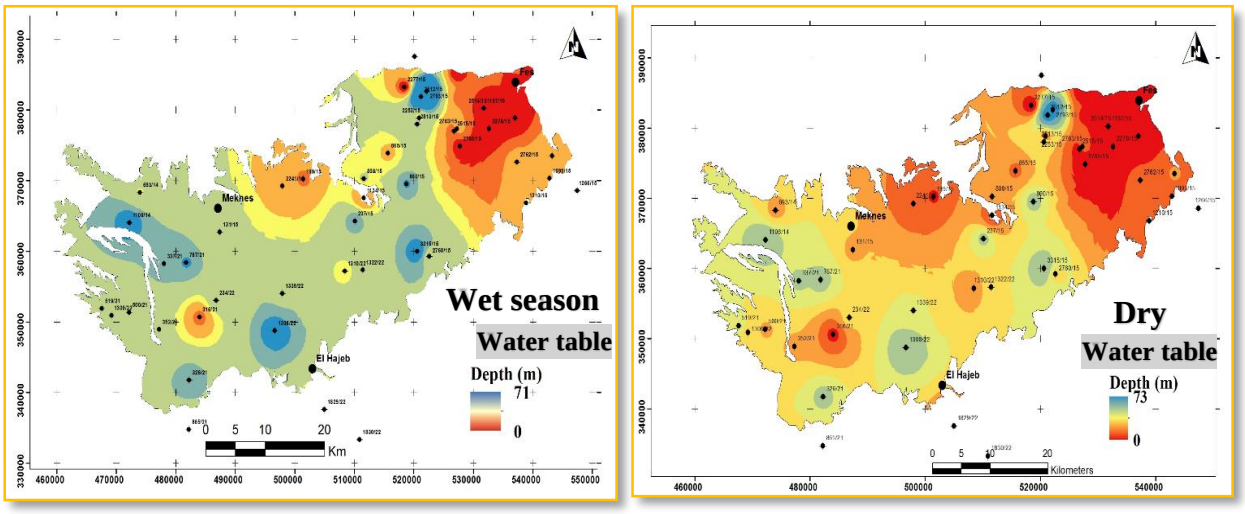

Figure 4.19: Long-term seasonal spatial distribution of Ground water table in Saiss basin

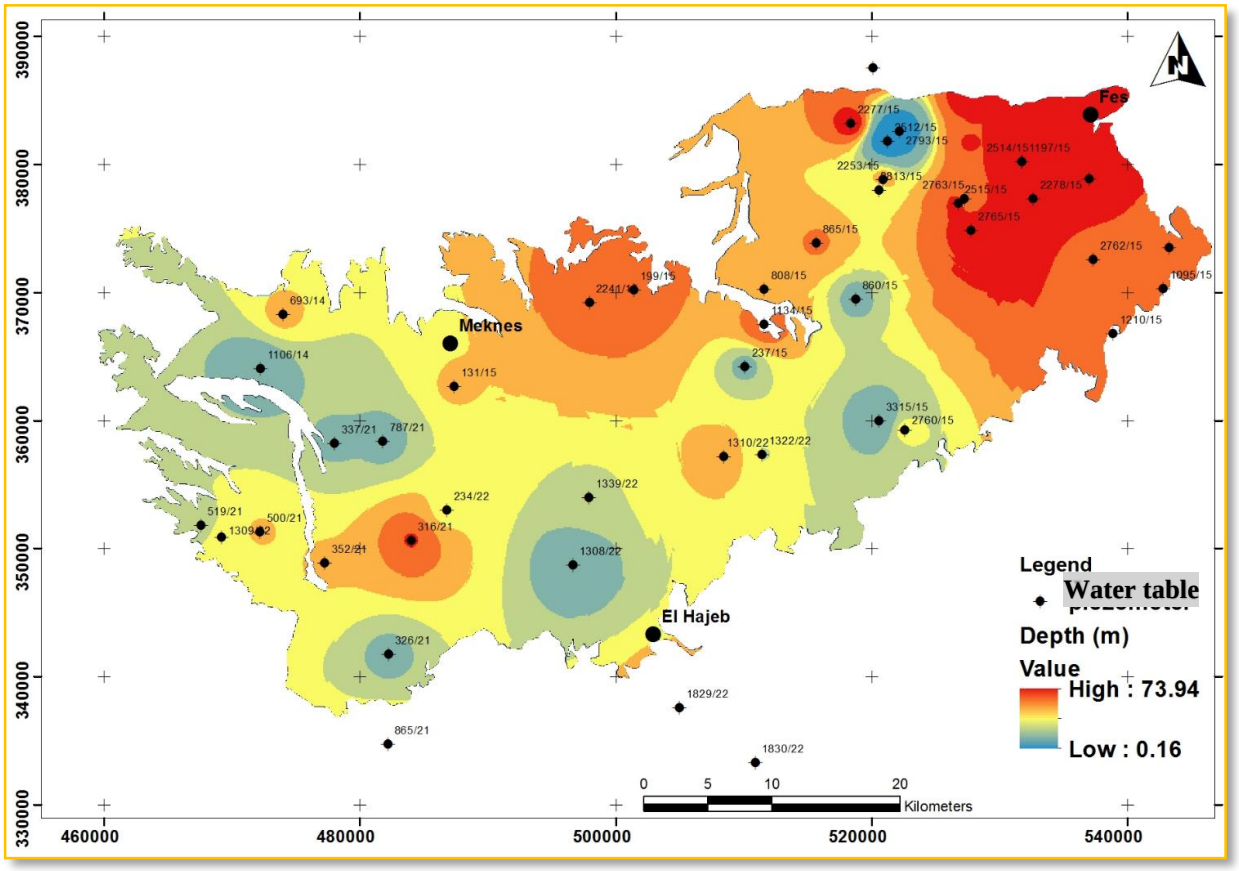

Figure 4.20: Long-term annual spatial distribution of Ground water table in Saiss basin

3.5 Land Use and Land Cover Change Classification

Understanding land use changes on any watershed is very vital as it enhances knowledge on the current trends in processes of deforestation, degradation, desertification and loss of biodiversity. The identification of spatio-temporal changes in land use in the study area Saiss plain was carried out from the ground reality, the interpretation and the picture classification of satellite images Landsat 5 TM and Landsat 7 ETM + (between 1987 and 2016), based on the radiometric values of the image data and various parameters specific to the photo-interpretation technique (specifically the texture and structure).

This was done by selecting and cutting the parts corresponding to the same portion of space from the geographical coordinates of the study zone. The Landsat images were georeferenced using the projection system Merchich North, general methodology shown in (figure 4.21).

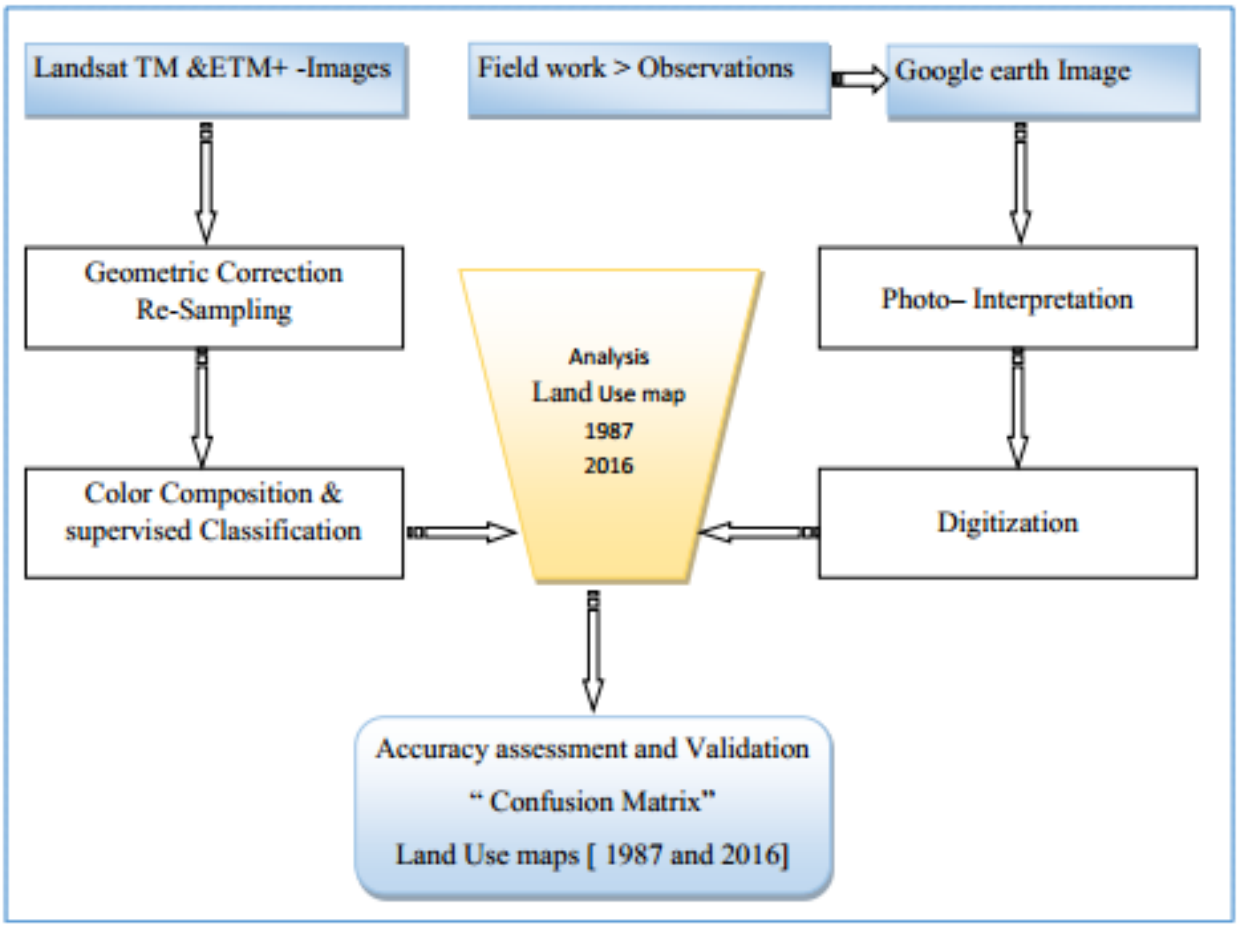

Figure 4.21: Diagram of the stages of processing of remote sensing images

3.5.1 Processing land use maps of Saiss plain for 1987 and 2016

Treatment of multi-source images is quite a complex process, involving analysis of technical procedures and appropriate specific choices. Indeed, the corrections of geometric and radiometric part of these image processing operations that allow formatting of data and decrease radiometric disturbances related to environmental conditions, presents a set of methods and choice of an appropriate method in order to get quality results.

The method used in this study includes processing and analysis satellite images as well data mining of existing complementary. This was done with the help of ArcGIS, google –earth and ENVI soft wares, in viewing images, conversion of file types vector and raster and image classification for mapping of the land use maps of the Saiss basin.

Regarding the acquisition of remote sensing data, two scenes Landsat TM and ETM + (1987 and 2016) were geometrically corrected having a spatial resolution of 30 m (Table 4.8).

Image processing Landsat TM and ETM + was achieved with the mentioned softwares, by preliminarily defining the limits of the Saiss basin and cutting of the spectral bands which were 7 in number (1, 2, 3, 4, 5.7 and 8). Channel 6 was not selected because its properties are focused on heat. The lane 8 shows the panchromatic band 15 m spatial resolution

Table 4.8: Characteristics of Landsat scenes

Name of Scene	Date of acquisition	Sensors	Path	Raw	Long	Lat
LM52010361987223AAA03	11_08_1987	TM	201	37	34.6	-5.5
LT52010362011209MPS00	28_07_2016	ETM+	201	37	34.6	-5.5

The next phase consisted of an image enhancement by raising contrast and principal component analysis performed on the raw images. This operation was used to improve the visual quality of each raw canal, decorrelating the neo- channels and to maximize information on the first three neo-channels (main components). At this step, data (neo-channels of the main component and indices) were the basis for the realization of colored compositions and directed classifications.

The land classification method adopted for this research was the directed classification, the principle goal in this method was to assign, to the thematic classification pixels that belong to a class defined by the spectral driving plots. This was a process that required choosing a most suitable classification algorithm to processed data.

The drive plots were defined according to their local homogeneity related. Their size was of the order of 30 pixels on average because the images show low spread and heterogeneous units. The choice of training areas was conducted in the ranges of consistent color, from visual interpretation of the colored composition.

The classical algorithm based on maximum likelihood was used as reference because it is the most used in classification (Eastman, 2006), represented by module *MAXLIKE*, file-based spectral signatures. It is considered that All classes have a prior probability identical. The pixels are assigned to the class they have the highest probability of belonging. *MAXLIKE* also has the option of reject a number of pixels with the possibility of belonging to a class is very low. This algorithm is based on a statistical method, which makes the calculation functions likelihood of a given pixel over existing classes and considers the parameters such as mean, standard deviation, distance, variance and covariance. All the scenes for this classification were taken in the dry season, with least cloud cover and not to compare images different seasons, which could result in non-comparable results.

3.5.2 Validation of the classification

For the validation of this supervised classification, the matrix confusion method was used, this matrix allows confronting the ground truth the results of Classification and evaluate the classification accuracy compared to the reference on field as a table (or matrix).

The evaluation of classifications was performed by analyzing the confusion matrix established from samples obtained from the map from the supervised classification and a card made from photo-interpretation of an image from Landsat georeferenced images (Reality on the ground)

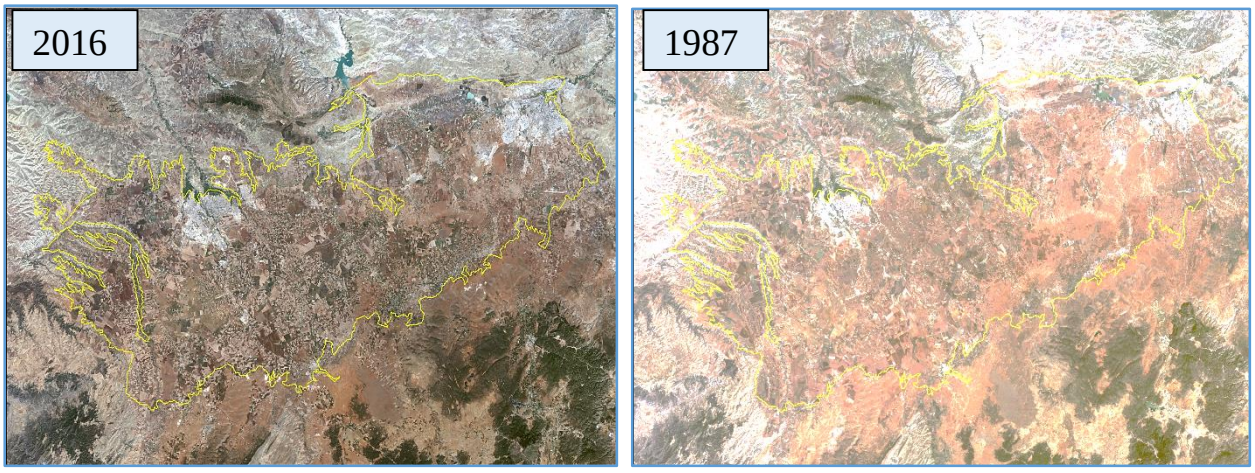

Figure 4.22: Landsat images of 2016 and 1987

The confusion matrix which is a double-entry table (contingency table) calculated by comparing the results from the supervised classification and those of the photo- interpretation of the Google Earth image granted as reality on the ground.

The columns of the matrix represent the sampling classes from (Image Google Earth-ground realities), and the lines represent the classes from the supervised classification. Crossing the values indicate the number of pixels (or % of pixels) belonging each learning class and assigned to the resulting classes, tables (4.9 and 4.10), and table (4.11) shows the generalized summary of points used for the classification of 1987 and 2016 land use maps.

The matrix cells are the number of pixels at each affiliated classes in the classified map and the reference card. In the diagonal was the number correctly classified pixels and the sum is the total number of pixels correctly classified. The pixels on the diagonal are classified, there is agreement between truth field and carried mapping and out of the diagonal, are the errors of classification, errors classifications were totaled and divided by the total marginal.

Errors of omission if reference points of a category are assigned to another category and commission Errors otherwise were points of a class to which they were erroneously assigned.

The errors of omission were considered as a way to judge the assignment (classification) and errors of commission as a way to improve this assignment.

The overall matrix tables provided the values of Kappa Index of Agreement (KIA), which is a relative accuracy index (Foody, 2002). When the: KIA = -1, the agreement is null, KIA = 0, the correlation is not significant and KIA = 1, the correlation is very strong.

The evaluation of the supervised classification was finally made with the coefficient kappa. It measures the residual quantity of the error obtained by classification.

The kappa value is between 0 and 1 (Cohen, 1960). The table shows confusion matrix for each class level reliability and major confusion made during image classification. For all classes defined, there was confusion is to say, the pixels of some units and use were confused with others. This matrix gave statistically acceptable and excellent indices of 0.979 and 0.993 for land use classification of 1987 and 2016 respectively.

Table 4.9: Confusion matrix of the different pixels of land use - 1987

Classification	Reality on ground								Precision user	Error ommision
	1	2	3	4	5	6	7	8		
1	1397	0	0	0	0	0	0	0	1397/1397	0/1397
2	0	158	0	0	0	0	0	0	158/158	0/158
3	0	0	836	0	0	0	0	0	836/836	0/836
4	0	0	1	4287	11	0	16	0	4287/4315	28/4324
5	22	0	0	20	408	0	0	52	408/502	94/502
6	0	0	0	10	0	1079	0	1	1079/1090	11/1090
7	0	0	0	0	0	0	1169	0	1169/1169	0/1173
8	0	0	0	0	96	0	0	6416	6416/6512	96/6512
IPC (%)	97	100	99.88	99.21	79.22	100	98.65	99.18		
PP	1397/1420	158/160	836/840	4287/4321	408/520	1079/1085	1169/1192	6416/6477	**Kappa Index = 0.979**	
Error Omissin	22/1420	0/160	1/840	30/4321	107/520	0/1085	16/1192	53/6477		

Table 4.10: Confusion matrix of the different pixels of land use - 2016

Classification	Reality on ground								Precision User	Error commision
	1	2	3	4	5	6	7	8		
1	1095	0	0	0	0	0	0	0	1095/1095	0/1095
2	5	2173	0	0	0	0	0	0	2173/2178	5/,2178
3	0	0	146	0	0	0	0	0	146/146	0/146
4	0	0	0	62	0	0	0	0	62/62	62/62
5	0	0	0	0	1737	0	0	0	1737/1737	0/1737
6	0	0	0	0	0	762	0	0	762/762	0/762
7	5	0	0	0	0	0	1582	0	1587/1587	5/1587
8	0	0	0	0	0	1	29	3916	3916/3946	30/3946
IPC(%)	*97*	*100*	*100*	*100*	*100*	*99.87*	*98.2*	*100*		
PP	1095/1105	2173/2173	146/146	62/62	1737/1737	762/763	1582/1611	3916/3916	**Kappa index = 0.993**	
Error ommision	10/1105	0/2173	0/146	0/62	0/1737	1/763	29/1611	0/3916		

Key: 1-Open water 2- Range lands 3- Orchards 4- Arable lands 5-Olives trees

6- Irrigated lands 7-Urban 8- Forests PP- precision production

Table 4.11: Land use class distribution summary for 1987 and 2017

Classification	1987	2016
Open water	3,097 points (0.055%) (2,515,538.2500 M²)	4,508 points (0.089%) (4,057,200.0000 M²)
Arable lands	171,028 points (3.042%) (138,917,493.0000 M²)	373,297 points (7.357%) (335,967,300.0000 M²)
Orchards	280,510 points (4.989%) (227,844,247.5000 M²)	733,381 points (14.454%) (660,042,900.0000 M²)
Range lands	3,870,025 points (68.825%) (3,143,427,806.2500 M²)	1,713,801 points (33.777%) (1,542,420,900.0000 M²)
Olives	770,441 points (13.702%) (625,790,702.2500 M²)	1,640,076 points (32.324%) (1,476,068,400.0000 M²)
Irrigated lands	82,824 points (1.473%) (67,273,794.0000 M²)	58,322 points (1.149%) (52,489,800.0000 M²)
Urban	48,557 points (0.864%) (39,440,423.2500 M²)	246,936 points (4.867%) (222,242,400.0000 M²)
Forests	386,429 points (6.872%) (313,876,955.2500 M²)	298,225 points (5.878%) (268,402,500.0000 M²)

Chapter 5: RESULTS AND DISCUSSION

5.1 Introduction

This chapter presents results and discussions of majorly two distinct sections; land use change analysis from 1978 to 2016 and WetSpass' simulated average spatially distributed seasonal and annual water balance components of Evapotranspiration, Surface run-off, Groundwater recharge and Interception under different land use conditions of 1987 and 2016, and discussion of individual variation due land use change during the study period.

5.2 Spatio-temporal Variation of the Land Use between 1987 and 2016

The diachronic study of the variation of the land use in Saiss plain was performed through classifications of two images at our disposal and covering a period of 29 years from 1987 and 2016, whose results were validated by the confusion matrix between the pixels of the land cover maps derived from the photo-interpretation of the Google Earth image and the results of supervised classification, which indicated satisfactory results with Kappa index of agreement of 0.979 and 0.993 for land use classification of 1987 and 2016 respectively, with eight (8) land use classes, Arable lands, Forests, Irrigated lands, Olive trees, Orchard, Range lands, Urban and open water . The results of the classification of Landsat TM and ETM + are represented in the (figures 5.1)

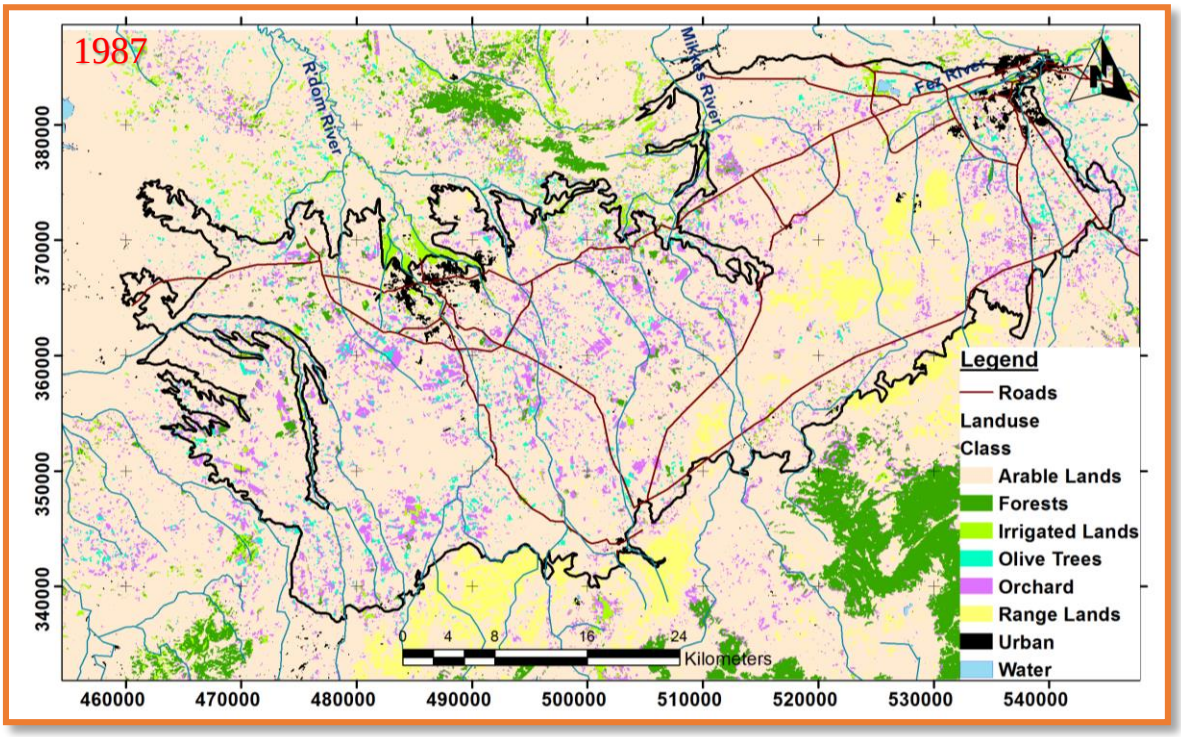

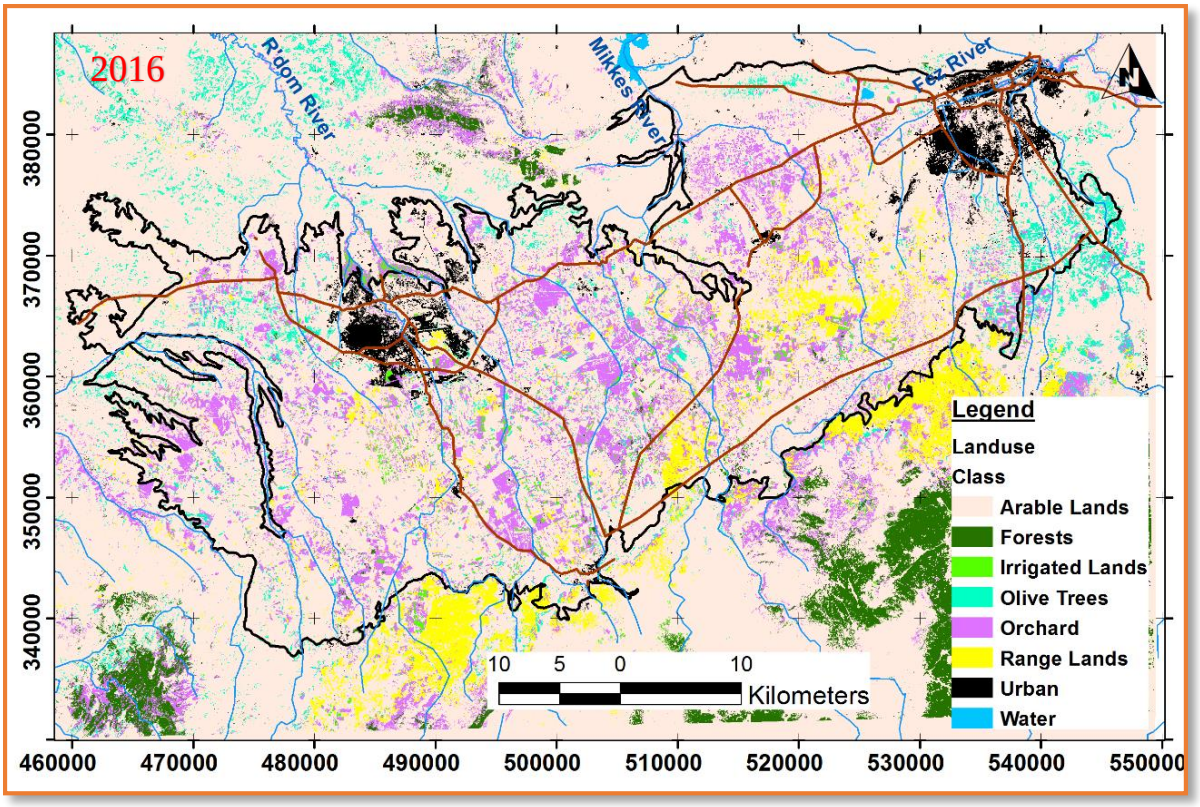

Figure 5.1: Evolution of land use in the Saiss plain between 1987 and 2016

Table 5.1: Land use change analysis between 1987 to 2016

LAND USE CLASS	1987 AREA (Km^2)	2016 AREA (Km^2)	CHANGE (2016-1987)	% CHANGE
Water	1.45	0.97	-0.48	**-33**
Range lands	65.06	115.76	50.70	78
Orchard	197.14	392.55	195.41	99
Irrigated lands	29.44	54.77	25.32	86
Urban	30.42	70.24	39.82	131
Forest lands	20.27	6.20	-14.07	**-69**
Olive trees	49.41	99.50	50.08	101
Arable lands	1,743.00	1,396.31	-346.70	**-20**

To get an idea of the spatial and temporal variation in the basin's land use changes between 1987 and 2016, areas of different types of land use and their corresponding percentages, were calculated

for each class surfaces of the two images, then the difference between them analyzed, (Table 5.1) shows the summary of the area change percentages per class.

From Table 5.1, land cover reveals significant changes between 1978 and 2016, in the individual land use classes, in the year 1987, arable land was the highest land use type by proportion and within a span of 29 years, it drastically decreased by -20% (347 km^2), followed by forest land reduction by -69 % (14 km^2) and open water surface reduction by -33% (0.48 km^2) in that sense, on the contrary there has been expansion of Urban by + 131% (40 km^2), Irrigated land by + 86% (25 km^2), range lands increased by +78% (51 km^2), Orchard fields expanded by + 99% (195 km^2), Olive tree plantations increased by 101 % (50 km^2). The dynamics of land use changes clearly show that the study area has experienced great changes in the transformations of land, the previously idle arable land converted into agricultural lands (Olives, Orchard and irrigated lands), the presence of Urban areas in the fields of agriculture shows an intrusion of local population with the urge to diversify agriculture which currently among the key economic activity in the study area. The decrease in the open water surface is attributed to drying up and shrinking of some rivers due to the influence of climate change that caused an increase of 1 ^oC of temperature as stated by (Benaabidate and Cholli, 2011).

In general, about 65 % of the total area of the Saiss basin currently is covered by agricultural related activities (Olives, Orchards, pasture, irrigated lands) while the remaining portion account for Urban areas, some arable lands especially in the hilly areas.

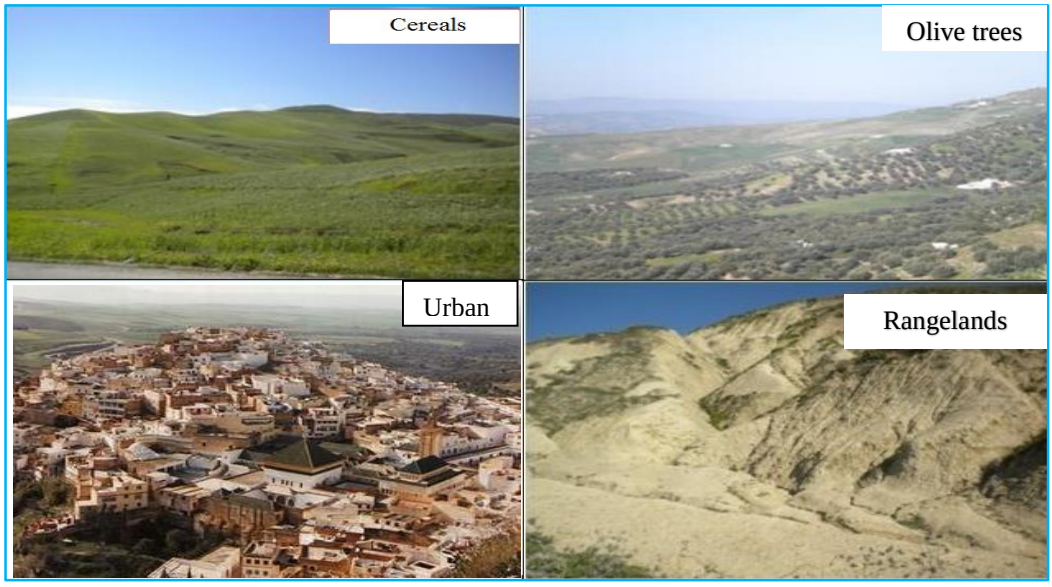

Figure 5.2: Landscapes corresponding to different types of land use characteristics

5.3 WetSpass simulated water balance components and analysis

The WetSpass model simulated spatially distributed mean values of the main water balance components of Actual evapotranspiration(E_a), surface run-off (R_o), ground water recharge(Rr) and Interception(I_r) for the study period of 29 years from 1987 to 2016, using long-term averaged input parameters mentioned earlier. The simulated results are presented on both seasonal scale (wet and dry) and annual scale for the entire study period.

All the output results from the model were represented in form of raster grid maps, from which every pixel constituted a magnitude of the individual water balance component, for this research a pixel size of (100m x 100m) was adopted, all expressed as a layer depth(mm), which were transformed into million cubic meters of water (Mm^3), by multiplying by the aquifer basin limit area.

For the purpose of seasonal variation analysis, two seasons were selected basing on two extreme conditions of dryness and wetness, the dry season was defined to be the four months of june, July, August and September, with minimal precipitation and the wet season, four months that received highest precipitation, November, December, January and February to give a vivid difference in water balance analysis.

The water balance results here represented and analyzed are based on majorly five water balance components, precipitation, actual evapotranspiration, surface run-off, interception and ground water recharge. Precipitation as the only inflow component into the system and the rest of the components as outflow of the system, precipitation determines and shapes how much water is portioned into other components which in turn depend on various factors. For instance, surface run off depends much on the slope, steep area generates a lot of run off unlike flat or low slope areas, also depends on the type of vegetation and soil type at hand.

Ground water recharge on the other hand depends on the soil type and condition, soils with high retention capacity hold more water and attracts more unlike clay high content soils that do not easily allow water to infiltrate through. Additionally, the vegetation cover also plays a role on improving the soil water holding capacity, as it impends the speed of running water allowing more water to percolate. while as evapotranspiration and interception are majorly dependent on solar radiation and vegetation cover respectively.

5.3.1 Dry season simulated water balance components for 1987 and 2016

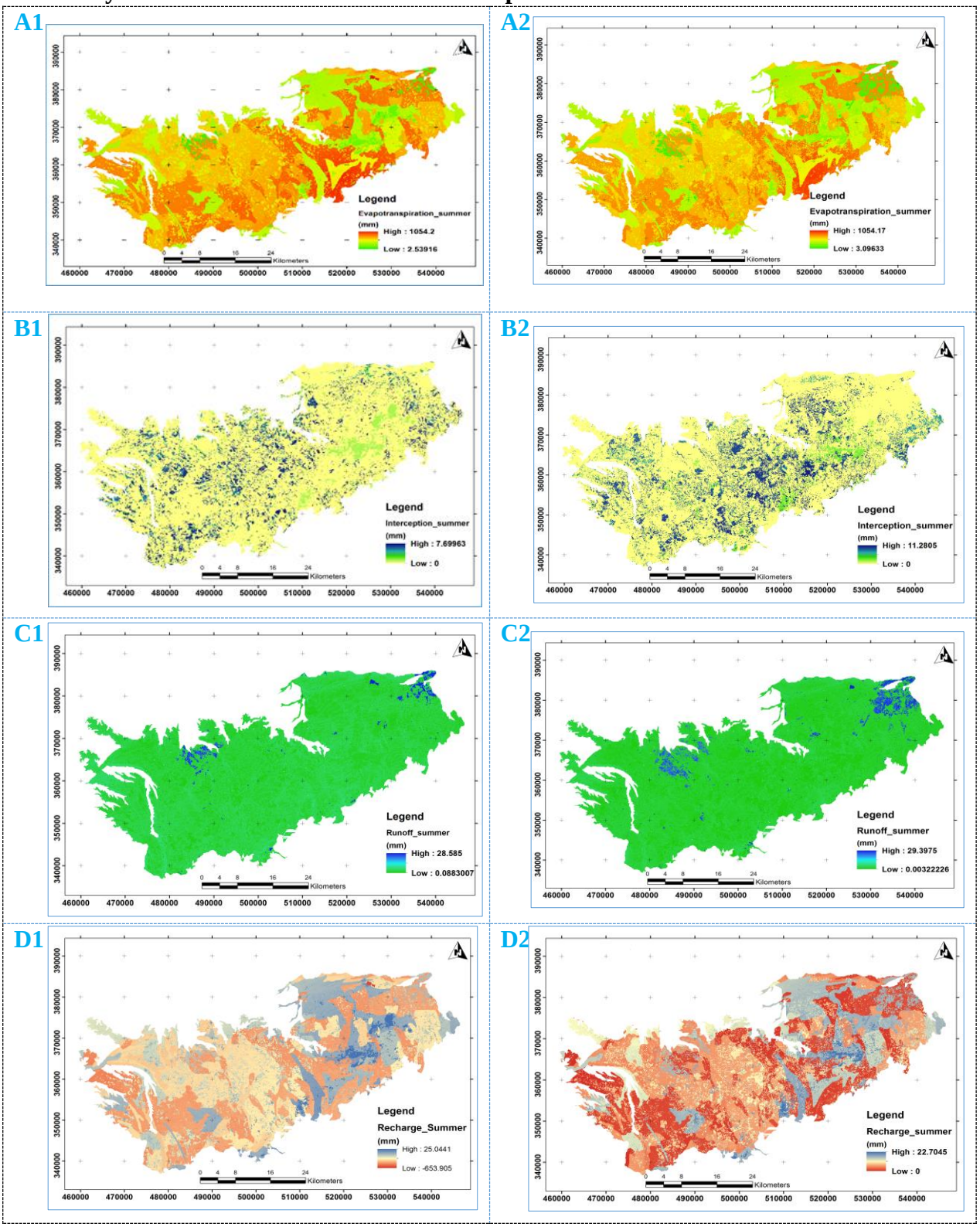

Figure 5.3: Summer simulated, E_a, I_r, R_o, R_e, (A1, B1, C1, D1)-1987 - (A2, B2, C2, D2) -2016

Table 5.2: WetSpass calculated dry season water balance components for 1987

Water balance component	Min	Max	Range	Mean (mm)	STD	% Precipitation	MEAN
Precipitation (P)				28.95			(Mm3/season)
Evapotranspiration (Ea)	2.53	1,054.24	1,051.71	**17.96**	4.94	62	**38.36**
Surface Run-off (Ro)	0.09	28.58	28.49	**1.00**	1.36	3	**2.14**
Interception (Ir)	0	7.69	7.69	**0.92**	3.09	3	**1.97**
Ground water recharge(Re)	-653.9	25.04	678.94	**10.19**	6.04	35	**21.77**
Water balance WB= P-Ea-Ro-Re				**-1.12**			
Error in water balance (WB/P) %				**-3.87**			

Table 5.3: WetSpass calculated dry season water balance components for 2016

Water balance component	Min	Max	Range	Mean (mm)	STD	% Precipitation	MEAN
Precipitation (P)				28.95			(Mm3/season)
Evapotranspiration (Ea)	3.09	1,054.17	1,051.08	**19.53**	5.02	67	**41.72**
Surface Run-off (Ro)	0.00	29.39	29.39	**0.77**	1.84	3	**1.64**
Interception (Ir)	0.00	11.28	11.28	**1.84**	3.23	6	**3.93**
Ground water recharge(Re)	0.00	22.70	22.70	**8.64**	6.92	30	**18.46**
Water balance WB= P-Ea-Ro-Re				**-1.84**			
Error in water balance (WB/P) %				**-6.34**			

Table 5.4: WetSpass calculated Wet season water balance components for 1987

Water balance component	Min	Max	Range	Mean (mm)	STD	% Precipitation	MEAN
Precipitation (P)				206.75			(Mm3/season)
Evapotranspiration (Ea)	58.68	206.01	147.33	**100.13**	26.17	48	**213.88**
Surface Run-off (Ro)	13.02	204.45	191.43	**34.35**	30.22	17	**73.37**
Interception (Ir)	0	16.00	16.00	**2.09**	14.30	1	**4.46**
Ground water recharge(Re)	0	143.79	143.79	**64.11**	21.12	31	**136.94**
Water balance WB= P-Ea-Ro-Re				**8.16**			
Error in water balance (WB/P) %				**3.95**			

Table 5.5: WetSpass calculated Wet season water balance components for 2016

Water balance component	Min	Max	Range	Mean (mm)	STD	% Precipitation	MEAN
Precipitation (P)				206.75			(Mm3/season)
Evapotranspiration (Ea)	83.39	206.09	122.70	**102.97**	24.41	50	**219.94**
Surface Run-off (Ro)	1.00	210.32	209.32	**9.60**	23.01	5	**20.51**
Interception (Ir)	0.00	46.34	46.34	**8.23**	15.40	4	**17.58**
Ground water recharge(Re)	0.00	149.42	149.42	**80.88**	25.38	39	**172.76**
Water balance WB= P-Ea-Ro-Re				**13.30**			
Error in water balance (WB/P) %				**6.43**			

5.3.2 WetSpass simulated Wet season water balance for 1987 and 2016

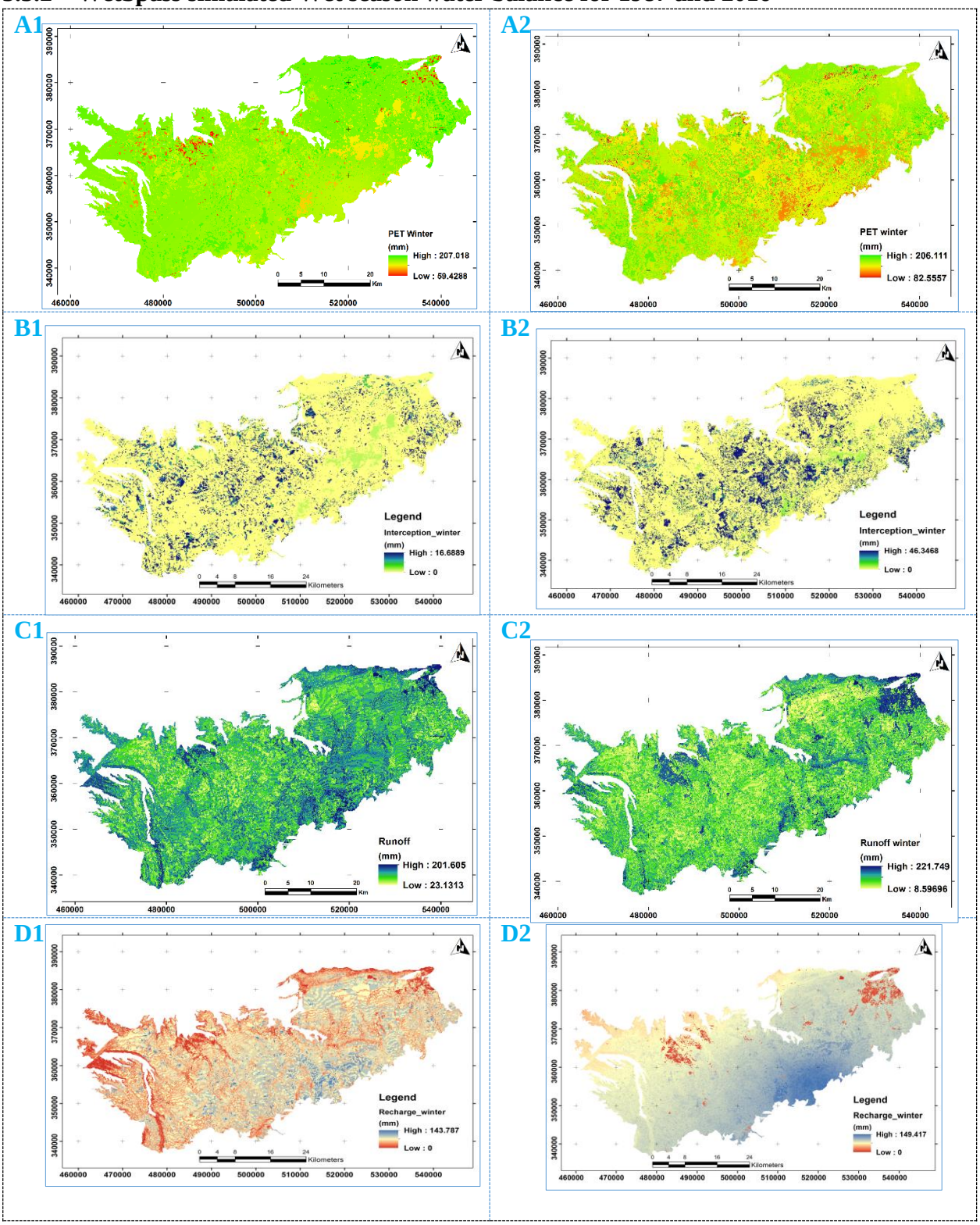

Figure 5.4: Wet simulated, E_a, I_r, R_o, R_e, (A1, B1, C1, D1)-1987 and (A2, B2, C2, D2) -2016

5.3.3 Average Annual WetSpass simulated water balance components (1987-2016)

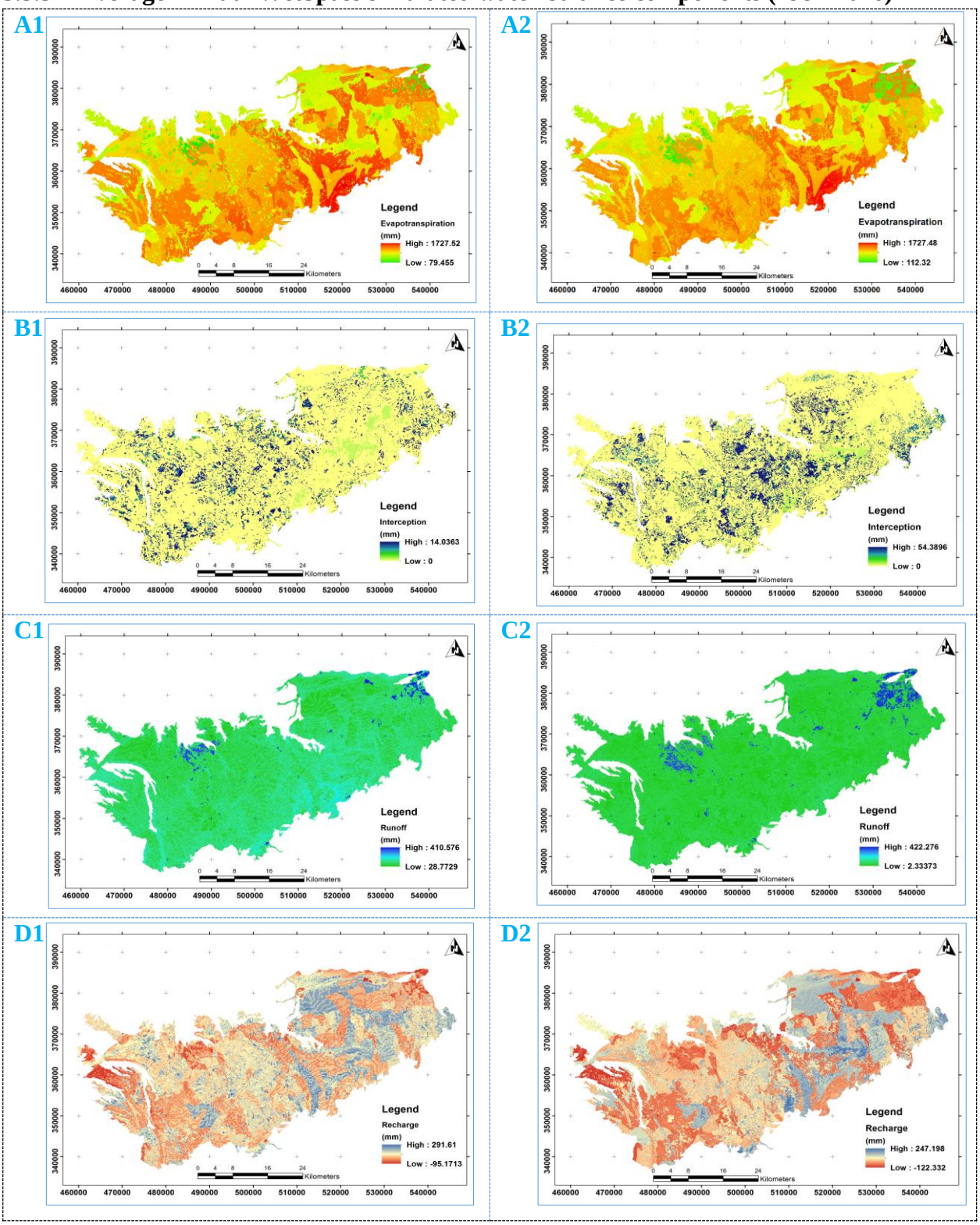

Figure 5.5: Annual simulated, E_a, I_r, R_o, R_e, (A1, B1, C1, D1)-1987 and (A2, B2, C2, D2) -2016

Table 5.6: WetSpass calculated Annual water balance components for 1987

Water balance component	Min	Max	Range	Mean (mm)	STD	% Precipitation	MEAN
Precipitation (P)				409.50			(Mm3/Yr)
Evapotranspiration (Ea)	79.45	1,727.52	1,648.07	**205.29**	46.16	50.13	**438.50**
Surface Run-off (Ro)	28.77	410.58	381.81	**76.19**	29.80	18.61	**162.74**
Interception (Ir)	0	14.04	14.04	**1.77**	15.31	0.43	**3.78**
Ground water recharge(Re)	-95.17	291.61	386.78	**126.38**	35.37	30.86	**269.95**
Water balance WB= P-Ea-Ro-Re				**-0.13**			
Error in water balance (WB/P) %				**-0.03**			

Table 5.7: WetSpass calculated Annual water balance components for 2016

Water balance component	Min	Max	Range	Mean	STD	% Precipitation	MEAN
Precipitation (P)				**409.50**			(Mm3/Yr)
Evapotranspiration (Ea)	112.32	1,727.48	1,615.16	**273.65**	47.89	67	**584.52**
Surface Run-off (Ro)	2.33	422.27	419.94	**26.35**	42.55	6	**56.28**
Interception (Ir)	0	54.38	54.38	**4.29**	16.69	1	**9.16**
Ground water recharge(Re)	-122.33	247.00	369.33	**107.53**	43.00	26	**229.68**
Water balance WB= P-Ea-Ro-Re				**1.97**			
Error in water balance (WB/P) %				**0.48**			

Actual evapotranspiration (E_a)

WetSpass model simulated actual evapotranspiration as a total of all evaporative elements of interception, bare soil evaporation, open water surfaces and vegetation transpiration. The average annual simulated results of actual evapotranspiration of the Saiss aquifer plain as indicated in the (figure 5.5) and depicted by the tables (5.2 -5.7), were in the range 79.45 mm to 1727.52 mm, with a mean value of 205.29 mm (438.50 Mm^3), standard deviation 46.16 and with 50% as fraction of the mean annual precipitation for the year 1987, while as for the year 2016, the results were in the range 112.32 mm to 1727.48 mm, with a mean value of 273.65 mm (584.52 Mm^3), standard deviation 47.89 and with 67% as fraction of the mean annual precipitation. Seasonal values in the dry period and wet period were respectively with means 17.96 mm (38.36 Mm^3) and 19.53 mm (41.72 Mm^3) in 1987 and 100.13 mm (213.88 Mm^3) and 102.97 mm (219.94 Mm^3) in 2016.

For both years of study, the actual evapotranspiration accounted for the highest proportion of water loss from the basin, these results are similar to related studies as also observed by (Kuisi *et al*., 2013 and Pan *et al.*, 2011), this is always true and majorly caused by high solar radiation which is averagely constant within the year and dry hot winds, and it is the main reason why the two mean values for both seasonal and annual for the two years 1978 and 2016 are nearly the same. The

spatially distributed actual evapotranspiration as indicated on maps in (figures 5.3 5.4 and 5.5) show that the high values are in the southern and central part which are majorly covered by vegetation and low values in the urbanized areas in the north east and northwest of the study area.

Interception (I_r)

Interception takes place due to presence of vegetative cover, its size broad or narrow and the growth rate. The shedding off of leaves cause a local reduction in the interception percentage (Babama, 2013), thick forests intercept and loose more water through transpiration than sparse forests, pastures and short crops.

The spatial seasonal and annual average interception in the Saiss plain as shown in the map (5.3-5.5), with summarized values indicated in the tables (5.2 -5.7), for annual values, were in the range 0 mm to 14.0 mm, with a mean value of 1.77 mm (3.78 Mm^3), standard deviation 15.31 and with 0.4 % as fraction of the mean annual precipitation for the year 1987, while as for the year 2016, the results were in the 0 mm to 54.38 mm, with a mean value of 4.29 mm (9.16 Mm^3), standard deviation 16.69 and with 1% as fraction of the mean annual precipitation. While as on seasonal scale, WetSpass model, estimated mean values of 0.92 mm and 1.84 mm for 1987 and 2.1 mm and 8.23 mm for 2016 respectively for dry and wet periods, with the highest proportion of seasonal precipitation of 4 % occurring in winter. The increase in the interception from 1987 to 2016, is attributed to land use change that almost increased the vegetated area by 65%. From the spatial maps (5.3 – 5.5), high interception was observed in the central and south eastern region which are highly vegetated and agricultural zone in the basin.

Surface run-off (R_o)

For estimation of surface run off of the catchment, WetSpass model uses the runoff coefficients generated in the look up table linked to the input soil map and land use map, these coefficients depend on types of vegetation, texture of the soil and slope (Batelaan *et al.*, 2003). The annual simulated mean surface runoff in the basin ranges from 28.77 mm to 410.58 mm, with a mean value of 76.19 mm (162.74 Mm^3), standard deviation 29.80 and with 18 % as fraction of the mean annual precipitation for the year 1987, while as for the year 2016, the results were in the range 2.33 mm to 422.27 mm, with a mean value of 26.35 mm (56.3 Mm^3), standard deviation 42.55 and with 6% as fraction of the mean annual precipitation. The noticeable reduction in the surface run

off is due to conversion of arable lands by -20% during the 29-year period and also opening up agricultural fields that led to improvement of the soil water holding capacity due to continuous tillage in addition to the increased vegetation that retards the flow of water thus reducing the amount surface run off.

From the maps (5.3 – 5.5) respectively for 1987 and 2016, the spatial run off distribution across the basin shows that the urbanized areas have high run off while as the central low plain zone with sand and sandy loam soils has lowest values of surface run off because of the high permeability of the soils, low run off is also observed in cultivated areas in the basin.

Ground water recharge (Rr)

Ground water recharge like surface run off depends also on soil texture, terrain, plant cover, water table depth and presence of permeable or impermeable surfaces, the basin long term annual and seasonal recharge averages were simulated under different land use conditions, 1987 and 2016 tables (5.2 – 5.7). The annual mean values for the year 1987 varied from -95.17 mm to 291.61 mm, with mean value of 126.38 mm (269.95 Mm^3), standard deviation of 35.37 and with 31 % as fraction of precipitation, while as for the year 2016, the results were in the range -122.3 mm to 247.0 mm, with a mean value of 107.53 mm (229.7 Mm^3), standard deviation 43.0 and with 26 % as fraction of the mean annual precipitation, additionally table (5.2 – 5.5) show average wet period recharge of 64.11 mm (136.94 Mm^3) and 80.88 mm (172.76 Mm^3) for 1987 and 2016 respectively and dry period averages were 10.19 mm (21.77 Mm^3) and 8.64 mm (18.46 Mm^3).

The negative annual recharge rate occurred in regions characterized by habitats in the city centers of Fes and Meknes, due to presence of impervious surfaces and in the southern zone with high elevation and in clay soil texture localities whiles higher ground water recharge rates were register flood plains in the central areas and in the agricultural gazetted areas. This variation in the recharge rates is also attributed to the spatial variation of soil types and land use practices. The negative recharge rates which were mainly observed in the summer season, may have happened due excessive loss of precipitation through the evaporative processes of transpiration, soil evaporation and withdraw moisture by the plant during this very hot period. Basing on annual recharges maps (figure 5.5), high recharge rates occurred cultivated low lands with loam soils and sandy soils and in the flat plain, minimum recharge observed in the built up areas in the northeast and northwest zones.

5.4 Impact of land use change on water balance components.

The WetSpass model was run separately under two land use conditions to quantity the differences between the simulated water balance components due to land use from 1987 to 2016 covering a period of 29 years. The average annual and seasonal components of actual evapotranspiration , surface runoff , interception and recharge were first simulated under land use condition of 1987 and then keeping all the model validated parameters and input files constant, except for the new land use condition 2016, the model simulated second set of respective components to give the differences and hence the impacts due to land use change (table 5.8), shows the individual components percentage changes and figures (5.6 and 5.7) show the variation of the simulated summer , winter and annual average values of the four major components in consideration , all compared with the mean precipitation values.

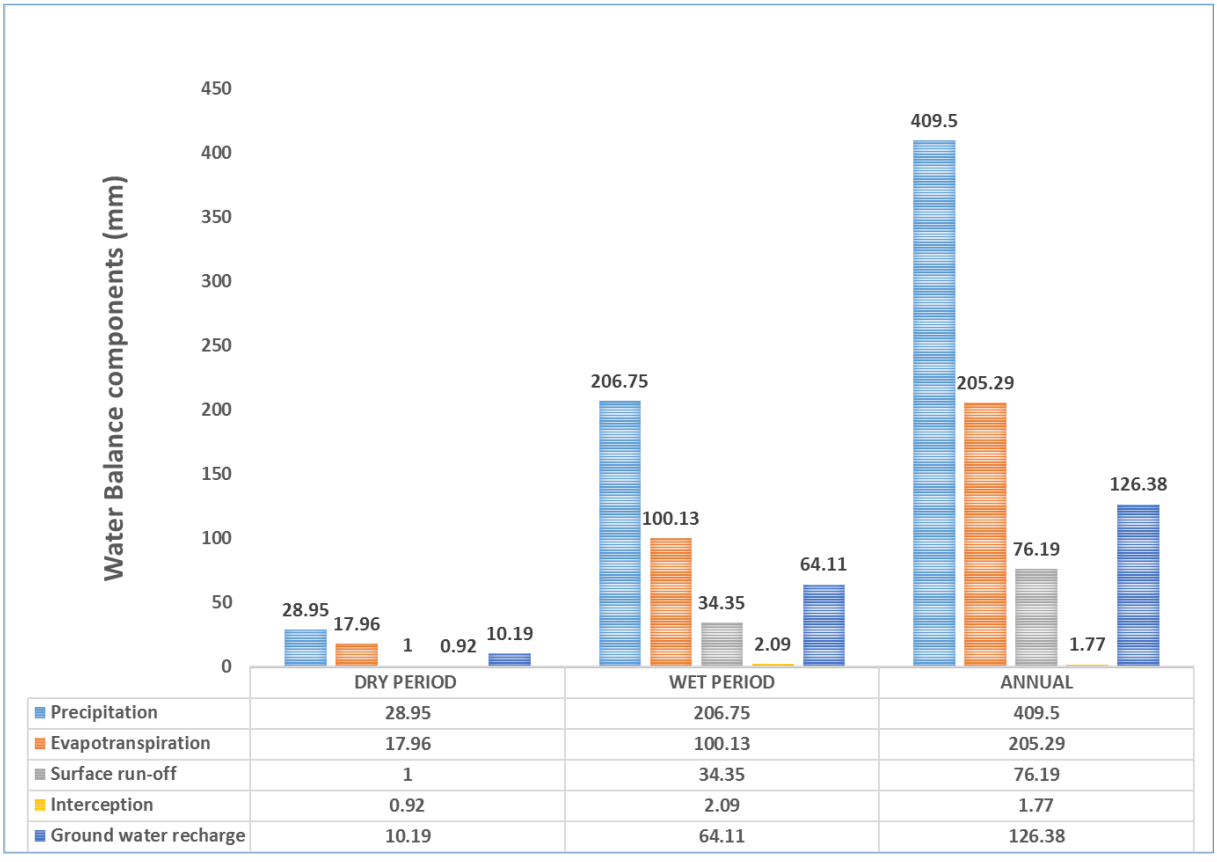

	DRY PERIOD	WET PERIOD	ANNUAL
Precipitation	28.95	206.75	409.5
Evapotranspiration	17.96	100.13	205.29
Surface run-off	1	34.35	76.19
Interception	0.92	2.09	1.77
Ground water recharge	10.19	64.11	126.38

Figure 5.6: Variation of average seasonal and annual water balance -1987

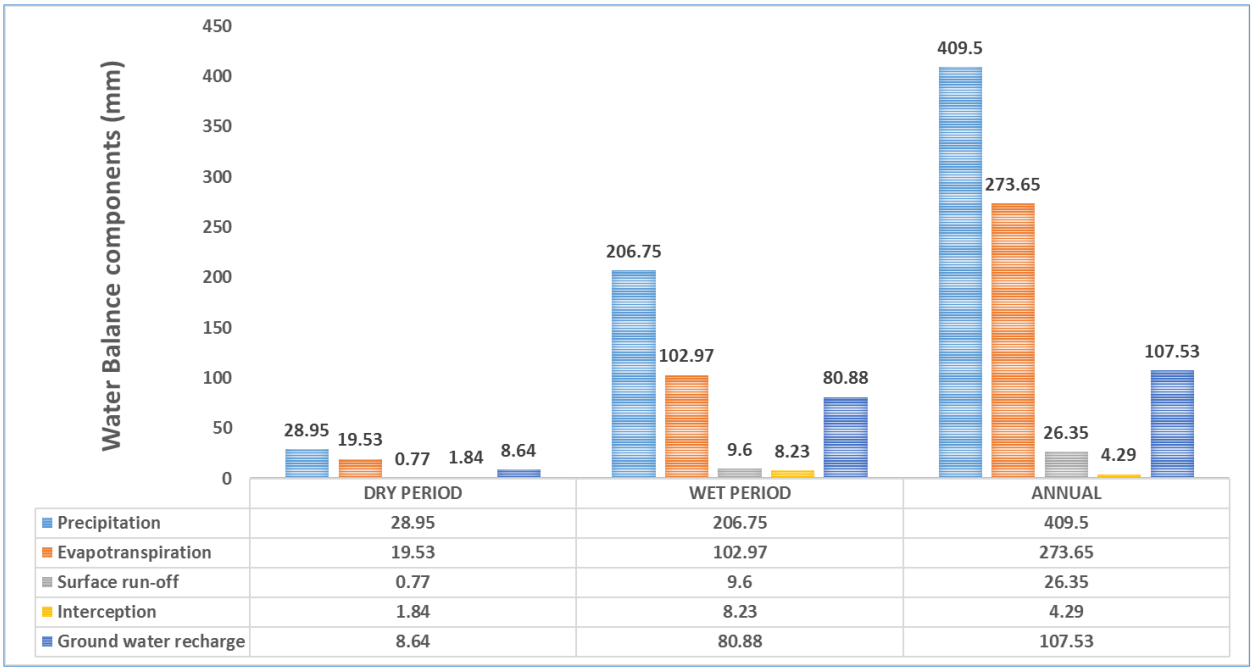

Figure 5.7: Variation of average seasonal and annual water balance -2016

Table 5.8: Seasonal and annual water balance change during the study period

Water balance component (mm)	**DRY PERIOD**			**WET PERIOD**			**ANNUAL**		
	1987	2016	**%Change**	1987	2016	**%Change**	1987	2016	**%Change**
Evapotranspiration (Ea)	17.96	19.53	**8.7**	100.13	102.97	**2.8**	205.29	273.65	**33.3**
Surface Run-off (Ro)	1.00	0.77	**-23.0**	34.35	9.60	**-72.1**	76.19	26.35	**-65.4**
Interception (Ir)	0.92	1.84	**100.0**	2.09	8.23	**293.8**	1.77	4.29	**142.4**
Ground water recharge(Re)	10.19	8.64	**-15.2**	64.11	80.88	**26.2**	126.38	107.53	**-14.9**

From the table 5.8, it is evident that due to land use change between the two reference years of 1987 and 2016, the dry, wet period and annual averages of actual evapotranspiration increased by 8.7%, 2.8% and 33.3 % respectively, this was due to the increase in the vegetative cover, since vegetative cover related land use types increased by about 65%. The increases per land use class are of the order, open water surfaces, Orchard fields, irrigated lands, olive fields and range lands as indicted by figure 5.9, the evapotranspiration accounted for the best percentage by proportion of annual mean precipitation.

Surface run off in the contrary decreased in the by 23%,72% and 65%., the decrease may be interpreted as a result of increased farm lands that improved upon the soil retention capacities,

though there were individual increases at land use class level, especially in the urban areas, is attributed to the increase in the urbans areas at a rate of 131%, with impervious surfaces leading to reduction in the local recharge and a little more run off instead. While as an eventual decrease in the dry and wet seasons values were caused by the resultant between the evaporative losses during high precipitation and improved soil holding abilities in the cultivated zones which increased between 1987 and 2016. The order of surface runoff decreases per land use classes are as; forested lands, irrigated lands, range lands and last urban centers with higher values.

Interception increased throughout the dry, wet and annual by 100%, 294% and 142 % respectively, and this is in agreement with the increase in vegetation from 1987 to 2016, since interception majorly depends on foliage cover in order of forest, fruit trees and general agricultural crops.

Ground water recharge, due to land use change, exhibited a decrease in ground water recharge during the dry and annual by 15% and 15% while there was a slight increase in the ground water recharge during wet period by 26 %. The annual decrease in recharge may be caused by increase in urban surface area, that comes with impermeable surfaces that limit infiltration rates, and similarly increase in the vegetative covers as a results of increase in agricultural crops, fruit trees and forest land through the evaporative losses and water discharge by plants leading to local decrease in the ground water recharge. At basin level the decrease in recharge of 19 mm is not very significant, though at pixel scale there is significant variation in recharge, some place with low to high recharge, various studies have also noted this observation like (Mustafa, 2017 and Pan et al., 2011) and land use change is not the only factor causing the decrease in recharge.

To further investigate the impacts of land use change on the water balance of the Saiss basin, ArcGIS zonal statistics (spatial analyst tools) was applied to extract water balance components per each land use class for both 1987 and 2016, figure (5.8 and 5.9), there was noticeable changes in the water balance simulated by each land use class for the two land use conditions, as shown by the figures, actual evapotranspiration highest from the open water surfaces and if examined between the two years there was change from 63% (1987) to 52 %(2016), interception in both condition recorded highest in the order orchards , olive trees, forestland and urban, though there are still differences within and across the boundary years. Surface run off noticeable in urban areas, and also exhibited changes between the two years, from 21% to 19% by proportion.

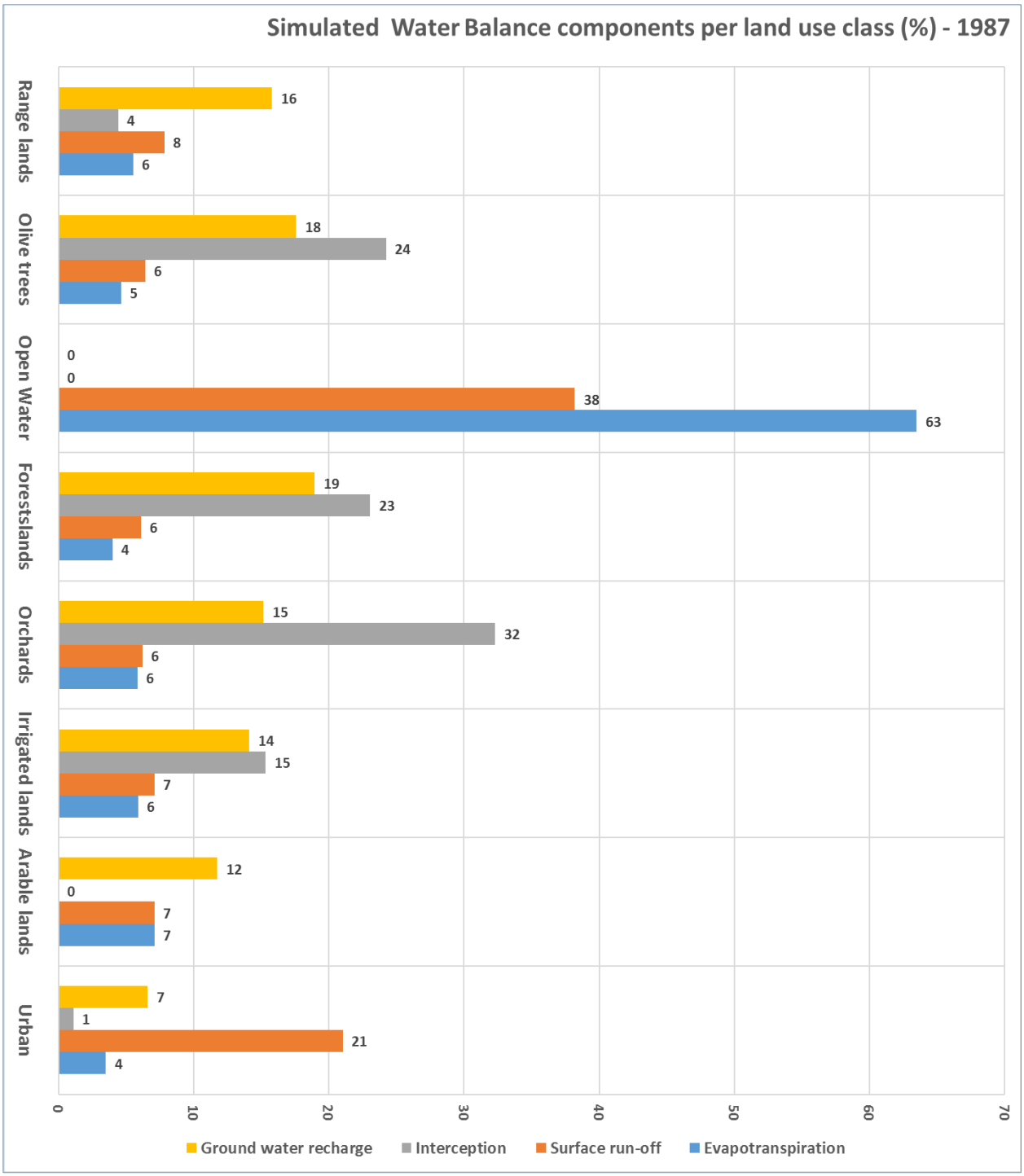

Figure 5.8: Simulated water balance components under different land use classes in 1987

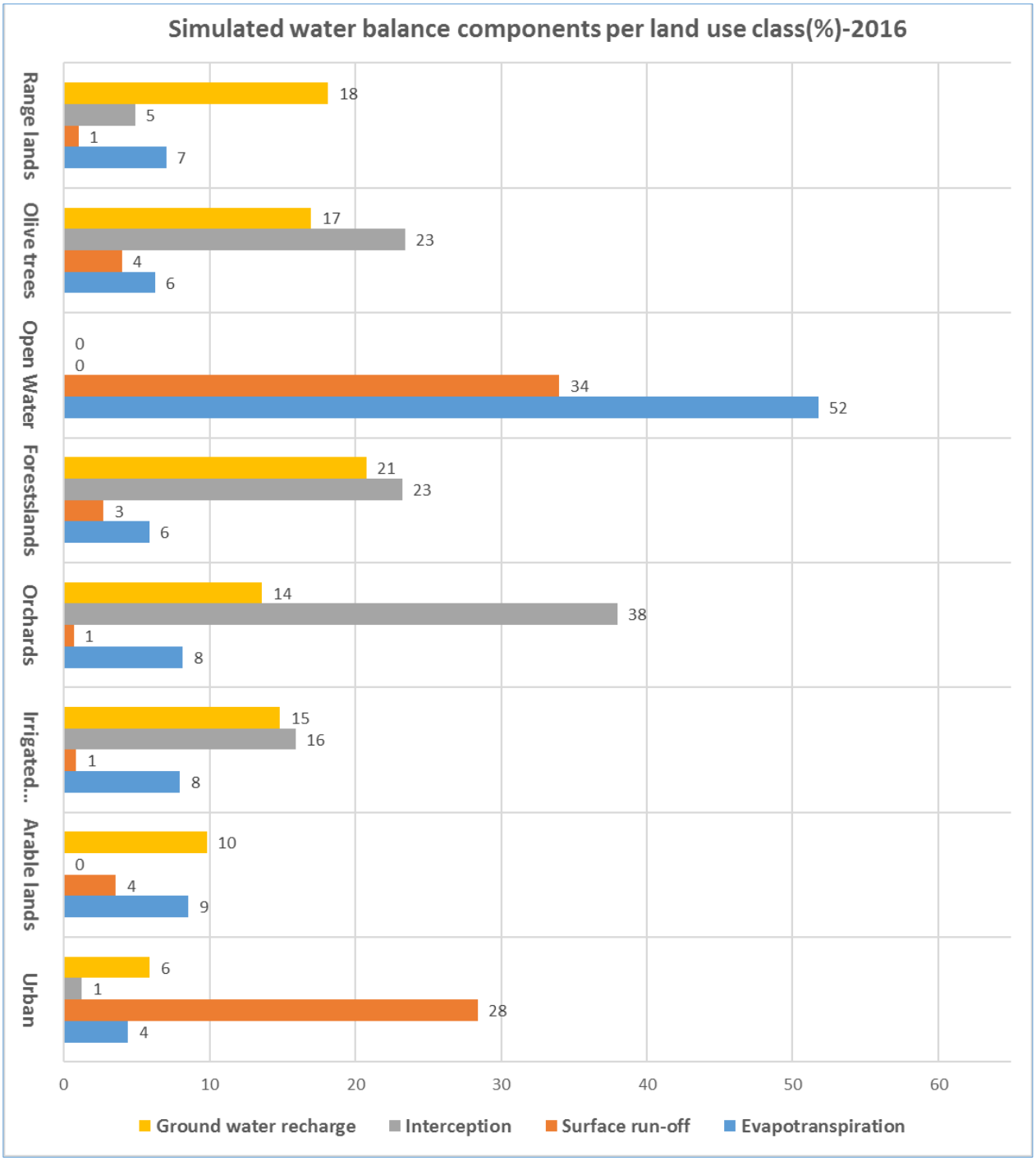

Figure 5.9: Simulated water balance components under different land use classes in 2016

5.5 WetSpass model validation analysis

For this study, the model was calibrated by comparing observed average annual ground water depth obtained from several piezometers within the study area for the period 1978 to 2016, a series of simulated ground water depth by the WetSpass were performed by manually adjusting the local model parameters whilst comparing with the calculated water depth, until a good fit was obtained between the observed and the calculated ground water depth, from the piezometers, with a correction R^2 of 0.948 and 0.960 for 1987 and 2016 respectively, as shown in the table (5.9 and 5.10). Related studies of (Woldeamlak et al., 2007 , Batelaan et al., 2003 and Mustafa, 2017) also used a similar method the validate the model.

Table 5.9. Comparison between measured and simulated ground water heads -1987

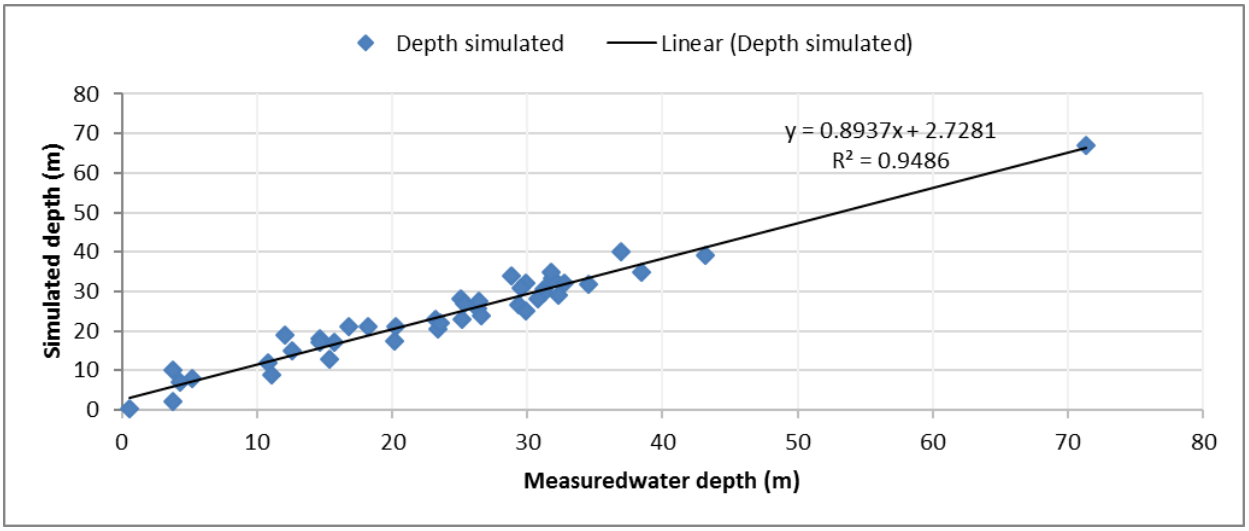

Table 5.10. Comparison between measured and simulated ground water heads -2016

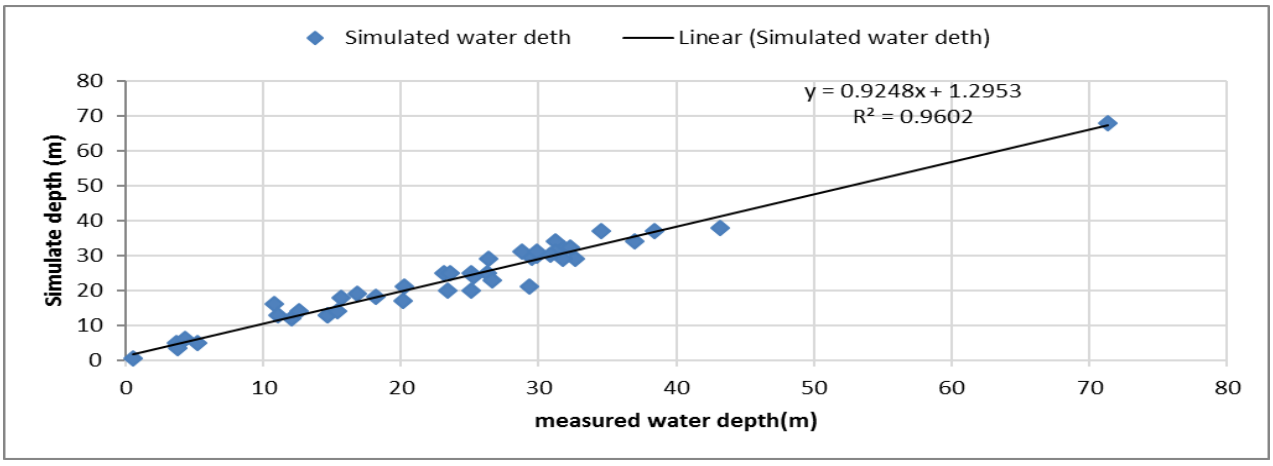

5.6 Results summary

The model simulated results for the two land use conditions of 1987 and 2016, indicated some considerable changes in the water balance components, an evidence that land use changes has impacted both positively and negatively on the water balance on the Saiss shallow aquifer basin.

The results are presented here as follows;

a. Actual evapotranspiration

For 1987

- Annual values range from 79.4 mm to 1727.4 mm, with a mean value of 205.3 mm (438.5 Mm^3), standard deviation 46.16 and with 40% as fraction of the mean annual precipitation.
- Wet season value range from 58.6 mm to 206 mm, with a mean value of 100.1 mm (213.9 Mm^3), standard deviation 26.17 and with 48% as fraction of the mean annual precipitation.
- Summer value range from 2.53 mm to 1054 mm, with a mean value of 17.9 mm (38.3 Mm^3), standard deviation 4.94 and with 62 % as fraction of the mean annual precipitation.

For 2016

- Annul value range from 112.3 mm to 1727 mm, with a mean value of 273.7 mm (584.5 Mm^3), standard deviation 47.89 and with 67% as fraction of the mean annual precipitation.
- Winter value range from 83.4 mm to 206 mm, with a mean value of 102.9 mm (219.9 Mm^3), standard deviation 24.41 and with 50% as fraction of the mean annual precipitation.
- Summer value range from 3.09 mm to 1054 mm, with a mean value of 19.5 mm (41.7 Mm^3), standard deviation 5.02 and with 67% as fraction of the mean annual precipitation.

b. Surface run off

For 1987

- Annual values range from 28.77 mm to 410.6 mm, with a mean value of 76.2 mm (162.7 Mm^3), standard deviation 29.80 and with 18 % as fraction of the mean annual precipitation.
- Wet period value range from 13.0 mm to 204.5 mm, with a mean value of 34.4 mm (734 Mm^3), standard deviation 30.22 and with 45% as fraction of the mean winter precipitation.
- Dry period value range from 0.09 mm to 28.5 mm, with a mean value of 1 mm (2.14 Mm^3), standard deviation 1.36 and with 3 % as fraction of the mean summer precipitation.

For 2016

- Annul value range from 2.33 mm to 422 mm, with a mean value of 26.4 mm (56.3 Mm^3), standard deviation 42.55 and with 20 % as fraction of the mean annual precipitation.
- Wet period value range from 1 mm to 210 mm, with a mean value of 9.6 mm (20.5 Mm^3), standard deviation 23.01 and with 5% as fraction of the mean winter precipitation.
- Dry period value range from 0 mm to 29.4 mm, with a mean value of 0.77 mm (1.64 Mm^3), standard deviation 1.84 and with 3 % as fraction of the mean summer precipitation.

c. Interception

For 1987

- Annual values range from 0.0 mm to 14 mm, with a mean value of 1.77 mm (3.8 Mm^3), standard deviation 15.31 and with 0.4 % as fraction of the mean annual precipitation.
- Wet period value range from 0.00 mm to 16. mm, with a mean value of 2.1 mm (4.4 Mm^3), standard deviation 14.3 and with 4% as fraction of the mean winter precipitation.
- Dry period value range from 0.0 mm to 7.6 mm, with a mean value of 0.92 mm (1.97 Mm^3), standard deviation 3.09 and with 3 % as fraction of the mean summer precipitation.

For 2016

- Annul value range from 0.0 mm to 54.38 mm, with a mean value of 4.3 mm (9.2 Mm^3), standard deviation 16.69 and with 1% as fraction of the mean annual precipitation.
- Wet period value range from 0.00 mm to 46.3 mm, with a mean value of 8.2 mm (17.6 Mm^3), standard deviation 15.40 and with 4 % as fraction of the mean winter precipitation.
- Dry period value range from 0.0 mm to 11.2 mm, with a mean value of 1.84 mm (3.93 Mm^3), standard deviation 3.23 and with 6 % as fraction of the mean summer precipitation.

d. Ground water recharge

For 1987

- Annual values range from -95 mm to 291.6 mm, with a mean value of 126.4 mm (269.9 Mm^3), standard deviation 35.37 and with 30 % as fraction of the mean annual precipitation.
- Wet period value range from 0 mm to 143.8 mm, with a mean value of 64.1 mm (136.9 Mm^3), standard deviation 21.12 and with 9% as fraction of the mean winter precipitation.

- Dry period value range from -653.9 mm to 25 mm, with a mean value of 10.2 mm (21.77 Mm^3), standard deviation 6.04 and with 44 % as fraction of the mean summer precipitation.

For 2016

- Annul value range from -122 mm to 247 mm, with a mean value of 107.5 mm (229.7 Mm^3), standard deviation 43.0 and with 26 % as fraction of the mean annual precipitation.
- Wet period value range from 0.0 mm to 149.4 mm, with a mean value of 80.9 mm (172.8 Mm^3), standard deviation 25.38 and with 9% as fraction of the mean winter precipitation.
- Dry period value range from 0.0 mm to 22.7 mm, with a mean value of 8.64 mm (18.46 Mm^3), standard deviation 6.92 and with 40% as fraction of the mean summer precipitation.

Considering annual average simulated water balance components, the results reveal that, there has been both negative and positive (decrease and increase) in the values of the water balance and these changes are directly linked to the changes in land use classes that have occurred during the 29 years.

- Actual evapotranspiration increased from **439 x 10^6** m^3 in 1987 to **585 x 10^6** m^3 in 2016, literally represented as 33 % increase.
- Surface run off decreased from **163 x 10^6** m^3 in 1987 to **56 x 10^6** m^3 in 2016, literally represented as 65 % decrease
- Interception increased from **4 x 10^6** m^3 in 1987 to **9 x 10^6** m^3 in 2016, literally represented as 142 % increase
- Ground water recharge decreased from **270 x 10^6** m^3 in 1987 to **230 x 10^6** m^3 in 2016, literally represented as 15 % decrease.

The results obtained in the study are related and quite consistent with similar studies in Africa; Tunisia,(Gafsa *et al.*, 2017), Ethiopia (Armanuos *et al.*, 2016,Tilahun and Merkel, 2009 and, Gebremeskel and Kebede, 2017), Chad (Babama, 2013), and many more all over the world including; (Batelaan *et al.*, 2003),(Pan *et al.*, 2011),(Mustafa, 2017),(Kuisi, *et al.*, 2013) and (Gharbia, 2013). WetSpass model validation was performed by comparing the measured ground water depth and simulated ground water level for the land use conditions of 1987 and 2016, and obtained acceptable agreements between the measured and simulated ground water depth, with correction coefficients of 0.948 and 0.960 respectively for the two boundary years.

CONCLUSION AND RECOMMENDATION

The main objective of this study was achieved by first studying the historical land use evolution of the study area for the period of 29 years from 1987 to 2016 to evaluate the land use changes that have occurred during this period and then simulated water balance components using water balance model. A spatially distributed water balance model, WetSpass was applied to simulate seasonal and annual average values of the main water balance components of actual evapotranspiration, surface run off, ground water recharge, using long term average climatological parameters of precipitation, temperature, potential evapotranspiration, wind speed and ground water depth, morphological and elevation characteristics of the study area.

To quantify the impact of land use change on water balance of the Saiss basin, the WetSpass was run separately under the two land use conditions of 1987 and 2016 and the two model output results compared and the simulated water balance components per land use class analyzed.

The results from this study revealed that, there has been significant land use changes between 1987 and 2016 and the model simulated results for the two land use conditions of 1987 and 2016, indicated some considerable changes in the water balance components, an evidence that land use changes has impacted both positively and negatively on the water balance on the Saiss shallow aquifer basin. The simulated results indicated that 2016, annual average recharge was 107 mm (230 Mm^3), surface run off was 26 mm (56 Mm^3) and actual evapotranspiration was 274 mm (585 Mm^3), this actual evapotranspiration was the main process through which water is lost from the Saiss basin. The decrease in the ground water recharge is an evidence of what is currently experienced in the Saiss shallow aquifer with declining ground water levels.

The results from this research can service as a principle indicator for resource base analysis and development of effective and appropriate response strategies for sustainable management of water and land resources in Saiss basin region and the entire morocco at large.

The following recommendations could help for sustainability of Saiss aquifer:

- Ground water abstraction for the purposes of irrigation, industrial and domestic consumption should be regulated to acceptable levels through continuous monitoring and issuing of water abstraction permits.
- Formulation water user's associations to manage and plan for the water with the basin sustainably and in case of illegal be levied huge penalties.
- Improve on the land use practices especially in the regions with agricultural activities, the adopted practices should aim at improving soil water retention capacities and minimizing water losses through evaporation through use of subsurface or drip irrigation system.
- Establishment of sound state waste water treatment plants at both the major cities of Fes and Meknes and this treated water pumped to agricultural zone to relieve on the over pumping of ground water for irrigation.
- Land use change should be integrated into the strategic planning as a key factor affecting the water of the aquifer.
- During periods of peak flows especially in the winter season, the excessive run off that even causes flooding in the low plain should be used to recharge the aquifer through artificial means.

REFERENCES

Abbas, I. I., Muazu, K. M., and Ukoje, J. A. (2010). Mapping Land Use-Land Cover and Change Detection in Kafur Local Government Katsina, Nigeria (1995–2008) Using Remote Sensing and GIS. Research Journal of Environmental and Earth Science, 2(1), 6–12.

Abbaspour, K. C. (2011). SWAT-CUP4: SWAT Calibration and Uncertainty Programs—A User Manual. Swiss Federal Institute of Aquatic Science and Technology, Department of Systems Analysis, Dübendorf.

Abdollahi, K., Bashir, I., Verbeiren, B., and Harouna, M. R. (2017). A distributed monthly water balance model: formulation and application on Black Volta Basin. Environmental Earth Sciences. https://doi.org/10.1007/s12665-017-6512-1

Abraha, L. (2007). Assessing the impact of land use and land cover change on groundwater recharge using RS and GIS; A case of Awassa catchement Southern Ethiopia. M.Sc Thesis, Addis Ababa University, Department of Earth Sciences; Addis Ababa.

Akram, S., and Driss, O. (2011). Simulation-Optimization Modeling for Sustainable Groundwater Development: A Moroccan Coastal Aquifer Case Study. Water Resources Management Journal, 25, 2855–2875.

Alvar, C., and Karen, V. G. (2016, August 19). Aquifer Contracts: A Means to Solving Groundwater Over-exploitation in Morocco? Groundwater Solutions Initiative for Policy and Practice (GRIPP) Case Study series, p. 20.

Armanuos, A. M., Negm, A., and Yoshimura, C. (2016). Application of WetSpass model to estimate groundwater recharge variability in the Nile Delta aquifer. Arabian Journal of Geosciences. https://doi.org/10.1007/s12517-016-2580-x

Asmamaw, A. G. (2013). Assessing The Impacts of Land Use and Land Cover Change On Hydrology of Watershed.

Awotwi, A. (2009). Detection of land use and land cover change in Accra, Ghana, between 1985 and 2003 using Landsat Imagery. Master Thesis, Royal Institute of Technology (KTH)., Division of Geoinformatics.

Awotwi, A., Yeboah, F., and Michael, K. (2014). Assessing the impact of land cover changes on water balance components of White Volta Basin in West Africa. Water and Environment Journal, 1-9.

Babama, R. (2013). Impacts of precipitation, land use land cover and soil type on the water balance of lake Chad basin.

Baker, T. J., and Miller, S. N. (2013). Using the Soil and Water Assessment Tool (SWAT) to assess land use impact on water resources in an East African watershed. Journal of Hydrology, 486, 100-111.

Batelaan, O., and De Smedt, F. (2007). GIS-based recharge estimation by coupling surface-subsurface water balances. Journal of Hydrology, 337(3–4), 337–355. https://doi.org/10.1016/j.jhydrol.2007.02.001

Batelaan, O., Smedt, F. De, and Triest, L. (2003). Regional groundwater discharge: phreatophyte mapping, groundwater modelling and impact analysis of land-use change, 275, 86–108. https://doi.org/10.1016/S0022-1694(03)00018-0

Bawahidi, K. S. (2005). Integrated land use change analysis for soil erosion study in ulu kinta catchment. Universiti Sains Malaysia.

Benaabidate, L., and Cholli, M. (2011). Groundwater Stress and Vulnerability to pollution of Saiss Basin Shallow Aquifer, Morocco. Fifteenth International Water Technology Conference, IWTC-15. Alexandria, Egypt.

Benaabidate, L; Fryar, A E. (2010). Controls on Ground Water Chemistry in the. Ground Water Journal, 48(2), 306-319.

Briak, H., Moussadek, R., Aboumaria, K., and Mrabet, R. (2016). International Soil and Water Conservation Research Assessing sediment yield in Kalaya gauged watershed (Northern Morocco) using GIS and SWAT model. International Soil and Water Conservation Research, 4(3), 177–185. https://doi.org/10.1016/j.iswcr.2016.08.002

CCAA. (2010). Balancing competing water needs in Morocco's Saiss basin.

Chadli, K., Kirat, M., Laadoua, A., and El Harchaoui, N. (2016). Runoff modeling of Sebou watershed (Morocco) using SCS curve number method and geographic information system. Modeling Earth Systems and Environment, 2(3), 158. https://doi.org/10.1007/s40808-016-0215-6

Chadli.K. (2016). Estimation of soil loss using RUSLE model for Sebou watershed (Morocco). Modeling Earth Systems and Environment, 2(2), 1–10. https://doi.org/10.1007/s40808-016-0105-y

Charles, G., Julius, M. N., and Ramadhan, W. (2016, September 12). Hydrological Responses to Land Use/Cover Changes in the Olifants Basin, South Africa. Water, p. 16.

Cirac, P. (2008). Le bassin sud rifain occidental au Néogène supérieur. Evolution de la dynamique sédimentaire etde la paléogéographique au cours d'une phase de comblement. Mém. Inst. Géol. Bassin d'Aquitaine N°21, Bordeaux, France.

Closas, A., and Villholth, K. G. (2016). Aquifer contracts: a means to solving groundwater over-exploitation in Morocco? Colombo, Sri Lanka: International Water Management Institute (IWMI).

Cohen, J. (1960). Educational and Psychological Measurement. https://doi.org/10.1177/001316446002000104

Dams, J., Woldeamlak, S. T., and Batelaan, O. (2008). Predicting land use change and its impact on the groundwater system of the Kleine Nete catchment, Belgium. Hydrology and Earth System Sciences, 12(6), 1369–1385.

Dams, J., Woldeamlak, S. T., and Batelaan, O. (2008). Predicting land-use change and its impact on the groundwater system of the Kleine Nete catchment, Belgium, (2003), 1369–1385.

Deng, Z., Zhag, X., Li, D., and Pan, G. (2015). Simulation of land use/land cover change and its effects on the hydrological characteristics of the upper reaches of the Hanjiang Basin. Environmental Earth Sciences, 73(3), 1119-1132.

Drobot, R. (2014). Groundwater Hydrology. Retrieved from < http://echo2.epfl.ch/VICAIRE/mod_3/chapt_9/main.htm>

Eastman, J. (2006). Idrisi Andes manual: Giude to SIG and image processing, Worcester USA, Clark University, Idrisi production, 327 P.

Ellen, N. (2008). Assesment of a catchment water balance using GIS and Remote Sensing Techniques: Mazowe, Zimbabwe. International Institute for Geo Information Science and Earth observation.

Emiru, W. K. (2009). Hydrological Responses to land Cover Changes in Gilgel Abbay cathment, Ethiopia. International Institute for Geo-Information and Earth Observation, Enschede, Netherlands.

Fadil, A., Rhinane, H., Kaoukaya, A., Kharchaf, Y., and Bachir, O. A. (2011). Hydrologic Modeling of the Bouregreg Watershed (Morocco) Using GIS and SWAT Model. Journal of Geographic Information System, 3, 279-289.

Foody, G. M. (2002). Status of land cover classification accuracy assessment, 80, 185–201.

Ford, C. R., Hubbard, R. M., Kloeppel, B. D., and Vose, J. M. (2007). A comparison of sap flux-based evapotranspiration estimates with catchment-scale water balance. Journal of Agriculture, Forestry and Meteorology, 145, 176–185.

Gafsa, N., Melki, A., Abdollahi, K., Fatahi, R., and Abida, H. (2017). Journal of African Earth Sciences Groundwater recharge estimation under semi-arid climate: Case of. Journal of African Earth Sciences, 132, 37–46. https://doi.org/10.1016/j.jafrearsci.2017.04.020

Gassman, P. W., Reyes, M. R., Green, C. H., and Arnold, J. G. (2007). The soil and water assessment tool: Historical development, applications, and future research directions. Transactions of the Asabe, 50, 1211−1250.

Gebremeskel, G., and Kebede, A. (2017). Spatial estimation of long-term seasonal and annual groundwater resources: application of WetSpass model in the Werii watershed of the Tekeze River Basin, Ethiopia. Physical Geography, 3646 (March), https://doi.org/10.1080/02723646.2017.1302791

Ghaffari, G., Keesstra, S., Ghodousi, J., and Ahmadi, H. (2010). SWAT-simulated hydrological impact of land-use change in the Zanjanrood basin, Northwest Iran. Hydrological Processes, 24(7), 892-903.

Gharbia, S. S. (2013). AL-Azhar University – Gaza. Impacts of Climate Change on Groundwater of the Gaza Coastal Aquifer Using GIS and MOD FLOW.

Groeneveld, D. P., Baugh, W. M., Sanderson, J. S., and Cooper, D. J. (2007). Annual groundwater evapotranspiration mapped from single satellite scenes. Journal of Hydrology, 344, 146–156.

Gumindoga, W. (2010). Hydrologic Impact of Land-Use Change in The Upper Gilgel Abay River Basin, Ethiopia; Application. M.Sc. Thesis, ITC Netherlands.

Guo, H., Hu, Q., and Jiang, T. (2008). Annual and seasonal streamflow responses to climate and land-cover changes in the Poyang Lake basin, China. Journal of Hydrology, 355(1–4), 106-122.

GWP. (2014). The links between Land use and groundwater. Global Water Partnership.

Homdee, T., Pongput, K., and Kanae, S. (2011). Impacts of Land Cover Changes on Hydrologic Responses: A Case Study of Chi River Basin, Thailand. Annual Journal of Hydraulic Engineering, 55, 31–36.

Hosseini, M., Ghafouri, A. M., Amin, M. M., Goodarzi, M., and Abde, A. K. (2012). Effects of Land Use Changes on Water Balance in Taleghan Catchment, Iran. Journal of Agricultural Science and Technology, 14, 1159-1172.

Houcyne, E. I., and Florimond, D. S. (2006). Modelling groundwater flow of the Trifa aquifer, Morocco. Hydrogeology Journal, 14, 1265–1276.

Houdret, A. (2012). The water connection: Irrigation, water grabbing and politics in Southern Morocco.:. Water Alternatives, 5(2), 284-303.

IFAD. (2010). Linking land and water governance. Rome, Italy: International Fund for Agricultural Development.

Im, S., Kim, H., Kim, C., and Jang, C. (2009). Assessing the impacts of land use changes on watershed hydrology using MIKE SHE. Journal of Environment and Geology, 57, 231–239.

IUCN. (2009). Pangani River Basin. Situation Analysis. IUCN Eastern Africa Programme.

José, A. G. (2007). Effects of land cover changes on the water balance of the Palo Verde Wetland, Costa Rica. International Institute for Geo-Information Science and Earth, Enschede, Netherlands.

K. Abdollahi, I. B. and O. B. (2012). WetSpass: Graphical User Interface.

Keisuke, K. (2017). Numerical Simulation of Saltwater Intrusion Caused by Land-Use Change and Groundwater Pumping in a Salinity-Affected Coastal Aquifer, Japan. Lund University, Department of Building and Environmental Technology. Lund, Sweden: Lund University.

Keith, E. S., Manoj, K. J., You-Kuan, Z., Philip, W. G., and Calvin, F. W. (2008). Impact of land use and land cover change on the water balance of a large agricultural watershed: Historical effects and future directions. Water Resources research, 44.

Kim, H. K., Parajuli, P. B., and Filip to, S. D. (2013). Assessing impacts of bioenergy crops and climate change on hydrometeorology in the Yazoo River Basin, Mississippi. Agricultural and Forest Meteorology, 169, 61-73.

Kimberly, M. (2012, 05 09). Information on Earth's wate-National Groundwater Association. Retrieved April 20, 2017, from National Ground Water Association: http://ga.water.usgs.gov/edu/earthwherewater.html

Kuisi, A., Kuisi, M. Al, and El-naqa, A. (2013). GIS based Spatial Groundwater Recharge estimation in the Jafr basin, Jordan – Application of WetSpass models for arid regions, 96–109.

Kumar, C. P. (2012, Oct.). Climate Change and Its Impact on Groundwater Resources. International Journal of Engineering and Science, 1(5), 43-60.

Laraichi, S., Hammani, A., and Bouignane, A. (2016). Data integration as the key to building a decision support system for groundwater management: Case of Saiss aquifers, Morocco. Groundwater for Sustainable Development, 2–3, 7–15. https://doi.org/10.1016/j.gsd.2016.04.003

Legrouri, A., Kettan, D., and Kalpak, J. (2012). Using a Demand Size Management to adapt to water scarcity and Climate Change in the Saiss Basin, Morocco. Final Technical Report, Al-Akhawayn University in Ifrane, Morocco, Ifrane, Morocco.

Li, H., Brunner, P., Kinzelbach, W., Li, W., and Dong., X. (2009). Calibration of a groundwater model using pattern information from remote sensing data. Journal of Hydrology, 377, 120–130.

Liu, M., Tian, H., Chen, G., Ren, W., Zhang, C., and Liu, J. (2008). Effects of Land-Use and Land-Cover Change on Evapotranspiration and Water Yield in China During 1900-20001. JAWRA Journal of the American Water Resources Association, 44(5), 1193-1207.

Manashi, P. (2016). Impacts of Land Use and Climate Changes on Hydrological Processes in South Dakota Watersheds. South Dakota State University.

Mao, D., and Cherkauer, K. A. (2009). Impacts of land-use change on hydrologic responses in the Great Lakes region. Journal of Hydrology, 374(1–2), 71-82.

McCuen, R. H. (2004). Hydrologic Analysis and Design. New Jersey: Prentice Hall.

Meiyappan, P., and Jain, A. K. (2012). Three distinct global estimates of historical land-cover change and land-use conversion for over 200 years. Frontiers Earth Science, 6, 122-139.

Mengistu, K. T. (2009). Watershed Hydrological Responses to Changes in Land Use and Land Cover, and Management Practices at Hare Watershade, Ethiopia. Research Institute for Water and Environment. Siegen, Germany: Universität Siegen.

Moriasi, D. N., Arnold, J. G., Van Liew, M. W., Bingner, R. L., Harmel, R. D., and Veith, T. L. (2007). Model evaluation guidelines for systematic quantification of accuracy in watershed simulations. T ASABE, 50(3), 885-900.

Münch, Z., and Conrad, J. (2007). Remote sensing and GIS based determination of groundwater dependent ecosystems in the Western Cape, South Africa. Hydrogeological Journal, 15, 19–28.

Mustafa, S. T. (2017). Identification of the influencing factors on groundwater drought and depletion in north-western Bangladesh. https://doi.org/10.1007/s10040-017-1547-7

Ndomba, P., Mtalo, F., and Killingtveit, A. (2008). SWAT model application in a data scarce tropical complex catchment in Tanzania. Phys. Chem. Earth, 626–632.

Nejadhashemi, A. P., Wardynski, B. J., and Munoz, J. D. (2011). Evaluating the impacts of land use changes on hydrologic responses in the agricultural regions of Michigan and Wisconsin. Michigan State University, Department of Biosystems and Agricultural Engineering, East Lansing, USA.

OPID. (2016). Saiss Water conservation Project – Environmental and social appraisal and action plan.

Öztürk, M., Copty, N. K., and Saysel, A. K. (2013). Modeling the impact of land use change on the hydrology of a rural watershed. Journal of Hydrology, 497, 97-109.

Pai, N., and Saraswat, D. (2011). SWAT 2009 _LUC: A Tool to Activate the Land Use Change Module in SWAT 2009. Transactions of the ASABE, 54(5), 1649-1658.

Pan Yun, Y., Gong Huili, H., Zhou, D., LI, X., and Nakagoshi, N. (2011). Impact of Land Use Change on Groundwater Recharge in Guishui River Basin, China. China Journal of Science, 21(6), 734–743.

Pan, Y., Gong, H., Zhou, D., Li, X., and Nakagoshi, N. (2011). Impact of land use change on groundwater recharge in Guishui River Basin, China. Chinese Geographical Science, 21(6), 734–743. https://doi.org/10.1007/s11769-011-0508-7

Pengfei, Z. (2004). Basic Hydrology. Lecture: Storage Properties of Aquifers.

Priyantha, R. S., So, K., and Masaki, S. (2006). Effects of climate and land use changes on groundwater resources. Journal of Environmental Management, 25-35.

Randall, E. F. (2011). Using water balance models to approximate the effects ofClimate change on spring catchment discharge: Mt. Hanang, Tanzania. Michigan Technological University. UMI Dissertation Publishing.

Renny, C. (2012). Effects of Land Use and Land Cover Changes on the Hydrology of Weruweru-Kiladeda Sub-Catchment in Pangani River Basin, Tanzania. Kenyatta University, Department of Geography.

Renny, C. (2012). Effects of land use and land cover changes on the Hydrology of Weruweru-Kiladeda Sub-Catchment in Pangani River Basin, Tanzania. Thesis Report, Kenyatta Univerity, Department of Geography, Nairobi, Kenya.

Rientjes, T. M. (2007). Modelling in Hydrology. Department of Water Resources, Enschede, Netherlandfs.

Rodhe, A. (2014). Grundvatten. Nationalencyklopedin. Retrieved April 20, 2017, from <http://www.ne.se/uppslagsverk/encyklopedi/lång/grundvatten>

Roy, A. H., Dybas, A. L., Fritz, K. M., and Lubbers, H. R. (2009). Urbanization affects: the extent and hydrologic permanence of headwater streams in a midwestern US metropolitan area. Journal of the North American Benthological Society, 28(4), 911-928.

Saadati, H., Gholami, S. A., Sharifi, F., and Ayoubzadeh, S. A. (2006). An Investigation of the Effects of Land Use Change on Simulating Surface Runoff Using SWAT Mathematical Model. Journal of Iran's Natural Resources, 301-313.

Salem, S. G. (2013). Impacts of Climate Change on Groundwater of the Gaza Coastal Aquifer Using GIS and MODFLOW. Master's thesis, Institute of Water and Environment, Gaza.

Sanna, N. (2015). Modelling and Simulation of a Groundwater aquifer in Vomb. Master's Thesis, Lund University, Department of Chemical Engineering.

Sayena, F. M. (2012). Water Budget Analysis and Groundwater Inverse Modeling. Master's Thesis, Texas AandM University, Texas, USA.

Schilling, K. E., Gassman, P. W., Kling, C. L., Campbell, T., Jha, M. K., Wolter, C. F., and Arnold, J. G. (2014). The potential for agricultural land use change to reduce flood risk in a large watershed. Hydrological Processes, 28(8), 3314-3325.

Sener, E., Davraz, A., and Ozcelik, M. (2005). An integration of GIS and remote sensing in groundwater investigations: A case study in Burdur, Turkey. hydrogeological Journal, 13, 826–834.

Shaban, A., Khawlie, M., and Abdallah, C. (2006). Use of remote sensing and GIS to determine recharge potential zones: The case of Occidental Lebanon. hydrogeological Journal, 14, 433–443.

Stephen, F., and Jan, C. (2014). The links between land use and groundwater – Governance provisions and management strategies to secure a 'sustainable harvest'. Stockholm, Sweden: Global Water Partnership.

Stigter, T. Y., Nunes, J. P., Pisani, B., Fakir, Y., Hugman, R., Li, Y., . . . El Himer, H. (2014). Comparative assessment of climate change and its impacts on three coastal aquifers in the Mediterranean. Reg Environ Change, 14, 41-56.

Stisen, S., Jensen, K. H., Sandholt, I., and Grimes, D. i. (2008). A remote sensing driven distributed hydrological model of the Senegal River basin. Journal of Hydrology, 354, 131–148.

Tadele, K. (2007). Impact of Land use/cover change on stream flow: the case of Hare River Watershed, Ethiopia. Thesis, Arba Minch University., Arba Minch Water Technology Institute.

Tilahun, K., and Merkel, B. J. (2009). Estimation of groundwater recharge using a GIS-based distributed water balance model in Dire Dawa, Ethiopia. Hydrogeology Journal, 17(6), 1443–1457. https://doi.org/10.1007/s10040-009-0455-x

Todd, S. M. (2000). Simulation of Ground-water Flow in an Unconfined Sand and Gravel Aquifer at Marathon, Cortland County, New York. New York: US Geological Survey.

Tu_Min. (2006). Assessment of the Effects of Climate Variability and Land-Use Change on the Hydrology of Meuse River Basin. PhD Thesis, UNESCO-IHE Institute for Water Education.

Tweed, S. O., Leblanc, M., Webb, J. A., and Lubczynski, M. W. (2007). Remote sensing and GIS for mapping groundwater recharge and discharge areas in salinity prone catchments, southeastern Australia. Hydrologeological Journal, 15, 75–96.

UNDP. (2013). Water Governance in the Arab region. New York: United Nations Publications.

Wagner, P. D., Kumar, S., and Schneider, K. (2013). An assessment of land use change impacts on the water resources of the Mula and Mutha Rivers catchment upstream of Pune, India. Hydrology and Earth System Sciences, 17, 2233–2246.

Warburton, M. L., Schulze, R. E., and Jewitt, G. P. (2012). Hydrological impacts of land use change. Journal of Hydrology, 414-415, 118-135.

Winchell, M., Srinivasan, R., Di Luzio, M., and Arnold, J. G. (2009). ArcSWAT 10.1 Interface for SWAT2010, Users Guide, Version September 2009. Texas Agricultural Experiment Station and Agricultural Research Service. US Department of Agriculture, Temple.

Woldeamlak, S. T., and Batelaan, O. (2007). ArcView Interface for WetSpass.

Woldeamlak, S. T., Batelaan, O., and Smedt, F. De. (2007). Effects of climate change on the groundwater system in the Grote-Nete catchment, Belgium. https://doi.org/10.1007/s10040-006-0145-x

Wu, Y., Liu, S., and Li, Z. (2013). Identifying potential areas for biofuel production and evaluating the environmental effects: a case study of the James River Basin in the Midwestern United States. GCB Bioenergy, 4(6), 875-888.

Wubishet, T., Stephanie, W., William, C., and Constance, W. (2015). Assessing the Impact of Land-Use Land-Cover Change on Stream Water and Sediment Yields at a Watershed Level Using SWAT. Open Journal of Modern Hydrology (5), 68-85.

Yang, J., Reichert, P., Abbaspour, K. C., Xia, J., and Yang, H. (2008). Comparing uncertainty analysis techniques for a SWAT application to the Chaohe Basin in China. Journal of Hydrology, 358, 1-23.

Zhang, Y. K., and Schilling, K. E. (2006). Increasing streamflow and base flow in Mississippi River since the 1940s: Effect of land use change. Journal of Hydrology, 324(1–4), 412-422.

Zhi, Y., Yangxiao, Z., Jochen, W., Stefan, U., and Li, W. (2015). Simulation of Groundwater-Surface Water Interactions under Different Land Use Scenarios in the Bulang Catchment, Northwest China. Water, 7, 5959-5985.

Zhou, F., Xu, Y., Chen, Y., Xu, C.-Y., Gao, Y., and Du, J. (2013). Hydrological response to urbanization at different spatio-temporal scales simulated by coupling of CLU E-S and the SWAT model in the Yangtze River Delta region. Journal of Hydrology, 485, 113-125.

Zhou, Y., Wenninger, J., Yang, Z., Yin, L., Huang, J., Hou, L., . . . Uhlenbrook, S. (2013). Groundwater— Surface water interactions, vegetation dependencies and implications for water resources management in the semi-arid Hailiutu River catchment, China—A synthesis. Hydrology, Earth Systems and Science Journal, 17, 2435–2447

APPENDIX

Appendix 8.1: WetSpass model simulations

```
**********************************************************************
Running at 16/07/2017 18:09:54 with the following parameters:
a:4.5 , alfa:1.5 , wSlope:0.4 , wLanduse:0.3 , wSoil:0.3 , x:0.5 , LP:0.85 , Mean intensity:3 , Beta:0.75 , Contribution:0.5
**********************************************************************
TimeStep        AET     Runoff  Interception    Recharge
1       101.232771099847        81.7572912889381        8.71136077036594        25.0672798380417
2       19.1929136759342        0.993751328983847       1.94525675499315        8.91637236378672
3       258.476907857891        134.726095527632        9.20807208101986        32.1813092426628
**********************************************************************
Running at 16/07/2017 18:22:24 with the following parameters:
a:4.5 , alfa:0.5 , wSlope:0.4 , wLanduse:0.3 , wSoil:0.3 , x:0.5 , LP:0.85 , Mean intensity:3 , Beta:0.75 , Contribution:0.5
**********************************************************************
TimeStep        AET     Runoff  Interception    Recharge
1       101.232771099847        81.7572912889381        8.71136077036594        25.0672798380417
2       13.6023085018386        0.890532680255665       1.94525675499315        14.6101966202476
**********************************************************************
Running at 16/07/2017 20:17:26 with the following parameters:
a:4.5 , alfa:0.5 , wSlope:0.4 , wLanduse:0.3 , wSoil:0.3 , x:0.5 , LP:0.85 , Mean intensity:3 , Beta:0.75 , Contribution:0.5
**********************************************************************
TimeStep        AET     Runoff  Interception    Recharge
1       101.232771099847        81.7572912889381        8.71136077036594        25.0672798380417
2       13.6023085018386        0.890532680255665       1.94525675499315        14.6101966202476
**********************************************************************
Running at 16/07/2017 20:31:33 with the following parameters:
a:4.5 , alfa:0.5 , wSlope:0.4 , wLanduse:0.3 , wSoil:0.3 , x:0.5 , LP:0.85 , Mean intensity:3 , Beta:0.75 , Contribution:0.5
**********************************************************************
TimeStep        AET     Runoff  Interception    Recharge
1       101.232771099847        81.7572912889381        8.71136077036594        25.0672798380417
2       13.6023085018386        0.890532680255665       1.94525675499315        14.6101966202476
3       115.423765020208        73.9969953084001        9.20807208101986        218.342196356214
**********************************************************************
```

```
Running at 16/07/2017 20:45:07 with the following parameters:
a:4.5 , alfa:0.9 , wSlope:0.4 , wLanduse:0.3 , wSoil:0.3 , x:0.5 , LP:0.85 , Mean intensity:4 , Beta:0.75 , Contribution:0.5
**********************************************************************
TimeStep        AET     Runoff  Interception    Recharge
1       101.177700432577        93.8880043910345        8.71136077036594        17.6187826234139
2       18.0781660161171        0.973032720812157       1.94525675499315        10.0518387514878
3       199.646916175485        119.146224255964        9.20807208101986        88.973798346645
**********************************************************************
Running at 16/07/2017 21:00:18 with the following parameters:
a:4.5 , alfa:0.48 , wSlope:0.4 , wLanduse:0.3 , wSoil:0.3 , x:0.5 , LP:0.85 , Mean intensity:3 , Beta:0.75 , Contribution:0.5
**********************************************************************
TimeStep        AET     Runoff  Interception    Recharge
1       101.232771099847        81.7572912889381        8.71136077036594        25.0672798380417
2       13.1615112969969        0.882408060750399       1.94525675499315        15.0591184688834
3       109.665189130243        71.5575055138686        9.20807208101986        226.54026204071
**********************************************************************
Running at 16/07/2017 21:21:17 with the following parameters:
a:4.5 , alfa:0.258 , wSlope:0.4 , wLanduse:0.3 , wSoil:0.3 , x:0.5 , LP:0.85 , Mean intensity:3 , Beta:0.75 , Contribution:0.5
**********************************************************************
TimeStep        AET     Runoff  Interception    Recharge
1       101.232771099847        81.7572912889381        8.71136077036594        25.0672798380417
2       6.36326181156482        0.757106255387139       1.94525675499315        21.9826700494307
3       39.4713338564912        41.8460288022829        9.20807208101986        326.445594026048
**********************************************************************
Running at 16/07/2017 21:35:59 with the following parameters:
a:4.5 , alfa:0.34 , wSlope:0.4 , wLanduse:0.3 , wSoil:0.3 , x:0.5 , LP:0.85 , Mean intensity:3 , Beta:0.75 , Contribution:0.5
**********************************************************************
TimeStep        AET     Runoff  Interception    Recharge
1       101.232771099847        81.7572912889381        8.71136077036594        25.0672798380417
2       9.21754614163617        0.809714816427739       1.94525675499315        19.0757770536797
3       65.6938283344566        52.9402182884828        9.20807208101986        289.128910061882
```

```
TimeStep        AET     Runoff  Interception    Recharge
1       101.232771099847        81.7572912889381        8.71136077036594        25.0672798380417
2       9.21754614163617        0.809714816427739       1.94525675499315        19.0757770536797
3       65.6938283344566        52.9402182884828        9.20807208101986        289.128910061882
**************************************************************************
Running at 16/07/2017 21:49:14 with the following parameters:
a:4.5 , alfa:0.46 , wSlope:0.4 , wLanduse:0.3 , wSoil:0.3 , x:0.5 , LP:0.85 , Mean intensity:3 , Beta:0.75 , Contribution:0.5
**************************************************************************
TimeStep        AET     Runoff  Interception    Recharge
1       101.232771099847        81.7572912889381        8.71136077036594        25.0672798380417
2       12.6907333275602        0.873730866081312       1.94525675499315        15.5385736580205
3       103.75221256864 69.0529354526867        9.20807208101986        234.957808663495
**************************************************************************
Running at 16/07/2017 22:04:54 with the following parameters:
a:4.5 , alfa:1.5 , wSlope:0.4 , wLanduse:0.3 , wSoil:0.3 , x:0.5 , LP:0.85 , Mean intensity:3 , Beta:0.75 , Contribution:0.5
**************************************************************************
TimeStep        AET     Runoff  Interception    Recharge
1       101.232771099847        81.7572912889381        8.71136077036594        25.0672798380417
2       19.1929136759342        0.993751328983847       1.94525675499315        8.91637236378672
3       258.476907857891        134.726095527632        9.20807208101986        32.1813092426628
**************************************************************************
Running at 16/07/2017 22:19:42 with the following parameters:
a:4.5 , alfa:0.7 , wSlope:0.4 , wLanduse:0.3 , wSoil:0.3 , x:0.5 , LP:0.85 , Mean intensity:4 , Beta:0.75 , Contribution:0.5
**************************************************************************
TimeStep        AET     Runoff  Interception    Recharge
1       101.177700432577        93.8880043910345        8.71136077036594        17.6187826234139
2       16.645720761599 0.946628682244081       1.94525675499315        11.5106881625234
3       164.311011600776        102.849114717207        9.20807208101986        140.602964136329
```

```
Running at 16/07/2017 22:34:32 with the following parameters:
a:4.5 , alfa:0.7 , wSlope:0.4 , wLanduse:0.3 , wSoil:0.3 , x:0.5 , LP:0.85 , Mean intensity:1.29 , Beta:0.75 , Contribution:0.5
**************************************************************************
TimeStep        AET     Runoff  Interception    Recharge
1       100.351415904231        45.0829045194763        18.2940622098815        58.0660137828029
2       14.1274095117464        1.01006515619609        4.15973628133606        13.8644117643054
3       150.335982750736        70.3139928563835        19.225509399994 186.94673300213
**************************************************************************
Running at 16/07/2017 22:47:46 with the following parameters:
a:4.5 , alfa:0.67 , wSlope:0.4 , wLanduse:0.3 , wSoil:0.3 , x:0.5 , LP:0.85 , Mean intensity:1.29 , Beta:0.75 , Contribution:0.5
**************************************************************************
TimeStep        AET     Runoff  Interception    Recharge
1       100.351415904231        45.0829045194763        18.2940622098815        58.0660137828029
2       13.910558938354 1.00584502942297        4.15973628133606        14.085482095703
3       144.957079858453        68.5328060826943        19.225509399994 194.106822668102
**************************************************************************
Running at 16/07/2017 23:00:09 with the following parameters:
a:4.5 , alfa:0.725 , wSlope:0.4 , wLanduse:0.3 , wSoil:0.3 , x:0.5 , LP:0.85 , Mean intensity:1.29 , Beta:0.75 , Contribution:0.5
**************************************************************************
TimeStep        AET     Runoff  Interception    Recharge
1       100.351415904231        45.0829045194763        18.2940622098815        58.0660137828029
2       14.2901264992981        1.01323176418534        4.15973628133606        13.698528444914
3       154.619424912765        71.7327604707393        19.225509399994 181.244523225745
**************************************************************************
Running at 16/07/2017 23:17:45 with the following parameters:
a:4.5 , alfa:0.88 , wSlope:0.4 , wLanduse:0.3 , wSoil:0.3 , x:0.5 , LP:0.85 , Mean intensity:1.29 , Beta:0.75 , Contribution:0.5
**************************************************************************
```

```
Running at 16/07/2017 23:44:42 with the following parameters:
a:4.5 , alfa:0.93 , wSlope:0.4 , wLanduse:0.3 , wSoil:0.3 , x:0.5 , LP:0.85 , Mean intensity:1.29 , Beta:0.75 , Contribution:0.5
**************************************************************************
TimeStep        AET     Runoff  Interception    Recharge
1       100.351415904231        45.0829045194763        18.2940622098815        58.0660137828029
2       15.1699965935991        1.03035431569077        4.15973628133606        12.8015372816193
3       183.834091190937        81.4177138037019        19.225509399994 142.344903614611
**************************************************************************
Running at 16/07/2017 23:57:57 with the following parameters:
a:4.5 , alfa:0.96 , wSlope:0.4 , wLanduse:0.3 , wSoil:0.3 , x:0.5 , LP:0.85 , Mean intensity:1.29 , Beta:0.75 , Contribution:0.5
**************************************************************************
TimeStep        AET     Runoff  Interception    Recharge
1       100.351415904231        45.0829045194763        18.2940622098815        58.0660137828029
2       15.2498756438286        1.03190874215811        4.15973628133606        12.7201039383219
3       187.35350756506 82.5855013491271        19.225509399994 137.657699695062
```

Appendix 8.2: WetSpass Calibration parameters

SOIL PARAMETER ATTRIBUTE TABLE

SOIL_NUM	SOIL_TPYE	Field_capacity	Wilting_point	Plant_AW	Residual_WC	A1	Evapo_Depth	Tension_Heigt	P_frac_sum	P_Frac_Winter	TERA
1	Sand	0.12	0.05	0.07	0.02	0.51	0.05	0.07	0.09	0.01	0.136
2	Loamy Sand	0.15	0.07	0.08	0.035	0.47	0.05	0.09	0.09	0.01	0.176
3	Sand Loam	0.21	0.09	0.12	0.041	0.44	0.05	0.15	0.09	0.01	0.266
4	Silty Loam	0.29	0.1	0.19	0.015	0.4	0.05	0.21	0.26	0.07	0.408
5	Loam	0.25	0.12	0.13	0.027	0.37	0.05	0.11	0.15	0.02	0.333
6	Silt	0.3	0.1	0.2	0.04	0.35	0.05	0.61	0.09	0.01	0.429
7	Sand Clayl	0.26	0.16	0.1	0.068	0.32	0.05	0.28	0.54	0.3	0.351
9	Clay Loam	0.33	0.19	0.14	0.075	0.27	0.05	0.26	0.62	0.41	0.493

RUN-OFF COEFFICIENT PARAMETERS

RUNOFF_VEG	LUSE_NUM	SLOPE_(%)	SLOPE_NUM	SOIL_TPYE	SOIL_NUM	RUNOFF_COEFF	UNIQUE_NUM	SOIL_BARE	SLOPE_BARE	BARE_COEFF	UNIQUE_BARE
Grass	4	<0.5	1	Sand	1	0.30	141	1	1	0.35	11
Bare soil	7	0.5-5	2	Loamy Sand	2	0.35	272	2	2	0.4	22
Crop	21	5,10	3	Sand Loam	3	0.40	513	3	3	0.55	33
Crop	27	>10	4	Silty Loam	4	0.45	674	4	4	0.6	44
Forest	33	<0.5	1	Loam	5	0.25	831	5	1	0.68	51
Open water	55	0.5-5	2	Silt	6	0.30	1152	6	2	0.7	62
Forest	303	5,10	3	Sand Clayl	7	0.35	3733	7	3	0.75	73
Grass	307	>10	4	Clay Loam	9	0.40	3974	9	4	0.8	94

Appendix 8.3: WetSpass soil codes and parameters

No	SOIL	FIELDCAPAC	WILTINGPNT	PAW	RESIDUALWC	A1	EVAPODEPTH	TENSIONHHT	P_FRAC_SUM	P_FRAC_WIN
1	Sand	0.12	0.05	0.07	0.020	0.51	0.05	0.07	0.09	0.01
2	loamy sand	0.15	0.07	0.08	0.035	0.47	0.05	0.09	0.09	0.01
3	sandy loam	0.21	0.09	0.12	0.041	0.44	0.05	0.15	0.09	0.01
4	silty loam	0.29	0.10	0.19	0.015	0.40	0.05	0.21	0.26	0.07
5	loam	0.25	0.12	0.13	0.027	0.37	0.05	0.11	0.15	0.02
6	silt	0.30	0.10	0.20	0.040	0.35	0.05	0.61	0.09	0.01
7	sandy clayl	0.26	0.16	0.10	0.068	0.32	0.05	0.28	0.54	0.30
8	silty clayl	0.36	0.19	0.17	0.040	0.29	0.05	0.33	0.62	0.41
9	clayloam	0.33	0.19	0.14	0.075	0.27	0.05	0.26	0.62	0.41
10	sandy clay	0.32	0.23	0.09	0.109	0.25	0.05	0.29	0.80	0.68
11	silty clay	0.43	0.27	0.16	0.056	0.23	0.05	0.34	0.84	0.75
12	clay	0.46	0.33	0.13	0.090	0.21	0.05	0.37	0.95	0.85

Appendix 8.4-: precipitation variation between stations

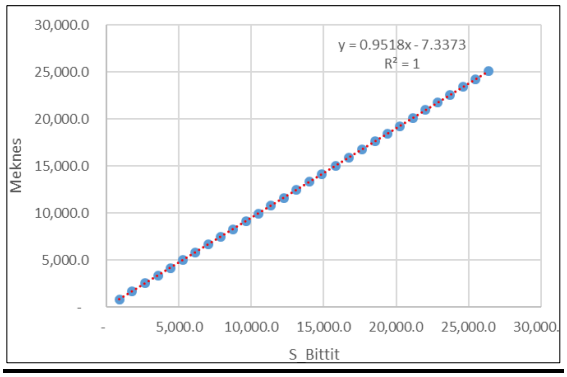

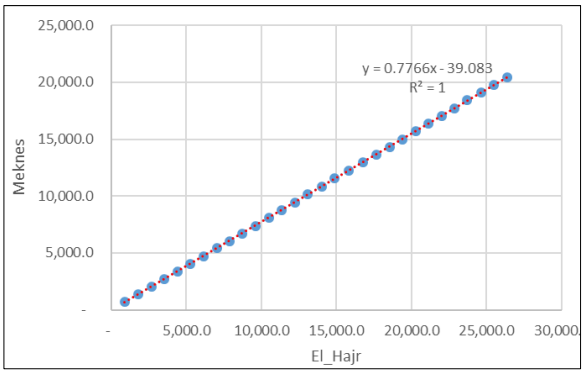

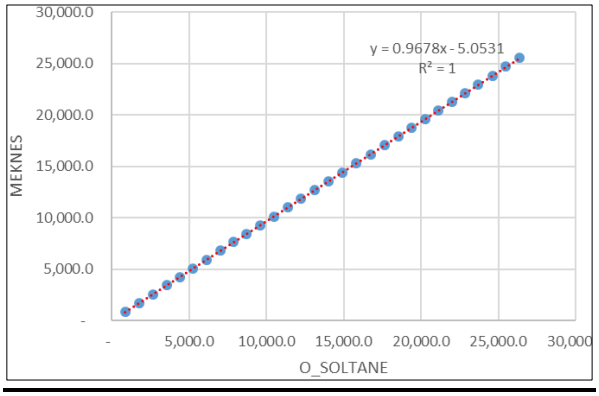

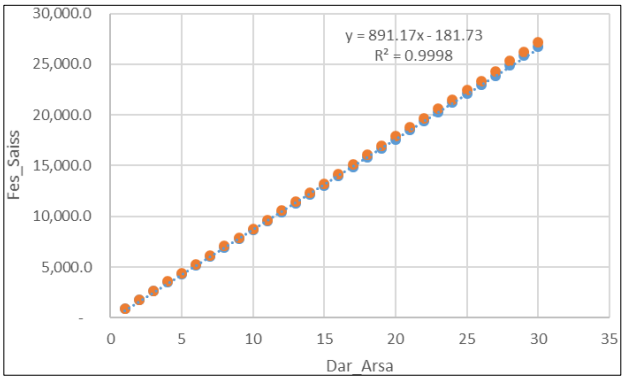

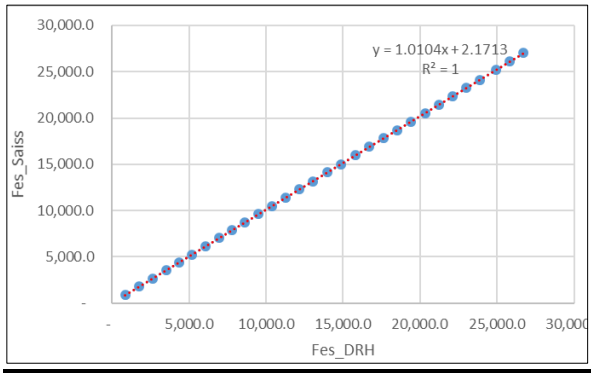

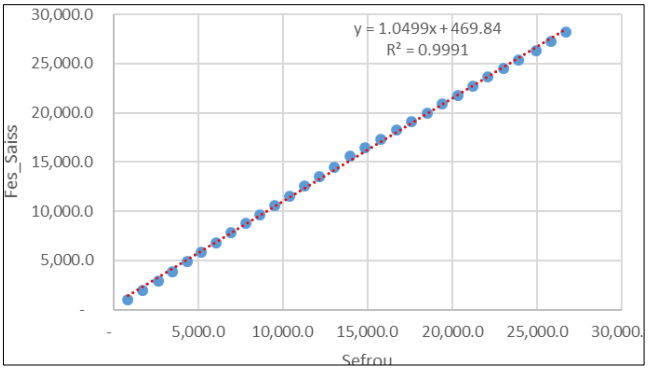

Appendix 8.5: Statistical adjustment to precipitation for various stations

Meknes Meteo

	GAUS: 2.35	GUMB: 7.244	Galt: 10.461	PEAR: 5.114	PEAV: 17.828	GOOD: 2.606	FREC: 29.619	Lgam: 17.338	Fuit: 3.45
Paramètre d'échelle	142.33	136.986	433.285	50.518	2809.64	490.504	356.553	36.965	23.599
Paramètre de position	458.348	387.971	0.05	0.05	0.05	17.512	0.05	36.965	0
Paramètre de forme premier	0	0	0.398	9.072	6.978	0.294	-0.459	40.241	19.423
Paramètre de forme second	0	0	0	0	0	0	0	0.061	0
Borne inférieure	0	0	0.05	0.05	0.05	17.512	0.05	36.965	0
Borne supérieure	0	0	0	0	0	0	0	0	0
Moyenne	458.348	467.042	469.119	458.348	470.04	458.185	585.502	505.694	458.348
Médiane	458.348	438.178	433.335	441.623	422.697	457.918	421.933	424.605	446.504
Mode	458.348	387.971	369.748	407.831	352.22	460.312	299.835	354.952	422.471
Variance	20257.896	30867.447	37843.548	23152.163	17049.115	20467.205	1145463.033	41024.138	21632.905
Coef. de variance	0.311	0.376	0.415	0.332	0.278	0.312	1.828	0.401	0.321
Coef. d'asymetrie	0	1.139	1.316	0.664	2.243	0.05	0	1.896	0.481
Coef. d'aplatissement	0	2.4	3.227	0.661	12.099	-0.289	0	7.598	0.309
Valeur de test	2.35	7.244	10.461	5.114	17.828	2.606	29.619	17.338	3.45
Freq. au dépassement	0.698	0.071	0.018	0.203	0.001	0.635	0	0.001	0.435

Récurrence	Probabilité	GAUS	GUMB	Galt	PEAR	PEAV	GOOD	FREC	Lgam	Fuit
10000 ans	0.0001	-70.598	83.817	98.526	90.888	132.307	50.235	128.721	131.448	70.331
1000 ans	0.001	18.544	123.226	126.556	125.595	155.662	81.908	146.886	155.039	108.427
100 ans	0.01	127.242	178.769	171.556	179.465	193.305	144.39	176.924	192.385	170.791
50 ans	0.02	166.041	201.115	191.231	202.135	209.638	173.295	190.678	208.833	196.433
20 ans	0.05	224.237	237.672	225.053	239.87	237.887	222.376	215.521	237.429	238.215
10 ans	0.1	275.946	273.72	260.093	277.333	267.515	270.651	243.187	267.507	278.692
5 ans	0.2	338.56	322.782	309.906	327.921	310.512	333.128	286.634	311.197	331.91
3.333 ans	0.3	383.711	362.543	351.646	368.096	347.482	379.783	327.479	348.703	373.131
2.5 ans	0.4	422.289	399.947	391.738	404.972	383.9	420.126	371.202	385.534	410.242
2 ans	0.5	458.348	438.178	433.335	441.621	422.699	457.918	421.933	424.603	446.501
2.5 ans	0.6	494.407	479.988	479.349	480.423	466.892	495.572	485.382	468.859	484.283
3.333 ans	0.7	532.986	529.194	534.002	524.378	521.218	535.524	572.385	522.849	526.397
5 ans	0.8	578.136	593.442	605.93	579.083	595.906	581.661	709.876	596.297	577.886
10 ans	0.9	640.752	696.24	721.99	660.931	724.525	644.292	1001.795	720.576	653.242
20 ans	0.95	692.461	794.846	834.419	733.899	859.215	694.701	1394.048	847.771	718.926
50 ans	0.98	750.659	922.482	982.031	821.945	1052.07	749.962	2138.083	1024.876	796.629
100 ans	0.99	789.458	1018.127	1094.679	884.21	1212.419	785.939	2945.894	1167.817	850.568
1000.03 ans	0.999	898.185	1334.168	1484.051	1074.014	1862.047	883.207	8494.876	1712.367	1012.476
10003.001 ans	0.9999	987.687	1649.652	1906.532	1244.947	2793.498	959.597	24450.551	2385.571	1160.465

FES METEO

	GAUS: 7.728	GUMB: 2.581	Galt: 2.881	PEAR: 3.06	PEAV: 4.803	GOOD: 4.038	Lgam: 5.953
Paramètre d'échelle	158.879	128.416	388.72	90.171	2465.279	277.099	53.6
Paramètre de position	417.664	344.484	0.05	116.562	0.05	167.333	53.6
Paramètre de forme premier	0	0	0.388	3.339	6.835	0.643	24.882
Paramètre de forme second	0	0	0	0	0	0	0.08
Borne inférieure	0	0	0.05	116.562	0.05	167.333	53.6
Borne supérieure	0	0	0	0	0	0	0
Moyenne	417.664	418.608	419.185	417.664	422.515	416.471	476.166
Médiane	417.664	391.551	388.77	388.2	379.022	386.244	378.614
Mode	417.664	344.484	334.401	327.493	314.681	310.177	312.027
Variance	25242.55	27126.143	28566.322	27150.562	14085.501	26782.162	36711.814
Coef. de variance	0.38	0.393	0.403	0.395	0.281	0.393	0.402
Coef. d'asymetrie	0	1.139	1.275	1.094	2.293	1.01	2.167
Coef. d'aplatissement	0	2.4	3.025	1.797	12.787	1.189	10.409
Valeur de test	7.728	2.581	2.881	3.06	4.803	4.038	5.953
Freq. au dépassement	0.06	0.636	0.568	0.533	0.249	0.338	0.141

Récurrence	Probabilité	GAUS	GUMB	Galt	PEAR	PEAV	GOOD	Lgam
10000 ans	0.0001	-172.783	59.359	91.821	127.804	117.808	168.074	122.705
1000 ans	0.001	-73.277	96.302	117.188	140.118	136.593	170.594	142.181
100 ans	0.01	48.059	148.37	157.619	166.877	172.058	181.714	173.669
50 ans	0.02	91.37	169.318	175.206	180.649	186.731	189.866	187.7
20 ans	0.05	156.332	203.588	205.334	206.383	212.11	208.359	212.281
10 ans	0.1	214.053	237.381	236.423	235.025	238.782	232.512	238.413
5 ans	0.2	283.948	283.373	280.438	277.882	277.552	272.942	276.807
3.333 ans	0.3	334.348	320.647	317.179	314.87	310.941	310.122	310.152
2.5 ans	0.4	377.413	355.711	352.363	350.809	343.883	347.229	343.214
2 ans	0.5	417.664	391.551	388.77	388.198	379.023	386.244	378.614
2.5 ans	0.6	457.915	430.745	428.939	429.408	419.107	429.283	419.083
3.333 ans	0.7	500.98	476.873	476.522	477.886	468.461	479.567	468.973
5 ans	0.8	551.38	537.101	538.956	540.591	536.43	543.646	537.669
10 ans	0.9	621.276	633.468	639.306	638.609	653.769	641.117	655.918
20 ans	0.95	678.997	725.906	736.119	729.585	777.041	728.484	779.303
50 ans	0.98	743.961	845.557	862.726	843.169	954.127	833.549	954.685
100 ans	0.99	787.272	935.218	959.012	925.571	1101.502	907.238	1098.909
1000.03 ans	0.999	908.64	1231.488	1290.012	1185.608	1702.697	1127.668	1667.041
10003.001 ans	0.9999	1008.549	1527.235	1646.632	1427.125	2555.295	1322.839	2408.585

FES DRH

	GAUS: 2.157	GUMB: 2.528	Galt: 3.13	PEAR: 1.327	PEAV: 5.809	GOOD: 1.233	FREC: 12.018	Lgam: 7.472
Paramètre d'échelle	132.076	115.914	354.089	48.753	2292.835	299.458	291.476	43.232
Paramètre de position	378.236	314.409	0.05	0.05	0.05	112.799	0.05	43.232
Paramètre de forme premier	0	0	0.387	7.757	6.969	0.475	-0.391	28.792
Paramètre de forme second	0	0	0	0	0	0	0	0.073
Borne inférieure	0	0	0.05	0.05	0.05	112.799	0.05	43.232
Borne supérieure	0	0	0	0	0	0	0	0
Moyenne	378.236	381.316	381.691	378.236	384.183	378.022	428.119	427.167
Médiane	378.236	356.893	354.139	362.115	345.434	364.439	336.423	345.642
Mode	378.236	314.409	304.86	329.483	287.774	333.409	256.26	286.707
Variance	17444.004	22101.246	23547.259	18437.901	11405.277	17506.32	172367.324	28955.742
Coef. de variance	0.349	0.39	0.402	0.359	0.278	0.35	0.97	0.398
Coef. d'asymetrie	0	1.139	1.271	0.718	2.247	0.563	0	2.059
Coef. d'aplatissement	0	2.4	3.005	0.773	12.142	0.126	0	9.218
Valeur de test	2.157	2.528	3.13	1.327	5.809	1.233	12.018	7.472
Freq. au dépassement	0.754	0.664	0.503	0.934	0.142	0.946	0.01	0.07

Récurrence	Probabilité	GAUS	GUMB	Galt	PEAR	PEAV	GOOD	FREC	Lgam
10000 ans	0.0001	-112.601	57.043	83.97	63.02	108.67	116.58	122.425	111.02
1000 ans	0.001	-29.881	90.389	107.096	90.577	127.073	124.081	136.989	129.303
100 ans	0.01	70.985	137.388	143.93	134.778	157.905	146.528	160.507	158.575
50 ans	0.02	106.989	156.296	159.944	153.79	171.255	159.782	171.071	171.57
20 ans	0.05	160.992	187.23	187.366	185.8	194.337	185.917	189.874	194.241
10 ans	0.1	208.975	217.733	215.653	217.959	218.56	215.7	210.439	218.244
5 ans	0.2	267.079	259.247	255.683	261.875	253.707	259.733	242.052	253.346
3.333 ans	0.3	308.976	292.892	289.084	297.085	283.931	296.372	271.127	283.691
2.5 ans	0.4	344.775	324.542	321.061	329.613	313.711	330.499	301.659	313.666
2 ans	0.5	378.236	356.893	354.139	362.114	345.435	364.439	336.423	345.64
2.5 ans	0.6	411.697	392.271	390.627	396.694	381.576	400.085	379.044	382.066
3.333 ans	0.7	447.497	433.908	433.837	436.043	426.01	439.841	436.173	426.789
5 ans	0.8	489.394	488.272	490.515	485.262	487.106	488.153	523.922	488.084
10 ans	0.9	547.498	575.257	581.578	559.319	592.318	557.71	702.498	592.893
20 ans	0.95	595.481	658.695	669.395	625.69	702.531	616.907	930.747	701.468
50 ans	0.98	649.486	766.696	784.191	706.158	860.389	684.987	1339.654	854.584
100 ans	0.99	685.49	847.628	871.464	763.267	991.461	731.053	1760.002	979.612
1000.03 ans	0.999	786.384	1115.053	1171.313	956.762	1523.493	862.269	4336.588	1465.835
10003.001 ans	0.9999	869.438	1382.006	1494.138	1093.78	2283.313	971.932	10668.331	2087.644

SEFROU.

	GAUS: 2.754	GUMB: 8.31	Galt: 8.923	PEAR: 4.97	PEAV: 16.579	GOOD: 3.381	FREC: 26.572	Lgam: 15.384
Paramètre d'échelle	136.528	132.983	466.456	42.531	4155.354	469.345	393.974	49.066
Paramètre de position	487.61	419.93	0.05	0.05	0.05	65.651	0.05	49.066
Paramètre de forme premier	0	0	0.338	11.464	9.404	0.297	-0.387	45.451
Paramètre de forme second	0	0	0	0	0	0	0	0.05
Borne inférieure	0	0	0.05	0.05	0.05	65.651	0.05	49.066
Borne supérieure	0	0	0	0	0	0	0	0
Moyenne	487.61	496.69	493.992	487.61	494.518	487.109	574.935	543.289
Médiane	487.61	468.67	466.506	473.509	458.065	486.625	453.993	458.877
Mode	487.61	419.93	416.037	445.08	399.462	488.434	347.261	400.11
Variance	18639.874	29089.994	29600.202	20736.205	13730.195	19044.813	293200.427	32162.845
Coef. de variance	0.28	0.343	0.348	0.295	0.237	0.283	0.942	0.33
Coef. d'asymetrie	0	1.139	1.087	0.591	1.7	0.059	0	1.564
Coef. d'aplatissement	0	2.4	2.173	0.523	6.245	-0.289	0	4.969
Valeur de test	2.754	8.31	8.923	4.97	16.579	3.381	26.572	15.384
Freq. au dépassement	0.601	0.044	0.037	0.225	0.002	0.465	0	0.003

Récurrence	Probabilité	GAUS	GUMB	Galt	PEAR	PEAV	GOOD	FREC	Lgam
10000 ans	0.0001	-19.773	124.663	132.564	120.842	165.141	96.161	167.042	164.934
1000 ans	0.001	65.735	162.92	163.981	159.216	191.029	126.083	186.686	190.965
100 ans	0.01	170.002	216.84	212.338	215.844	222.526	185.494	218.358	230.809
50 ans	0.02	207.219	238.533	232.853	239.102	248.657	213.085	232.568	247.988
20 ans	0.05	263.042	274.022	267.4	277.254	278.019	260.046	257.837	277.371
10 ans	0.1	312.643	309.017	302.373	314.547	308.195	306.341	285.442	307.712
5 ans	0.2	372.706	356.645	350.902	364.179	350.995	366.38	327.821	350.866
3.333 ans	0.3	416.015	395.244	390.66	403.117	386.959	411.29	366.743	387.168
2.5 ans	0.4	453.021	431.555	428.182	438.549	421.712	450.171	407.566	422.234
2 ans	0.5	487.61	468.67	466.506	473.506	458.067	486.625	453.993	458.876
2.5 ans	0.6	522.199	509.258	508.26	510.28	498.717	522.977	510.842	499.751
3.333 ans	0.7	559.205	557.026	557.078	551.675	547.68	561.577	586.932	548.823
5 ans	0.8	602.515	619.397	620.2	602.859	613.388	606.189	703.596	614.326
10 ans	0.9	662.578	719.191	719.747	678.845	722.783	666.804	940.384	722.403
20 ans	0.95	712.179	814.917	813.894	774.41	833.091	715.634	1242.086	830.012
50 ans	0.98	768.004	938.823	934.665	826.695	984.88	769.203	1780.643	975.733
100 ans	0.99	805.221	1031.673	1024.981	883.378	1106.357	804.1	2332.366	1090.391
1000.03 ans	0.999	909.516	1338.48	1327.321	1055.112	1566.829	898.522	5690.253	1508.821
10003.001 ans	0.9999	995.37	1644.746	1642.056	1207.229	2139.614	972.751	13860.737	1997.307

El-HAJRA

	GAUS: 5.555	GUMB: 4.835	Galt: 5.261	PEAR: 32.11	PEAV: 5.02	GOOD: 7.253	FREC: 6.935	Lgam: 6.565
Paramètre d'échelle	133.554	109.95	244.792	293.56	4076.137	185.735	350.935	72.689
Paramètre de position	430.756	366.78	152.539	251.7	0.05	250.744	0.05	72.689
Paramètre de forme premier	0	0	0.522	0.61	10.431	0.905	-0.282	29.737
Paramètre de forme second	0	0	0	0	0	0	0	0.058
Borne inférieure	0	0	152.539	251.7	0.05	250.744	0.05	72.689
Borne supérieure	0	0	0	0	0	0	0	0
Moyenne	430.756	430.245	433.098	430.756	432.246	429.684	445.785	505.083
Médiane	430.756	407.078	397.331	348.599	403.634	384.057	389.168	402.448
Mode	430.756	366.78	338.894	251.7	356.629	272.866	327.273	353.094
Variance	17836.694	19885.771	24682.669	52563.747	9404.328	26283.823	51318.373	22531.308
Coef. de variance	0.31	0.328	0.363	0.532	0.224	0.377	0.508	0.297
Coef. d'asymetrie	0	1.139	1.856	2.561	1.563	1.722	8.879	1.609
Coef. d'aplatissement	0	2.4	6.687	9.837	5.167	4.29	0	5.319
Valeur de test	5.555	4.835	5.261	32.11	5.02	7.253	6.935	6.565
Freq. au dépassement	0.161	0.228	0.201	0	0.224	0.071	0.083	0.108

Récurrence	Probabilité	GAUS	GUMB	Galt	PEAR	PEAV	GOOD	FREC	Lgam
10000 ans	0.0001	-65.575	122.654	187.637	251.7	152.215	250.789	187.764	159.584
1000 ans	0.001	18.071	154.285	201.279	251.703	175.051	251.103	203.615	180.979
100 ans	0.01	120.066	198.866	225.175	251.829	210.468	253.636	228.255	213.776
50 ans	0.02	156.473	216.801	236.288	252.101	216.975	256.184	238.99	227.925
20 ans	0.05	211.08	246.143	256.225	253.507	250.912	263.385	257.652	252.138
10 ans	0.1	259.601	275.078	277.889	257.378	276.869	274.989	277.481	277.181
5 ans	0.2	318.355	314.456	310.266	269.857	313.416	298.552	306.943	312.857
3.333 ans	0.3	360.721	346.37	338.686	288.377	343.9	323.823	333.1	342.921
2.5 ans	0.4	396.921	376.392	366.993	313.569	373.179	351.888	359.738	372.01
2 ans	0.5	430.756	407.078	397.331	347.016	403.635	384.057	389.168	402.445
2.5 ans	0.6	464.592	440.636	431.96	391.751	437.492	422.354	424.117	436.457
3.333 ans	0.7	500.792	480.131	474.452	453.758	478.021	470.446	469.29	477.363
5 ans	0.8	543.158	531.699	532.455	546.818	532.003	536.431	535.592	532.098
10 ans	0.9	601.913	614.209	630.586	715.661	620.96	645.767	661.708	622.709
20 ans	0.95	650.433	693.354	730.465	892.195	709.629	751.964	810.504	713.303
50 ans	0.98	705.043	795.8	868.048	1132.795	830.187	888.849	1053.849	836.544
100 ans	0.99	741.45	872.568	977.521	1318.332	925.565	990.334	1282.992	933.907
1000.03 ans	0.999	843.472	1126.236	1381.983	1948.116	1279.991	1318.118	2457.912	1293.158
10003.001 ans	0.9999	927.456	1379.455	1859.949	2585.771	1718.505	1635.457	4703.43	1718.991

Appendix 8.6: Wind speed Data

STATION	SEPT	OCT	NOV	DEC	**JAN**	**FEB**	**MAR**	**APR**	**MAY**	**JUN**	**JUL**	**AUG**
336-44	1.79	1.55	1.64	1.60	1.60	1.74	1.88	1.99	2.04	2.12	2.13	2.00
336-47	1.69	1.51	1.62	1.60	1.58	1.74	1.86	1.87	1.93	2.03	2.00	1.87
336-50	1.81	1.68	1.79	1.78	1.76	1.92	2.05	2.00	2.04	2.15	2.10	1.97
339-44	2.05	1.92	2.03	2.02	2.02	2.19	2.31	2.30	2.30	2.38	2.34	2.20
339-47	1.97	1.93	2.13	2.18	2.16	2.25	2.31	2.31	2.21	2.20	2.19	2.08
339-50	2.04	2.00	2.19	2.23	2.22	2.33	2.40	2.36	2.28	2.31	2.29	2.18
342-44	2.11	2.05	2.19	2.19	2.22	2.34	2.44	2.40	2.36	2.41	2.38	2.26
342-47	2.13	2.06	2.20	2.18	2.24	2.36	2.46	2.46	2.40	2.42	2.37	2.25
342-50	2.51	2.58	2.58	2.56	2.40	2.37	2.37	2.28	2.16	2.24	2.47	2.58
342-59	2.17	2.24	2.31	2.34	2.15	2.09	2.05	1.95	1.90	1.96	2.14	2.14

Appendix 8.7: Location of piezometers

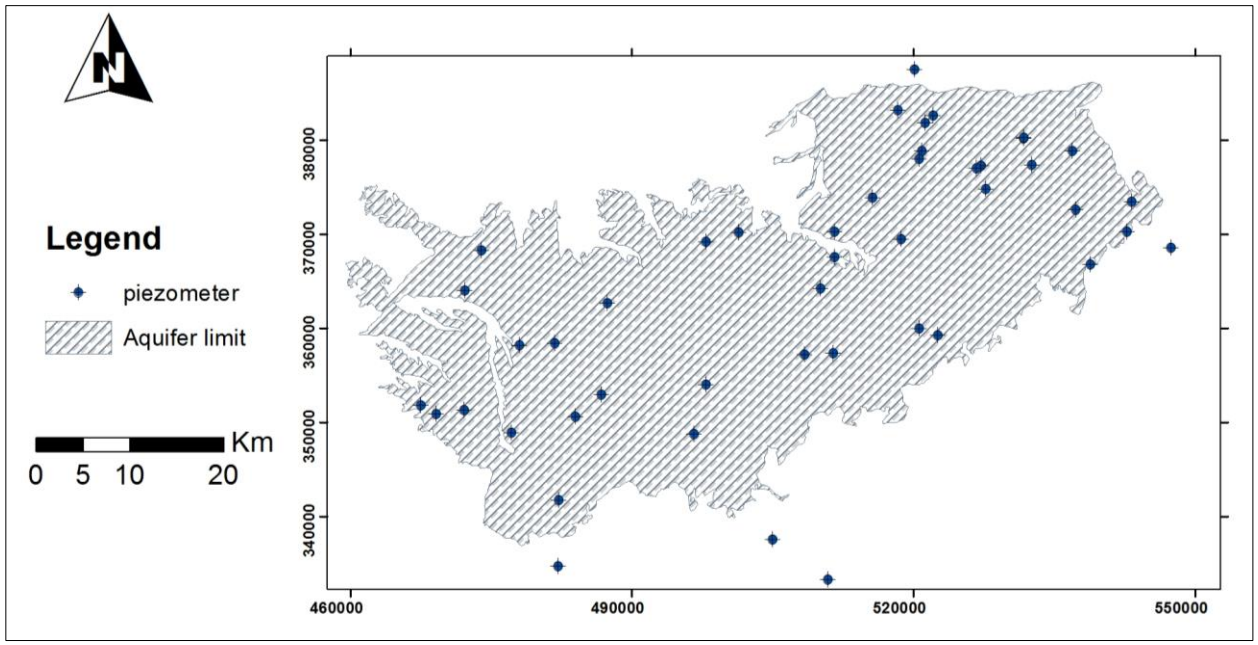

Appendix 8.7: Piezometer Data

Piezom-	JAN	FEB	MAR	APR	MAY	JUN	JUL	AUG	SEP	OCT	NOV	DEC
3362-15	36.3	36.7	35.7	35.7	35.7	36.5	36.6	37.1	37.0	37.4	36.9	37.0
3321-15	26.1	25.2	27.0	25.0	23.6	22.6	23.0	23.7	23.9	23.8	23.5	20.8
2813-15	15.4	14.4	15.3	15.5	15.1	18.0	20.9	20.2	20.7	19.7	17.5	16.9
2607-15	11.9	11.6	12.0	11.8	12.2	12.9	11.7	11.1	10.9	11.1	10.8	10.9
2604-15	8.0	8.2	8.0	7.5	7.5	8.6	8.4	8.3	7.3	7.6	7.3	7.7
2366-15	47.6	49.8	47.3	46.9	46.8	49.1	48.6	51.6	51.1	51.1	49.3	51.1
1314-22	2.6	1.9	2.1	1.8	2.2	2.5	3.3	3.8	4.2	4.2	3.5	3.0
290-22	51.4	52.5	50.9	49.2	54.8	55.9	59.5	59.6	60.6	56.4	56.8	55.6

8.8 Appendix: WetSpass Land use parameters

No	LUSE_TYPE	RUNOFF_VEG	NUM_VEG_RO	NUM_IMP_RO	VEG_AREA	BARE_AREA	IMP_AREA	OPENW_AREA	ROOT_DEPTH	LAI	MIN_STOM	INTERC_PER	VEG_HEIGHT
1	city center build up	grass	2	1	0.20	0.00	0.80	0.00	0.30	2.00	100.00	10.00	0.1200
2	build up	grass	2	2	0.50	0.00	0.50	0.00	0.30	2.00	100.00	10.00	0.1200
10	open build up	grass	2	3	0.60	0.10	0.30	0.00	0.30	2.00	100.00	10.00	0.1200
4	infrastructure	grass	2	4	0.60	0.10	0.30	0.00	0.30	2.00	100.00	10.00	0.1200
201	highway	grass	2	5	0.60	0.10	0.30	0.00	0.30	2.00	100.00	10.00	0.1200
202	district road	grass	2	6	0.60	0.10	0.30	0.00	0.30	2.00	100.00	10.00	0.1200
5	sea harbour	grass	2	7	0.60	0.10	0.30	0.00	0.30	2.00	100.00	10.00	0.1200
6	airport	grass	2	8	0.20	0.00	0.80	0.00	0.30	2.00	100.00	10.00	0.1200
3	industry	grass	2	9	0.40	0.00	0.60	0.00	0.30	2.00	100.00	10.00	0.1200
7	excavation	bare soil	4	0	0.00	1.00	0.00	0.00	0.05	0.00	110.00	0.00	0.0010
21	agriculture	crop	1	0	0.00	1.00	0.00	0.00	0.35	0.00	180.00	0.00	0.6000
27	maize and tuberous p	crop	1	0	0.00	1.00	0.00	0.00	0.40	0.00	180.00	0.00	1.5000
23	meadow	grass	2	0	1.00	0.00	0.00	0.00	0.30	2.00	100.00	10.00	0.2000
28	wet meadow	grass	2	0	1.00	0.00	0.00	0.00	0.30	2.00	100.00	10.00	0.3000
29	orchard	forest	3	0	0.20	0.80	0.00	0.00	0.80	0.00	200.00	10.00	3.0000
31	deciduous forest	forest	3	0	0.20	0.80	0.00	0.00	2.00	0.00	250.00	10.00	18.0000
32	coniferous forest	forest	3	0	0.90	0.10	0.00	0.00	2.00	4.50	500.00	45.00	15.0000
33	mixed forest	forest	3	0	0.50	0.50	0.00	0.00	2.00	4.50	500.00	38.00	15.0000
36	shrub	grass	2	0	0.20	0.80	0.00	0.00	0.60	0.00	110.00	5.00	2.0000
35	heather	grass	2	0	0.20	0.80	0.00	0.00	0.20	4.00	110.00	15.00	0.7500
54	sea	open water	5	0	0.00	0.00	0.00	1.00	0.05	0.00	110.00	0.00	0.0000
53	estuary	open water	5	0	0.00	0.00	0.00	1.00	0.05	0.00	110.00	0.00	0.0000
44	mud flat/salt marsh	open water	5	0	0.40	0.20	0.00	0.40	0.30	2.00	110.00	10.00	0.5000
37	beach/dune	bare soil	4	0	0.30	0.70	0.00	0.00	0.50	2.00	110.00	15.00	1.0000
51	navigable river	open water	5	0	0.00	0.00	0.00	1.00	0.05	0.00	110.00	0.00	0.0000
55	unnavigable river	open water	5	0	0.00	0.00	0.00	1.00	0.05	0.00	110.00	0.00	0.0000
52	lake	open water	5	0	0.00	0.00	0.00	1.00	0.05	0.00	110.00	0.00	0.0000
301	spruce	forest	3	0	0.90	0.10	0.00	0.00	2.00	11.00	320.00	55.00	13.0000
302	pine	forest	3	0	0.90	0.10	0.00	0.00	2.00	4.50	550.00	40.00	15.0000
303	beech	forest	3	0	0.20	0.80	0.00	0.00	2.00	0.00	320.00	10.00	20.0000
304	birch	forest	3	0	0.20	0.80	0.00	0.00	2.00	0.00	320.00	10.00	16.0000
305	oak	forest	3	0	0.20	0.80	0.00	0.00	2.00	0.00	150.00	10.00	17.0000
306	poplar	forest	3	0	0.20	0.80	0.00	0.00	2.00	0.00	250.00	10.00	18.0000
307	reference grass	grass	2	0	1.00	0.00	0.00	0.00	0.30	2.00	140.00	10.00	0.1200

8.9 Appendix WetSpass parameter table

Parameter	Full name	Unit
Veg_area	Vegetation area fraction	-
Bare_area	Bare area fraction	-
Imp_area	Impervious area fraction	-
Openw_area	Open water area fraction	-
Root depth	Rooting depth	M
Lai	Leaf Area Index	- area fraction
Min_stom	Minimal stomatal resistance	s/m
Interc_per	Interception percentage	%
Veg_height	Vegetation height	M

Parameter	Full name	Unit
Porosity	Porosity	- (volume fraction)
Wilting point	Wilting point	- (volume fraction)
Field capacity	Field capacity	- (volume fraction)
Residual wc	Residual water content	- (volume fraction)
a_1	a1 soil empirical parameter for ET calculation	-
PAW	Plant Available Water	- (volume fraction)
tensionhht	Tension saturated height	M
evapodepth	Soil evaporation depth	M
P_frac_winter	Precipitation fraction in winter which has an intensity higher than the soil infiltration rate	- (volume fraction)
P_frac_summer	Precipitation fraction in summer which has an intensity higher than the soil infiltration rate	- (volume fraction)